Aus der
Klinik für Orthopädie und Unfallchirurgie
Klinik der Universität München
Direktoren: Prof. Dr. Wolfgang Böcker und Prof. Dr. Boris Holzapfel

Overexpression of PAX3 in immortalised human mesenchymal stem cells initiates a myogenic program

Dissertation
zum Erwerb des Doktorgrades der Zahnmedizin
an der Medizinischen Fakultät
der Ludwig-Maximilians-Universität zu München

vorgelegt von
Marlene Zimmermann

aus
Graz

Jahr
2025

Mit Genehmigung der Medizinischen Fakultät
der Universität München

Berichterstatter:	PD Dr. Attila Aszódi
Mitberichterstatter:	Prof. Dr. Florian Haasters
	Prof. Dr. Eric Hesse
Mitbetreuung durch den promovierten Mitarbeiter:	Dr. Maximilian Saller
Dekan:	Prof. Dr. med. Thomas Gudermann
Tag der mündlichen Prüfung:	18.03.2025

Für Ilse, Paula, Elke, Walter, Lisbeth und Birgit

Abstract

The loss of skeletal muscle tissue has many causes, including age-related muscle loss (sarcopenia), inactivity (muscle atrophy) or disease (cachexia). It is an important topic of current research, as satisfactory treatment of patients suffering from muscle loss is often not possible. In general, the self-repair mechanisms of skeletal muscle tissue are so impressive that injured and subsequently repaired muscle fibres are indistinguishable from uninjured ones. However, when it comes to sarcopenia, cachexia, muscle atrophy or muscular dystrophy, the treatment of lost muscle tissue is unsatisfactory. New applications and treatments need to be discovered to achieve a proper recovery of affected patients. To date, various approaches in regenerative medicine have been developed, and some promising options have been identified, although most still have drawbacks that prevent their clinical application. The medical needs of patients suffering from muscle loss remain unmet.

In this study, I chose *PAX3* as the gene of interest because of its role as a master regulator of early myogenesis. The *PAX3* gene encodes a vital transcription factor in muscle precursor cells. PAX3 is expressed at early stages of development in the dermomyotome, where it is required for the proper development of the epaxial and hypaxial dermomyotome. PAX3 also controls the delamination of muscle progenitor cells from the dermomyotome. This gene is essential for the migration of muscle precursor cells to distant sites during myogenesis, such as the limbs, where muscle precursors differentiate and give rise to mature muscle. The limbs and most hypaxial muscles in mammals require the expression of PAX3 to develop. PAX3 also plays an important role in cell proliferation, cell motility and cell survival. *Pax3* mutant embryos were found to lack muscles of migratory origin and the development of trunk musculature in these embryos was also severely defective.

For this reason, I focused on the gene *PAX3* and generated PAX3-overexpressing mesenchymal stem cell populations (SCP1 cell populations) using a Sleeping Beauty transposon system: SCP1$^{PAX3}{}_{high}$ cells and SCP1$^{PAX3}{}_{low}$ cells. I aimed to generate PAX3-overexpressing SCP1 cell populations, characterise them *in vitro* and identify the muscle-related molecular signatures of SCP1$^{PAX3}{}_{high}$ cells and SCP1$^{PAX3}{}_{low}$ cells. Accordingly, I characterised these newly generated cell populations *in vitro* by analysing changes in cell proliferation, clonogenic potential, random migration, cell morphology and fusion properties compared to native SCP1 cells and/or C2C12 cells. I evaluated the muscle-related molecular signatures of the PAX3-overexpressing cell populations using next generation RNA-sequencing.

I found that overexpression of PAX3 in SCP1 cells alone was not sufficient to fully transform these cells into functional myoblasts. The proliferation of SCP1 cells was not affected by PAX3-overexpression. The clonogenic potential of SCP1 cells was unaffected by PAX3-overexpression, as was cell morphology and random cell migration. Fusion of SCP1 cell populations could not be induced by PAX3. Furthermore, I could not detect MYH1E expression or terminal myogenic differentiation in the newly created cell populations. However, overexpression of PAX3 shifted the transcriptome of SCP1 cells. Using GO enrichment analysis, I was able to show that the overexpression of PAX3 activated the “muscle organ development” pathway in SCP1 cells. This suggests that the overexpression of PAX3 induces slight changes in the transcriptome of SCP1 cells towards a more myogenic lineage.

Taken together, my data indicate that overexpression of PAX3 allows for minor myogenic changes in the transcriptome of SCP1 cell populations that were not translated into any of the functions explored by the aforementioned assays. My work provides a basis for characterising the potential changes in mesenchymal stem cells by overexpressing PAX3. Furthermore, my data suggest that the constant overexpression of PAX3 may prevent the cells from terminal myogenic differentiation and that downregulation of PAX3 must be included in any future studies to allow the initiation of myogenic cascades as they naturally occur *in vivo*. A transient upregulation of PAX3 would more closely resemble the physiological myogenic program and could therefore be an interesting alternative to explore in the future.

Zusammenfassung

Es gibt verschiedene Gründe für den Abbau von skelettaler Muskelmasse. Diese Gründe für Muskelabbau können entweder durch Alter (Sarkopenie), Inaktivität (Muskelatrophie) oder Krankheit (Kachexie) bedingt sein. Obwohl der menschliche Körper grundsätzlich beeindruckende Ressourcen besitzt, um verletztes Muskelgewebe wieder aufzubauen, sind der Medizin aktuell in der Therapie von Muskelabbau im Zuge von Sarkopenie, Muskelatrophie oder Kachexie Grenzen gesetzt. Die gänzliche Wiederherstellung der verlorenen skelettalen Muskelmasse ist oft nicht möglich. Daher sollte in der zukünftigen Forschung ein Hauptaugenmerk auf dieses Gebiet gelegt werden, um bessere Behandlungsmöglichkeiten für betroffene Patienten/Patientinnen zu ermöglichen. In der regenerativen Medizin gibt es bereits viele Ansätze für die Therapie von Muskelabbau. Viele dieser Ansätze sind jedoch nach wie vor mit Kehrseiten verbunden. Eine gänzlich zufriedenstellende Lösung für die Behandlung von Muskelabbau wurde noch nicht gefunden. Durch Forschung über muskuläre Entwicklung und Regeneration und die damit einhergehende Identifikation wichtiger Gene und Faktoren, könnten die Therapiemöglichkeiten für betroffene Patienten/Patientinnen verbessert werden.

In meiner Arbeit habe ich *PAX3* als zu untersuchendes Gen ausgewählt, weil es für die frühe Muskelentwicklung essenziell ist. Das *PAX3* Gen codiert einen Transkriptionsfaktor, dessen Transkription in Muskelvorläuferzellen wesentlich ist. Die Expression von PAX3 wurde im frühen Stadium der Muskelentwicklung im Dermomyotom nachgewiesen, wo das Gen für die korrekte Entwicklung des epaxialen und hypaxialen Dermomyotoms essenziell ist. PAX3 kontrolliert die Delamination von Muskelvorläuferzellen vom Dermomyotom. Außerdem ist PAX3 unverzichtbar für die Migration von Muskelvorläuferzellen zu Orten der Myogenese wie zum Beispiel den Extremitäten. Säugetiere brauchen zur korrekten Entwicklung der Muskeln der Extremitäten sowie der meisten hypaxialen Muskeln PAX3. Außerdem spielt PAX3 eine wichtige Rolle in der Proliferation, der Motilität und auch im Überleben von Zellen. In *Pax3* mutanten Embryonen wurden fehlende Muskeln migratorischen Ursprungs festgestellt, was auch mit schweren Defekten in der Entwicklung der Rumpfmuskulatur einherging.

Aus diesem Grund habe ich mich in meiner Arbeit auf den Transkriptionsfaktor PAX3 fokussiert und mithilfe des Sleeping Beauty Transposon Systems aus mesenchymalen Stammzellen (SCP1 Zellen) Zellpopulationen generiert, die das Gen *PAX3* stabil überexprimieren: SCP1$^{PAX3}_{high}$ Zellen und SCP1$^{PAX3}_{low}$ Zellen. Das Ziel der Studie war, PAX3-überexprimierende SCP1 Zellpopulationen zu kreieren, diese *in vitro* zu charakterisieren und Veränderungen dieser Zellen hinsichtlich einer potenziellen myogenen Differenzierung aufzuzeigen. Ich habe die neu geschaffenen Zellpopulation *in vitro* analysiert, um

Veränderungen bezüglich ihrer Proliferation, ihres klonogenem Potentials, Migrationsverhaltens, Morphologie und der Zellfusion zu erforschen. Ich habe die Ergebnisse jeweils mit nativen SCP1 Zellen und/oder C2C12 Myoblasten verglichen. Außerdem wurde eine Next-Generation RNA-Sequenzierung durchgeführt, um Änderungen im Transkriptom der PAX3-überexprimierenden SCP1 Zellpopulationen festzustellen.

Meine Daten zeigen, dass die alleinige Überexpression von PAX3 in SCP1 Zellen nicht ausreicht, um diese Zellen in funktionelle Myoblasten zu verwandeln. Ich konnte keine Veränderungen in der Proliferation der neuen Zellpopulationen aufgrund von PAX3 Überexpression feststellen. Das klonogene Potential dieser Zellen blieb ebenso unverändert wie auch die Morphologie oder das Migrationsverhalten. SCP1 Zellen, die PAX3 überexprimierten, fusionierten nicht und exprimierten auch kein MYH1E. Die neu geschaffenen Zellen differenzierten in Summe nicht aus und entwickelten sich nicht zu Myoblasten. Dennoch konnte durch die Überexpression von PAX3 das Transkriptom der SCP1 Zellen verändert werden. Von großer Bedeutung für meine Studie war hier das Ergebnis, dass der Signalweg der „Muskel Organ Entwicklung“ in PAX3-überexprimierenden SCP1 Zellen aktiviert wurde. Dies zeigte die GO Enrichment Analyse. Dieses Ergebnis deutet darauf hin, dass durch Überexpression von PAX3 leichte Veränderungen des Transkriptoms von SCP1 Zellen in Richtung einer myogenen Linie ermöglicht wurden.

Zusammengefasst zeigen meine Daten, dass die Überexpression von PAX3 eine beginnende Induktion des myogenen Programms in SCP1 Zellen ermöglicht. Meine Studie bietet eine Basis, um Möglichkeiten der Veränderung von mesenchymalen Stammzellen durch PAX3 Expression aufzuzeigen. Außerdem konnte ich zeigen, dass eine konstante Überexpression von PAX3 die Zellen an der terminalen, myogenen Differenzierung hindern könnte. Und, dass PAX3 in zukünftigen Studien herunter reguliert werden muss, um den Beginn von myogenen Kaskaden zu ermöglichen, wie es auch *in vivo* der Fall ist. Hierfür wäre eine transiente Transfektion von PAX3 eine Möglichkeit, welche die physiologischen Abläufe der Myogenese besser nachahmen könnte.

Contents

List of Figures

List of Tables

1. Introduction

1.1 Skeletal muscle loss

For this study, I define the loss of skeletal muscle as a decrease in muscle mass (1). Skeletal muscle loss comes with an imbalance in the metabolism of protein, as more protein is degraded than produced (1). There are various reasons why muscle loss occurs: due to ageing, which is known as sarcopenia (2); due to disease, called cachexia; or by inactivity, known as atrophy (2). Sarcopenia, cachexia and atrophy are all based on a loss of muscle mass (2). Other reasons for the loss of skeletal muscle tissue are trauma through injury or degenerative diseases such as muscular dystrophies (3, 4).

1.1.1 Sarcopenia

With age, the lean body mass is reduced, and fat mass is increased (2). The resulting condition of sarcopenia was first described in 1993 by Evans and Campbell (2, 5) and in 1995 Evans defined it as an age-related loss of muscle mass (2, 6). In 2010, Muscaritoli et al. modified the definition of sarcopenia (7). It was then defined as low muscle mass (> two standard deviations under the mean muscle mass measured in young adults) combined with low gait speed (meaning a walking speed under 0.8 m/s in a walking test of four meters) (7). Humans reduce about 30% of muscle mass from age 20 to 80 (2, 8) as the amount and size of muscle fibres decreases over a lifetime (2, 9). The aetiology of sarcopenia has various causes such as a lack of physical activity, lower levels of androgens, poor nutrition especially concerning vitamin D and protein intake or chronic inflammation (2, 10-14). 50% of people over 80 years and 5-13% of 60 to 70-year-olds suffer from sarcopenia, making it a global health concern (15, 16). Diagnosing sarcopenia is difficult as there are no specific or sensitive measures (16-18). Currently, imaging methods such as magnetic resonance imaging (MRI) or computed tomography (CT), calf circumference, handgrip strength, walking speed or bio-impedance analysis are used to evaluate sarcopenia (16). The European Working Group on Sarcopenia in Older People (EWGSOP) defined the diagnostic criteria for sarcopenia as follows:

- Low muscle mass is defined by a skeletal muscle mass index of ≤ 6.37 kg/m^2 in women and ≤ 8.90 kg/m^2 in men
- Low muscle strength measured by handgrip strength of < 20 kg in women or < 30 kg in men

- Low physical performance measured by gait speed ≤ 0.8 m/s (16, 19)

Depending on the levels of muscle mass and functional impairment, sarcopenia can be staged into three levels: pre-sarcopenia (low muscle mass, normal muscle strength and normal performance), sarcopenia (low muscle mass, low muscle strength and normal or low performance) and severe sarcopenia (low muscle mass, low muscle strength and low performance) (16, 19).

Early diagnosis of sarcopenia is important in order to start interventions and improve outcomes for those affected (16). A distinction can be made between the non-pharmacological and pharmacological treatment of sarcopenia (16). Regarding non-pharmacological treatment, establishing an exercise regimen is vital to counteract physical inactivity in patients (16). Both strength training and resistance training should be included (16). Resistance training can increase the rate of protein synthesis and hormone concentrations, which is beneficial for the neuromuscular system (16, 20). When it comes to the pharmacological treatment of sarcopenia, no agents have been approved by the US Food and Drug Administration (FDA) (16). Attempts using growth hormone increased muscle mass and protein synthesis but did not improve muscle strength or function (16). Anabolic steroids, especially testosterone, can increase muscle mass and strength (16, 21, 22). Nevertheless, clinical use is limited due to an elevated risk of cardiovascular events, the risk of virilisation in women and prostate cancer in men (16, 21, 22).

New treatment pathways for sarcopenia are currently in development (16). Promising options being investigated include selective androgen receptor modulators, vitamin D, myostatin, eicosapentaenoic acid, angiotensin-converting enzyme inhibitors (16, 21, 22), thalidomide, anabolic agents such as ghrelin, MT-102 (anabolic catabolic transforming agent (ACTA) (23)), celecoxib, or omega-3 supplements or BYM338 (bimagrumab) (16, 24). Pötsch et al. showed that MT-102 could reverse sarcopenia in old rats (23), and its potential in human sarcopenia treatment is currently being considered (16). Herbal supplements also present an interesting option to increase muscle mass in patients suffering from sarcopenia (16). In 2016, Rondanelli et al. showed that some herbal compounds positively affect skeletal muscle (16, 25). These include steroidal lactones and alkaloids from *Withania somnifera* (Solanaceae), curcumin from *Curcuma longa*, shogaols and gingerols from Zingiber *officinale*, proanthocyanidin of *grape seeds* or catechins from *Camellia sinensis* (16, 25). Still, further studies are needed to prove the efficacy and safety of herbal supplements in humans (16). In 2013, Harimoto et al. found that the prognosis of the recurrence-free and overall survival of patients suffering from hepatocellular carcinoma, undergoing hepatectomy, with sarcopenia was significantly worse than without sarcopenia (26). Sarcopenia raises the risk of mortality in critically ill patients

(27). Future research should concentrate on improving diagnostic biomarkers for sarcopenia and analysing biological pathways leading to sarcopenia (16). Currently, the best practice to minimise sarcopenia lies in elevated awareness among healthcare providers and patients, a multi-disciplinary treatment approach and early screening (16, 28).

1.1.2 Cachexia

Cachexia can be defined as unintentional weight loss during a chronic illness (29). By definition, cachectic patients suffer from a chronic disease, have lost ≥ 5% of their body weight in the past twelve months or less, and face at least three of the following conditions: decrease in muscle strength, low albumin, fatigue, anaemia, anorexia, inflammation, atypical biochemistry or a low Fat-Free Mass Index (29, 30). Cachexia is characterised by a rapid loss of skeletal muscle tissue (2). It can also come with a loss of adipose tissue (2, 30). It is associated with inflammation, insulin resistance, anaemia, muscle weakness, fatigue and increases in the breakdown rate of muscle proteins (2, 30).

Several conditions can entail cachexia such as malignant cancer, chronic obstructive pulmonary disease (COPD), Alzheimer's disease, cystic fibrosis, chronic heart failure, rheumatoid arthritis, infectious diseases, chronic kidney disease and several other chronic diseases (29). The most prevalent subtypes of cachexia are COPD cachexia, chronic kidney disease cachexia, cancer cachexia and cardiac cachexia (in chronic heart failure) (29).

Many patients suffer from cachexia (29). 60%-80% of advanced cancer patients and 5%-15% of patients suffering from chronic heart failure or chronic obstructive pulmonary disease develop cachexia (29).

Cachexia comes with an impaired quality of life, high-mortality, and poor-symptom status (29). It is thought that the rate of cancer patients dying from cachexia presumably exceeds the 30% mark (29). Mortality rates range from 80% in cancer cachexia patients, 10%-15% in COPD cachexia patients to about 30% in patients suffering from chronic kidney disease cachexia or cardiac cachexia (29).

Therapy of affected patients is restricted; there is no proven treatment for cachexia. Current approaches focus on nutritional interventions, administering anabolic steroids, appetite stimulants or anti-catabolic therapies (29, 31). These treatments are currently being investigated (29, 31). To date, the pathophysiology of cachexia is not well understood, and future research should focus on cachexia as a serious medical problem, which is often under-recognised and underestimated (29).

1.1.3 Muscle atrophy

Muscle atrophy is properly defined as a loss of skeletal muscle tissue caused by reduced physical activity (2). Confusingly, the term “muscle atrophy” is also used when discussing sarcopenia or cachexia, since muscle atrophy occurs physiologically with age (age-related sarcopenia) (1) and muscle atrophy is a clinical feature of cachexia (1). Commonly, these terms are used fluidly and synonymously; however, in this study, muscle atrophy will be defined as a loss of skeletal muscle mass caused by inactivity (2). Causes for disuse-induced skeletal muscle atrophy (32) can be a sedentary lifestyle, long-term immobilisation or long periods of rest (1). Furthermore, enforced lockdowns such as during the COVID-19 pandemic, disabilities or pain due to chronic diseases, diseases affecting mental health such as depression, decreased ambulatory activity, infections compelling bed rest or hospitalisations can promote skeletal muscle atrophy due to reduced physical activity (32-36). Affected patients suffer from a reduced quality of life, a decrease in individual independence and overall reduced mobility (32, 37, 38). This loss of skeletal muscle mass in muscle atrophy increases the risk of various chronic diseases such as cardiovascular diseases, depression or type 2 diabetes mellitus and is linked to a higher mortality (2, 32, 39, 40). Therefore, it is important to understand and prevent muscle atrophy (32).

Therapeutic approaches to counteract muscle atrophy include exercise training targeting the atrophying muscles (1, 41-43), dietary interventions e.g. using appetite stimulants (1, 44), using compounds with anabolic activity such as steroidal androgens (1, 45) or growth factors (1, 46), using anti-inflammatory drugs (1, 47-49) or using muscle-wasting inhibitors like proteasome inhibitors (1, 50, 51). The most widely accepted, effective non-pharmacological treatment of muscle atrophy is resistance training (32). Muscle loss that occurs after disuse-events can often be restored via rehabilitation therapy or ambulation; however, in the older population, multifaceted treatment approaches including increased activity and protein intake, seem to be the most efficient (32, 52).

1.1.4 Other reasons for loss of muscle mass

As stated before, trauma caused by injury and degenerative diseases such as muscular dystrophies are grave reasons for loss of muscle mass as well (3, 4). Various types of traumas or injuries can result in loss of muscle mass and strength such as contraction-induced injuries, myotoxic injuries, freeze injuries, volumetric muscle loss injuries or burn injuries (53). Throughout a lifetime, injuries of skeletal muscle happen frequently and differ in levels of impact to a person (54, 55). Skeletal muscle can rebuild itself to the point where newly regenerated myofibers cannot be distinguished from uninjured ones

(54). Recovering from injured muscles can depend upon immobilisation and, thereby, muscle disuse, which leads to muscle loss and decreases in the functional capacity and metabolic health of skeletal muscle (56). The rehabilitation period after injury depends on the extent of muscle loss (56). Muscle loss due to disuse after injury can be prevented by neuromuscular electrical stimulation (56).

Muscular dystrophies are characterised by genetic modifications that lead to progressive loss of power and strength, resulting in degeneration of skeletal muscle (57). Patients experience muscle weakness, spasms, atrophic muscle tissue or myalgias (58). Widespread muscular dystrophies are, for instance, myotonic dystrophy, facioscapulohumeral muscular dystrophy, Duchenne muscular dystrophy or Becker muscular dystrophy (59). Duchenne muscular dystrophy also affects children and young patients (60). To date, muscular dystrophies are incurable and can come with premature death due to cardiac failure or respiratory dysfunction (58). Novel genome editing technologies are promising in curing muscular dystrophies, enabling the insertion of genetic alterations into the cells of mammals (61).

Taken together, there are many forms and causes for the loss of skeletal muscle, and a satisfactory treatment leading to a complete cure is yet to be found. A deeper understanding of the underlying control mechanisms of the maintenance and loss of muscle mass will help tackle clinical problems (62). Future research needs to focus on providing more effective diagnostic and treatment pathways for patients. This will improve the prognosis of diseases associated with a loss of muscle mass by identifying new therapeutic targets and drugs (62). The activation of the Akt pathway through specific IGF1 memetics (62), beta-adrenergic antagonists (62, 63), myostatin (62, 64) or the proteasome system (62, 65-67) are promising therapeutic approaches (62). After all, healthy muscles are vital for healthy ageing, and for the energy supply to essential organs in periods of stress and preventing metabolic disorders (62).

1.2 Adult muscle regeneration and the role of satellite cells

During the development of skeletal muscles, multinucleated myofibers are built by the fusion of mononucleated muscle progenitor cells (68). Some of these muscle progenitor cells stay associated with adult myofibers as satellite cells (68). Satellite cells, located under the basal lamina of the muscle fibres (69), are known to be a muscle-specific type of stem cell (68).

Mammalian skeletal muscles can regenerate after injury, a mechanism also known as the formation of myofibers caused by necrosis (68). This regeneration process is mediated by satellite cells (68). Neuronal activity is essential to support the growth of the regenerated muscle (68). Three sequential stages of muscle regeneration, which can also overlap, can be differentiated (68). First, there is an inflammatory response with macrophages involved in phagocytosis, simultaneously with the promotion of muscle differentiation, second, the activation and differentiation of satellite cells takes place and finally, the growth and remodelling of muscle tissue occurs (68).

Throughout the whole lifetime, they reside in the muscle tissue (68). Their regenerative capacity, however, declines with age and disease (68, 70). Satellite cells are located in a stem cell niche, a specialised microenvironment containing stem cells, stromal cells, neural inputs, vascular networks, soluble factors, cell adhesion molecules and components of extracellular matrix (68, 71). This niche protects the inactive stem cell populations from decreasing in number and regulates their activation, which can be induced by factors such as disease, injury or exercise (68, 71). Satellite cells are identified by certain markers such as Pax7, M-cadherin, CD34 and, in some adult muscles, Pax3 (68). After muscle tissue is injured, satellite cells activate and proliferate to form a pool of myoblasts (68). These myoblasts differentiate and fuse, providing the myonuclei required to replace or repair the damaged myofibers (68, 72). When activated, the satellite cells migrate out of the stem cell niche and either undergo symmetric division, expanding their number and, thereby, the stem cell pool or asymmetric division, giving rise to cohorts of committed satellite cells and, therefore, progenitor cells by creating one differentiating cell and one self-renewing stem cell (68, 73, 74). Various signals can activate satellite cells (68). For instance, the generation of sphingosine-1-phosphate in the inner side of the plasma membrane of muscle cells (75), the production of nitric oxide (NO) due to an increase of NO synthase activity (which occurs due to an activation of matrix metalloproteinases, which in turn cause the release of *hepatocyte growth factor (HGF)* from the extra-cellular matrix) (76) or HGF binding to its receptor c-met (which satellite cells express) (68, 77).

On the second day after injury, satellite stem cells undergo rapid proliferation (3, 68). This is promoted by endothelial cells, which secrete antiapoptotic and mitogenic factors, such as the vascular endothelial growth factor (VEGF) (3, 68).

Wnt and Notch signalling appears to control the switch from satellite cell proliferation to differentiation (68). During proliferation, Notch signalling seems to predominate (68, 78), whereas in the differentiation phase Wnt signalling prevails (68, 79).

The proliferation of satellite cells generates both new undifferentiated stem cells and myogenic progenitor cells, which express the myogenic regulatory factors (MRFs) Myf5,

MyoD, Myogenin and Mrf4 (68, 80). Most satellite cells simultaneously express Myf5 and MyoD, followed by moygenin (68). MyoD plays an essential role in this process since MyoD-null satellite cells showed no expression of Mrf4 and decrease in the levels of Myogenin (68, 81). As a result, a deficit in the differentiation of those cells occurs (68, 82).

Satellite cells proliferate and differentiate into myofibers (80). They can differentiate into various mesenchymal lineages due to the heterogeneity in their differentiation potential (83). Satellite cells can differentiate into osteocytes, myocytes or adipocytes *in vitro* (83). Still, the prevalent fate of satellite cells in healthy muscle *in vivo* is myogenesis (68, 80).

Many factors affect the growth of muscle tissue after injury, such as the type of injury, whether blood vessels are damaged and whether the re-establishment of myotendinous and neuromuscular connections is possible (68). The preservation of the basal lamina is essential for the regeneration of muscle tissue (68).

The remodelling of muscle is frequently observed in muscle regeneration (84). Myotubes might fuse outside the basal lamina, forming clusters of smaller fibres (68); or the myotubes may only fuse at one extremity, and form forked fibres (68); new myotendinous junctions may be formed due to scar tissue separating the two stumps (68). Furthermore, myofibers may form outside the basal lamina and persist as small fibres in the interstitial tissue (68).

As previously stated, nerve activity also plays an important role in the regeneration of muscle tissue (68); however, the activation, proliferation, differentiation and fusion of satellite cells are not dependent on neural activity (68). These stages of muscle regeneration can function without neural activity (68). Nonetheless, the newly formed myofibers ultimately need neural activity to enable further growth and maturation (68). If not, the newly formed myofibers remain atrophic (68).

Although satellite cells hold enormous regenerative capacities, including the ability to restore damaged muscle fibres or completely rebuild fresh muscle tissue, fibrosis, the formation of scar tissue reducing proper muscle function, still occurs in healing muscle tissue (68, 85, 86). This goes hand in hand with aesthetic deficits and insufficient recovery of the impaired area (68, 85, 86). Subsequently, identifying factors which can help decrease the formation of scar tissue and improve the healing process of muscle tissue overall is of great interest in current research (68, 85). By identifying essential bioactive factors involved in muscle regeneration, the treatment of muscle injuries, dysfunction or diseases could be improved (68, 85).

To sum up, satellite cells are vital for the regeneration of muscle tissue. The proliferation of satellite cells ensures the persistence of stem cell populations in adult muscle tissue, important for the proliferation, differentiation and fusion of myogenic cells, to form myofibers after injury and, ultimately, to maintain a normal muscle function (68, 80).

1.3 Approaches to regenerative medicine for treating muscle loss

The following chapter features possibilities of future treatments for muscle regeneration and combatting muscle loss. I will also review factors and cell lines which may be suitable for further research.

Ghrelin and Insulin-like growth factor 1 (IGF1) analogues are appealing aspects for research and future therapy of muscle loss (87). IGF1 is one of the best-characterised regulators of muscle growth (68), promoting the growth of muscle tissue and muscle regeneration (68), and regulating protein synthesis in skeletal muscle (68, 88). Barton-Davis et al. showed that skeletal muscle loss caused by ageing could be prevented by injecting a recombinant adeno-associated virus that induces the overexpression of IGF1 (89). These findings could be a starting point for human gene therapy, preserving muscle function despite ageing, via a gene transfer of IGF1 into muscle tissue (89). However, IGF1 is unsuitable as a therapeutic agent due to its fast clearance (87). A modified form has therefore been developed: long arginine IGF1, which is more potent, has a longer circulation time and binds to more tissue targets (87, 90).

Ghrelin is a hormone which raises the levels of growth hormone, IGF1 and overall body mass (87, 91). Ghrelin can reduce muscle atrophy caused by denervation or fasting (87, 92). In 2015, Chen et al. showed that Ghrelin ameliorates muscle wasting by increasing muscle strength and lean body mass (93). Human synthetic ghrelin can enhance the left ventricular function, combat muscle loss in patients suffering from chronic heart failure after intravenous dispensing for three weeks (94), boosting muscle mass for patients with COPD (95, 96), and benefiting patients suffering from cardiopulmonary-associated cachexia (97).

Another way of stimulating muscle tissue growth, independent of IGF1, is through activating the G protein-coupled β2-adrenoreceptor (87). This causes cAMP to accumulate, activating the protein kinase A (87, 98) and stimulating the PI3K–AKT–mTOR signalling (87, 99). β2-adrenoreceptor agonists, such as formoterol or clenbuterol, impede protein degradation and lower muscle atrophy due to ageing (100), immobilisation (63), dener-

vation (101) or cancer (87, 102). cAMP levels can also be increased by selective inhibitors of phosphodiesterase 4 (87). This class of drugs is known for anti-inflammatory qualities and the reduction of obstruction in airflow (87, 103), making them suitable for the treatment of COPD (87, 104). cAMP has been reviewed many times regarding the repair and regeneration of muscle tissue (105). Since many forms of cancer and musculoskeletal disorders display dysfunctions in the cAMP signalling cascade (105, 106), it is an interesting target to create model systems for future research (105, 107). Recently, musculoskeletal regenerative engineering has focused on cAMP (105). cAMP signalling is necessary for the proper regeneration of adult skeletal muscle since it is associated with the differentiation (105, 108) and migration (105, 109) of myoblasts as well as myoblast fusion (86, 105, 108, 110, 111). For this reason, studies in animal models revolving around muscular dystrophy, age-related muscle loss or muscular atrophy because of disuse have shown that by maintaining the activation of the cAMP signalling cascade, the hypertrophic reactions of myofibers can be accomplished (86, 105, 112, 113). Taken together, cAMP is a promising candidate for the future treatment of muscle loss as it modulates musculoskeletal regeneration (105). That said, the activation of cAMP cascades activates other signalling cascades, which might be harmful and unwelcome during specific treatments (105). Site-selective analogues of cAMP need to be identified in the future to offer more therapeutic agents that can be used in musculoskeletal regenerative engineering (105).

Another method of treating muscle loss could lie in androgens such as steroids and selective modulators of the androgen receptors (87). Testosterone increases the muscle mass and protein synthesis by binding to nuclear receptors in the muscle tissue (87). Testosterone induces the growth of muscle (87, 114) and raises the number of satellite cells in muscle tissue (87, 115). Clinical use of this androgen is very limited due to severe side effects, including masculinisation, cancer or prostate hypertrophy (87, 116). To overcome these side effects, non-steroidal selective androgen receptor modulators could be an alternative drug (87, 117).

Satellite cells are promising for future treatment as they are muscle-specific stem cells, assuring the regenerative capacity of skeletal muscle (3, 118). Transplanting satellite cells could be therapeutically feasible (3, 119). For instance, engrafting muscles with mice was enhanced after transplanting mouse muscle fibres with as few as one to seven satellite cells enclosed in them (3, 69, 120). Moreover, Xu et al. isolated human satellite cells from muscle biopsies and sorted them via fluorescence-activated cell sorting (FACS) before transplanting those satellite cells into immune-compromised mice (121-123); the mouse satellite cell niche was colonised, and mouse fibres formed, which expressed human markers (121-123). This is an essential step for recovering damaged

muscle tissue (121-123). Still, several obstacles are involved in working with satellite cells (3). Their regenerative capacity is reduced when cultured, compared to freshly isolated cells (3, 123). Moreover, they survive and migrate poorly in culture (3, 124, 125). After only three days of expansion *ex vivo*, satellite cells reduce their proliferative capacity (3); however, results could be improved by transplanting more cells (126) or immunosuppression (3, 127). Delivering satellite cells through means other than direct transplantation might avoid those challenges (3). For instance, Collins et al. showed that after implanting single myofibers into muscle, as few as seven satellite cells can regenerate more than 100 myofibers (3, 69). High levels of technical skill and expertise, however, are needed to implement such interventions (3). Another obstacle to the clinical use of satellite cells in therapy is that only a few satellite cells can be isolated from a biopsy (123). This means that the yield of satellite cells is low, especially when they come from already dystrophic muscle (123). Overall, satellite cells are difficult to isolate, expand or engraft (128).

Induced pluripotent stem cells (iPSCs) could be beneficial in the future treatment of muscle loss due to their capacity for self-renewal, ability to give rise to various cell types, and suitability for genetic editing (3). Other advantages of iPSCs are that their origins are easily accessible and can be established flexibly, regardless of the donor's age (3, 129). After *in vivo* transplantation, iPSCs can fuse with existing myofibers (3, 130). Mafioletti et al. showed that iPSCs can build functional skeletal muscle on a three-dimensional level *in vitro* (3, 131). Murine iPSCs differentiated efficiently into skeletal muscle *in vitro* as shown by Mizuno et al.(3, 132). The disadvantages of iPSCs, however, lie in the high costs of iPSC preparations from every patient and the extended time, more than three months, that is necessary to generate iPSCs (3, 129). Although rare, tumour formation following iPSC transplantation has been observed (3, 133). For clinical use, iPSCs require genetic correction to fix these errors (132).

Due to their regenerative capacity, hematopoietic stem cells (HSC) are an attractive avenue for muscle loss research (3). Gussoni et al. showed that, when injected intravenously, HSCs can restore the expression of dystrophin in dystrophic mice (mdx), contributing to myogenesis (3, 134). HSCs are an origin for both blood and muscle tissue as they increasingly integrate into myofibers after injury (3, 135). Still, their potential for clinical use is still controversial due to other findings (3). Goldman et al. showed that in treating volumetric muscle loss injuries, HSCs do not significantly alter the transcription of key myogenic factors or gains in muscle force (3, 136).

Mesenchymal stem cells (MSCs) also hold promise (3). MSCs can self-renew, exhibit a multi-lineage potential (3, 137) and can be accessed from various tissues, including adipose tissue or bone marrow (3). MSCs can differentiate into chondrocytes, adipocytes, and osteoblasts (3, 138). However, MSCs are challenging to acquire in the amounts necessary for successful transplantation (3, 139, 140).

Bone marrow-derived MSCs, when applied intramuscularly in rats, have proven to enhance muscle function in crush trauma models, as shown by Matziolis et al. (3, 141). They also contribute functionally to the phenotype of muscle cells and can reprogramme them (3, 142).

Muscle-derived MSCs have also been investigated to combat muscle wasting (3). They secrete numerous beneficial growth factors and anti-inflammatory cytokines and contribute to the regeneration and repair of muscle tissue (3, 137). Challenges in the clinical use of muscle-derived MSCs are the low engraftment efficiency and the limitations in functional improvements despite histological improvements, which were accomplished (128, 143, 144).

Fibro/adipogenic progenitor cells (FAPs) are another exciting area of research (3). In muscle tissue, FAPs are involved in the fat cell formation (3, 145). After damage, these otherwise quiescent cells proliferate and provide a source of signals, such as IL-6, beneficial for differentiating myogenic precursor cells (3, 146), though they do not fuse with existing myofibers (3, 146). Factors that modulate FAP activity need to be identified (3). Modulating the activity of FAPs to promote myogenic differentiation without fatty or fibrotic tissue might offer numerous benefits in the future treatment of muscle loss (3).

Furthermore, several other stem cell populations in the skeletal muscle could be of interest in the future treatment of muscle loss, such as the muscle side-population (SP) (3). SP cells are capable of self-renewal (3). Tanaka et al. showed that, when injected directly into the injured muscle, SP cells engrafted into the satellite cell niche successfully (3, 147). Doyle et al. found that ABGC2-expressing SP cells increased after injury, and mice lacking these cells had fewer satellite cells and decreased myofibers sizes (3, 148). Muscle SP cells' myogenic potential is under investigation (3).

Overall, stem-cell-based approaches to muscle regeneration currently prove problematic because of the difficulties in deliverability and cell expansion *in vitro* (3, 128). To implement stem-cell-based approaches to combat muscle loss in everyday clinical practice, the technical and financial obstacles and the regulatory difficulties must be overcome (3, 128).

The function and regeneration of skeletal muscle tissue is a complex process with numerous parties included. Cellular therapies will benefit from future studies into the mechanisms that coordinate muscle repair and improve skeletal muscle regeneration (3). As discussed in this chapter, several promising approaches already exist, but have substantial drawbacks and obstacles in clinical use. In the future, the solutions for the treatment of muscle loss might be found in tissue engineering, stem cell therapy or a combination of bioengineered scaffolds with stem cells (3). New genome editing technologies are promising in curing muscular dystrophies by inserting genetic alterations into the cells of mammals (61). Moreover, identifying bioactive factors involved in the growth and repair of skeletal muscle will help better understand the mechanisms, pathways, signalling cascades of biological factors which enable muscle regeneration (3, 105). Thus, therapeutic measures can be developed to improve the treatment of muscle loss, injuries or diseases (3, 105).

Taken together, current treatment options regarding muscle loss remain unsatisfactory due to the downsides of the abovementioned pathways (3). The medical care given to patients suffering from muscle loss needs to be improved, and finding new therapies could offer relief (3).

To improve options for future treatment, it is essential to also extend the knowledge of muscle development in embryogenesis. As complex as it is, this process usually has a successful outcome. Therefore, it provides an essential guide to be considered. PAX3 plays an important role in orchestrating early myogenesis (149). Analysing this gene and its possibilities more precisely could stimulate future research since regenerative medicine has not focused on PAX3 regarding muscle loss, hence my choice to focus on PAX3 in this study.

1.4 PAX3 and its role in myogenesis

The PAX3 protein belongs to the paired-homeobox family (150) and is a transcription factor with a highly-conserved paired box motif (151). The protein expression of PAX3 lasts throughout skeletal-muscle development (151). In embryonic myogenesis, PAX3 is described as a major regulator of the muscle progenitor cells (150, 151). Myogenic progenitor cells of the whole embryo express Pax3 (152). Hutcheson et al. showed that the loss or lack of Pax3 results in the failure of embryonic myogenesis (153). Pax3 expression is vital in forming limb muscles (153) and is necessary to ensure the proper formation of the ventrolateral dermomyotome (154-156). Borycki et al. found that a lack of Pax3 causes apoptosis of the cells in the dermomyotome (157). Furthermore, PAX3/Pax3 plays a crucial role in the survival and migration of the limb muscle precursor

cells (155, 156, 158). In the ventrolateral dermomyotome, PAX3/Pax3 regulates *Met* gene expression (156, 159). MET/Met is necessary for the limb muscle precursors to de-epithelialize from the dermomyotome and their following migration (156, 160). Thus, PAX3 regulates the liberation of the migrating muscle precursor cells by activating *MET* (156). Pax3 is expressed in these migrating muscle precursors (161-163).

In 1991, Epstein et al. discovered a naturally- occurring mutation in the *Pax3* allele in mice (164), which he named “splotch” (164). Homozygous splotch mutant mice die in the embryonic stage (164, 165). Several developmental defects were identified in splotch mutant mice, such as deficient closure of the neural tube, a lack of limb muscles due to the impaired migration of muscle precursors and defects concerning the neural crest (166-170).

PAX3 is first expressed at day 8,5 in the presomitic mesoderm (151). This is before the somite begins to segment and form (151, 161, 171, 172). During somite formation, the initial expression of PAX3/Pax3 all over the somite later restricts to the dermomyotome (151, 173). The epaxial and hypaxial regions of the dermomyotome become the focus of PAX3/Pax3 expression (151, 174, 175). As myogenesis starts in the somite, cells delaminate from the dermomyotome to build the myotome (174). Some of these cells migrate from the hypaxial dermomyotome, enabling muscle to form at different locations, such as the limbs (170, 174). These limb muscle precursor cells need Pax3 to delaminate and migrate, as was shown in *Pax3*$^{-/-}$Splotch mutant mice, which lack limb muscles (170, 172, 176). The expression of PAX3 downregulates after muscle precursor cells detach from the dermomyotome (151). At this point, Myf5 and Myod1 are activated (151, 174). Some cells expressing PAX3/Pax3 separate themselves from the dermomyotome and move to distant sites of myogenesis like the limbs, hypoglossal chord or diaphragm (151, 171, 172, 176-178).

Early myotome formation also depends on the expression of PAX3 (150). Myogenic progenitor cells expressing PAX3, delaminate from the lips of the dermomyotome and migrate in between the sclerotome and the dermomyotome, where they differentiate (150). The absence of PAX3 results in flawed myotome formation and is linked to errors in the localisation of structural proteins (150).

Limb muscles depend on the migration of skeletal muscle precursor cells to develop (156), and this step of myogenesis revolves around PAX3 activity (156). Loss-of-function mutations of *Pax3* in splotch mice showed that PAX3 is essential for myoblasts to migrate to the limbs (151, 179). PAX3/Pax3 is a crucial element in the signalling cascade mediating the delamination process in muscle progenitor cells and their subsequent migration to distant locations of myogenesis such as the limbs or paired appendages, where they

form muscle tissue (151, 180). Pax3 leads the migration process of muscle precursor cells in mice and birds (154, 155). In summary, PAX3/Pax3 plays an important role for the muscle progenitor cells as they delaminate from the dermomyotome and subsequently migrate to far-off locations of myogenesis such as limbs to form muscle tissue (151, 180).

PAX3 is not only essential for the migration of muscle precursor cells, but it is also involved in regulating cell proliferation (151). The interaction of PAX3 with PAX3/7BP (an adaptor that links *PAX3* and *PAX7* with the *H3K4* methyltransferase complex) induces muscle precursor proliferation (151, 181). Wang et al. showed that, in melanocytes, isoforms of PAX3 (PAX3c, PAX3e and PAX3g) control gene sets linked to cell differentiation and proliferation (182). Many target genes of PAX3, such as *FGFR4*, *HES1*, *MET*, *MITF* or *RET*, positively regulate the cell proliferation (151). Wang et al. found that PAX3 and its isoforms are essential for controlling the genes involved in cell proliferation and differentiation (151, 182).

Myogenesis is a complex process involving numerous factors, such as regulatory RNAs, transcriptional regulators or chromatin remodelling factors (183). This intricate genetic network, including Pax3 (183), controls myogenesis (183). Together with Pax7, Six1 and Six4, Pax3 is a master regulator of early muscle lineage specification *in vivo* (183, 184). These factors orchestrate different stages of myogenesis and induce the expression of other factors. For instance, MyoD acts downstream of Pax7 and Pax3 and Myf5 expresses simultaneously with Pax transcription factors (183, 185-187). Studies demonstrate that Pax3 acts upstream of myogenic regulatory factor genes (MRFs) (158, 188-190) such as *Myf5*, *Myf6*, and *Myod1* (191). Interestingly, the gene expression of *Pax3* downregulates before Myogenin is activated and myoblasts begin to differentiate into skeletal muscle fibres (192). Myogenin functions as a myoblast differentiation factor (193). In summary, Pax3 and Pax7 are essential for specifying early muscle lineage (183). Myf5 and MyoD are necessary to commit cells to the myogenic program (183). Therefore, PAX3 operates at very early stages of myogenesis and is downregulated later in the process.

In regenerative medicine, Birlea et al. reported that PAX3 had been analysed regarding the repigmentation in vitiligo via mobilisation of melanocyte stem cells due to its role in regulating melanocyte maturation (194). Pax3/PAX3 was also used in studies where mouse fibroblasts were reprogrammed into melanocytes (195, 196). However, PAX3 is yet to be a predominant factor in research regarding the muscle-related aspects of regenerative medicine. For this reason, I decided to focus on PAX3 in my thesis. Specifi-

cally, I want to demonstrate the potential myogenic changes in immortalised human mesenchymal stem cells (SCP1 cells) overexpressing PAX3. As explained in this chapter, PAX3 holds an important role as the initiator of the myogenic program in early myogenesis. That is why I chose PAX3 as the gene of interest in this study, after all, most muscles derive from $PAX3^{+}/PAX7^{+}$ progenitor cells which emerge from the somites (197).

2. Aim of the study

As mentioned in the introduction, there are many reasons for the loss of skeletal muscle tissue, and treatment options for affected patients are often unsatisfactory. Although regenerative medicine has approached the problem in various ways, using different factors and cell lines to overcome the obstacles in treating muscle loss, most of these methods have substantial drawbacks.

For instance, the activation of cAMP during specific treatments for musculoskeletal regeneration (105) can start other, potentially unintended or dangerous signalling cascades, which might be unwanted or even dangerous during certain treatments (105). Treatment with androgens can increase muscle mass (87), but is complicated by serious side effects such as cancer formation, masculinisation or prostate hypertrophy (87, 116). Although satellite cells may offer promising treatment options to combat muscle loss, satellite cells in culture have shown a reduced capacity for regeneration (3, 123) and poor cell survival rates, when compared to freshly isolated cells (3, 124, 125). Technical skill and experience are necessary to engraft satellite cells (3), as they are difficult to isolate and multiply (128). Treatment of muscle loss using induced pluripotent stem cells (iPSCs) is also problematic as iPSCs are expensive and time-consuming to prepare, taking at least three months to generate (3, 129). Moreover, tumour formation can also occur after iPSCs are transplanted (3, 133). Mesenchymal stem cells (MSCs) are difficult to acquire in numbers adequate for a successful transplantation (3, 139, 140). Fibro/adipogenic progenitor cells (FAPs) do not fuse with myofibers (3, 146), and additional factors modulating FAP activity must be identified to enable proper clinical use (3). The myogenic potential of muscle side-population cells might offer new treatments, and thus, their potential is currently investigated (3). In general, stem-cell-based approaches are challenging in everyday clinical practice because of the difficulties in deliverability and cell expansion *in vitro*, as well as technical and financial obstacles and regulatory difficulties (see 1.3) (3, 128).

PAX3 has not been used as a regenerative approach to muscle loss treatment yet. This transcription factor plays a crucial role in early myogenesis and could be a promising candidate for future research. I, therefore, chose PAX3 as the gene of interest in my study. My objectives are:

1. To generate PAX3-overexpressing cell populations

I believe that PAX3 is a suitable candidate to investigate. It has potential to induce a myogenic program in SCP1 cells, as PAX3 performs important functions in muscle development (149).

2. To characterise PAX3-overexpressing cell populations *in vitro*

After creating SCP1 cell populations which overexpress PAX3, I intend to analyse their characteristics *in vitro*. I will investigate their proliferation, clonogenic potential, morphology, random migration and fusion capacity of the newly created PAX3-overexpressing SCP1 cell lines.

3. To Identify the muscle-related molecular signatures of PAX3-overexpressing cell populations

I aim to do this by characterising the transcriptomic changes via next-gen RNA-sequencing analysis. It was already shown that the expression of Pax3 can start the myogenic program in embryonic stem cells of mice (191, 198) and in the P19 embryonal carcinoma cell line (191, 199). I expect to see shifts in the transcriptomes of PAX3-overexpressing SCP1 cells towards muscle tissue.

3. Materials & Methods

3.1 Chemicals

Table 1: Chemicals.

Chemical	Supplier
1,4-Dithiothreitol (DTT)	Sigma-Aldrich, USA
10 x Trypsin - EDTA-Solution (0,5%/ 0,2%) w/o Ca, w/o Mg	Sigma Aldrich, USA
Acetic acid	Merck, Germany
Ammoniac solution (30%)	Sigma-Aldrich, USA
Ampicillin	Thermo Fisher Scientific, USA
Aquadest	Thermo Fisher Scientific, USA
Beta (β)-Mercaptoethanol	Sigma-Aldrich, USA
Bovine serum albumin (BSA)	Ruth, Germany
Crystal violet (C.I. 42555)	Sigma-Aldrich, USA
DAPI	Sigma-Aldrich, USA
Dimethyl sulfoxide (DMSO)	Sigma Aldrich, USA
Dulbecco's Modified Eagle Medium (DMEM) (4,5g/l D-Glucose, Pyruvate)	Thermo Fisher Scientific, USA
Dulbecco's Phosphate Buffered Saline (D-PBS)	Sigma-Aldrich, USA
EDTA	Sigma-Aldrich, USA
Ethanol	Merck, Germany
Fluoroshield™	Sigma-Aldrich, USA
Foetal bovine serum (FBS)	Sigma-Aldrich, USA
Formaldehyde	Merck, Germany
Heat-inactivated horse serum (HS)	Life Technologies, USA
Laemmli buffer	Merck, Germany
LB (lysogeny broth) medium	Merck, Germany
Methanol	Merck, Germany
Mouse anti-β-actin-HRP #sc-47778	Santa Cruz Biotechnology, USA
NaCl	Merck, Germany
Nucleofector solution	Lonza, Switzerland

Opti-MEM	Thermo Fisher Scientific, USA
Paraformaldehyde	Sigma-Aldrich, USA
Penicillin-Streptomycin-Solution	PAA, Austria
Pierce ECL Western Blotting Substrate	Thermo Fisher Scientific, USA
Primary antibody against the myosin heavy chain 1E (MYH1E, clone MF20)	Developmental Studies Hybridoma Bank, USA
Primary antibody Pax3 AB_528426	Developmental Studies Hybridoma Bank, USA
Puromycin	Thermo Fisher Scientific, USA
rCutSmart buffer	NEB, USA
Secondary antibody anti-mouse-HRP 7076S	Cell Signaling Technology, USA
Secondary antibody Donkey Anti-Mouse (Alexa Flour 647)	Abcam, UK
Skimmed milk powder	Sigma-Aldrich, USA
Tris	Sigma-Aldrich, USA
Triton X-100	Sigma-Aldrich, USA
Trizol Reagent	Thermo Fisher Scientific, USA
Tween 20	Sigma-Aldrich, USA
Type I Collagen	Sigma Aldrich, USA

3.2 Kits

Table 2: Kits.

Kits	**Supplier**
Amaxa™ Cell Line Nucleofactor™ Kit V	Lonza, Switzerland
Prime Time Gene Expression Master Mix (IDT 1055772)	LubioScience GmbH, Switzerland
Promega PureYield^{TM} Plasmid Miniprep System (#A1223)	Promega, Switzerland
RNeasy Micro Kit	Qiagen, Germany
SENSE mRNA-Seq Library Prep Kit V2	Lexogen, Austria
SYBR green	Roche, Switzerland

Transcriptor First Strand cDNA Synthesis Kit	Roche, Switzerland

3.3 Devices

Table 3: Devices.

Device	Supplier
4D-Nucleofector™ Core Unit	Lonza, Switzerland
Centrifuge 5415 D	Eppendorf, Germany
FACS AriaFusion™ machine	BD Biosciences, USA
Fluorescence microscope Axio Observer Z1	Zeiss, Germany
HiSeq1500 device	Illumina, USA
Incubator (cell culture)	Thermo Fisher Scientific, USA
Incubator XL 100/135	Pecon, Germany
LightCycler 96 Instrument	Roche, Switzerland
Neubauer counting chamber	Brand, Germany
pH meter	WTW, Germany
Spectrophotometer	Thermo Fisher Scientific, USA
Steam sterilizer	H+P Labortechnik, Germany
Thermocycler	VWR, USA
Time lapse microscope Axiovert S100	Zeiss, Germany
Trans-Blot SD semi-dry Transfer Cell	Bio-Rad Laboratories Inc., USA
Transmitted light microscope Leica M165 FC	Leica, Germany
Water bath	GFL, Germany
Western Blot developer	Vilber Lourmat, France

3.4 Software

Table 4: Software.

Software	Use of Software
Adobe Illustrator CS6 (Version 16.0)	For editing images

Adobe Photoshop CS6 (Version 13.0)	For editing images
AxioVision, Version 4.8.1, Zeiss, Germany	For time lapse microscopy
DESeq2 (version 1.28.1)	For analysing differential gene expression
FlowJo 10.1-Software (FlowJo LLC, Oregon, USA).	For processing FACS samples
Graphpad Prism 5, Version 5.02, Graphpad Software Inc., USA	For evaluations, statistics
ImageJ (Version 2.0, NIH, USA)	For editing and evaluating images (cell morphology, cell migration, cell fusion etc.)
Microsoft Excel Version 14.0.7190.5000 (32bit), Microsoft Corporation, USA	For analysing data
Microsoft Office Professional Plus 2010;	For general use
Microsoft Word Version 14.0.7190.5000 (32bit), Microsoft Corporation, USA;	For writing
R software (Version 4.0.3)	For statistical computing and graphs
STAR (version 2.7.2b)	For aligning reads to the human genome
ZEN lite 2012 (blue edition), Version 1.1.2.0, Zeiss, Germany	For taking and editing pictures

3.5 Plasmids

Table 5: Plasmids.

Plasmid	**Supplier**
MGC Human *PAX3* Sequence-Verified cDNA, #40024658	Horizon Discovery, UK
SB transposon plasmid pSBbi-GP vector #60511	Addgene, USA
SB transposon plasmid pSBbi-RP vector; #60513	Addgene, USA
Transposase plasmid pCMV(CAT)T7-SB100, #34879	Addgene, USA

3.6 Enzymes

Table 6: Enzymes.

Enzyme	Supplier
Antarctic Phosphatase Antarctic #M0289	NEB, USA
BamHI	NEB, USA
EcoRI-HF	NEB, USA
T4 DNA ligase	Sigma-Aldrich, USA

3.7 Media

Media for cultivating SCP1 and C2C12 cells

10% FBS

1% penicillin/streptomycin

In DMEM high glucose

Media for freezing cells

10% DMSO

10% FBS

80% DMEM high glucose

Media for differentiation of cells

2% horse serum

1% penicillin/streptomycin

In DMEM high glucose

3.8 Cell culture materials

Table 7: Cell culture materials.

Cell culture material	Supplier
24-well plates	Greiner Bio One, Germany
25 cm^2,175 cm^2,225 cm^2 flasks	Nunc, Germany
6-well plates	Nunc, Germany
Eppendorf reaction vessel	Thermo Fisher Scientific, USA

3.9 Fluorescence-activated cell sorting

To obtain homogeneous cell populations which express GFP in different intensities, fluorescence-activated cell sorting (FACS) (FACSAriaFusion™, BD Biosciences, USA) was executed as SCP1^{GFP} cells were sorted into SCP1$^{GFP}_{high}$ cells (which were used as a control group in future assays) and SCP1$^{GFP}_{low}$ cells. SCP1^{PAX3} cells were sorted according to different GFP intensities into SCP1$^{PAX3}_{high}$ and SCP1$^{PAX3}_{low}$ cells. At this stage, I assumed that expression levels of GFP and PAX3 correlated.

To perform flow cytometry and cell sorting, the cells were resuspended using Trypsin, diluted in FACS buffer (100 ml PBS, 400 µl EDTA, 1 g BSA) and diluted to a concentration of 1-5 * 10^6/ml. The cells were filtered through a 30 µm filter (Sysmex, Japan) to break up cell clusters.

Using the cell sorter FACSAriaFusion™ (BD Biosciences, USA), the cells were sorted into populations exhibiting varying GFP intensities according to cell debris and cell cluster exclusion (side scatter (SSC) vs forward scatter (FSC)). Samples were analysed with FlowJo 10.1-Software (FlowJo LLC, Oregon, USA).

3.10 Cell populations

3.10.1 SCP1 cells

SCP1 (Single cell picked clone 1) is an immortalised human mesenchymal stem cell line based on human bone marrow-derived mesenchymal stem cells which stably expresses the gene *hTERT (human Telomerase Reverse Transcriptase)* upon retroviral transduction (200). Thereby, the ageing process is prevented (200).

The SCP1 cell line (200) was used as a basis for creating SCP1 cell populations used in my experiments: SCP1^{GFP}, SCP1$^{PAX3}_{low}$ and SCP1$^{PAX3}_{high}$ cells.

3.10.2 SCP1^{GFP} cell population

The coding sequence for the green fluorescent protein (*GFP*) was stably inserted into native SCP1 cells to create SCP1^{GFP} cells.

For this, 0.4 µl of SB plasmid (pSBbi-GP, #60511, Addgene, USA), 0.9 µg transposase (pCMV(CAT)T7-SB100, #34879, Addgene, USA) (201) and 20 µl of nucleofector solution (Amaxa™ Cell Line Nucleofactor™ Kit V, Lonza, Switzerland) were mixed with 500,000 SCP1 cells and electroporated in the 4D-Nucleofector™ Core Unit (program FF 104, Lonza, Switzerland) for 2 sec. Then, the cells were seeded onto 6-well plates. After 3

days, they were selected with 1 µg/ml Puromycin. After 10 days, the cells were sorted into SCP1$^{GFP}{}_{high}$ and SCP1$^{GFP}{}_{low}$ cells by FACS. SCP1$^{GFP}{}_{high}$ cells served as a control group (called SCP1^{GFP} cells) with which to compare the PAX3-overexpressing cells.

3.10.3 Generation of PAX3-positive SCP1 cell populations

For cloning the plasmid containing the coding sequence of *PAX3* and green fluorescent protein (*GFP*) as a reporter gene, a restriction digest of *PAX3* purchased as cDNA (MGC Human *PAX3* Sequence-Verified cDNA, #40024658, Horizon Discovery, UK) and the pSBbi-GP vector (#60511, Addgene, USA; see Figure 3.1) including a multiple cloning site (MCS) using EcoRI was performed as follows.

Table 8: Reaction mixture for restriction digest.

Insert (*PAX3* cDNA) or Vector (pSBbi-GP)	3 µg
10x rCutSmart buffer	5 µl
10x BSA	5 µl
EcoRI-HF	1 µl (20U)
ddH_2O	ad 50 µl

For vector dephosphorylation, 1 µl of Antarctic Phosphatase (#M0289, NEB, USA) was added to the digestion mix. The reaction was incubated at 37°C for 1h. A small volume of the reaction mix was analysed on an agarose gel to confirm vector linearisation.

As the next step, the ligation mix containing the components below was incubated at room temperature overnight.

Table 9: Reaction mixture for ligation.

Insert (*PAX3* cDNA)	300 ng
Vector (pSBbi-GP)	100 ng
10x T4 DNA ligase buffer	2 µl
T4 DNA ligase	1 µl (5U)
dH_2O	ad 20 µl

After the reaction, the ligase was inactivated for 10 min at 65°C.

For transformation into competent E. coli (DH5α, #C2987, NEB, USA), bacteria were thawed on ice for 20 min. 3 µl of ligation mix were added to 30 µl of bacteria and incubated on ice for 20 min. Following heat shock at 42°C for 45 sec and incubation on ice for 2 min, the bacteria were left to recover in LB medium for 45 min at 37°C while shaking. Bacteria were plated on LB agar plates containing Ampicillin and incubated at 37°C overnight.

The next day, single colonies were picked and inoculated in LB medium and Ampicillin overnight at 250 rpm at 37°C. The next day, plasmid isolation was performed using the Promega PureYield™ Plasmid Miniprep System (#A1223, Promega, Switzerland) according to the manufacturer's instructions. Correct *PAX3* integration into the plasmid (see Figure 3.2) was confirmed by a qualitative restriction digest using EcoRI and BamHI.

For the generation of PAX3-positive cells, the Sleeping Beauty Transposon system was employed following nucleofection. For this, 250,000 SCP1 cells were incubated with 0.4 µl of pSBbi-GP-PAX3 plasmid (see Figure 3.2) and 0.9 µl transposase plasmid (pCMV(CAT)T7-SB100, #34879, Addgene, USA) and electroporated in the 4D-Nucleofector™ Core Unit (program FF 104, Lonza, Switzerland) for 2 sec using the Amaxa™ Cell Line Nucleofactor™ Kit V (Lonza, Switzerland). Cells recovered in DMEM complete for 3 days, after which selection with 1 µg/ml Puromycin was started.

After two weeks of cultivation, two populations exhibiting different GFP intensities became apparent. They were sorted on a FACS AriaFusion™ machine (BD Biosciences, USA) into SCP1$^{PAX3}_{high}$ cells and SCP1$^{PAX3}_{low}$ cells (see 3.9), assuming that the different GFP intensities correlate with the expression levels of PAX3.

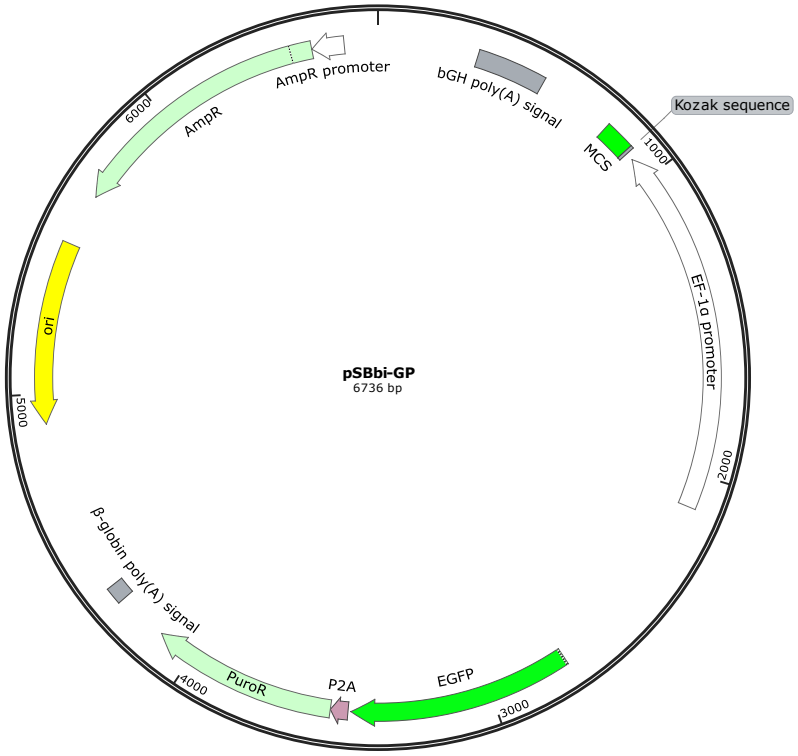

Figure 3.1: Sleeping Beauty vector pSBbi-GFP.

Original SB vector which was integrated into native SCP1 cells to create green fluorescent SCP1 cells (SCP1^{GFP}), the control group. Further, the gene of interest PAX3 was cloned into this plasmid to create SCP1$^{PAX3}{}_{high}$ and SCP1$^{PAX3}{}_{low}$ cells.

Ori = origin of replication
AmpR = Ampicillin resistance (for use in bacteria)
PuroR = Puromycin resistance (for use in eucaryotic cells)
MCS = multiple cloning site; contains restriction sites to enable insertion of DNA in this region
Kozak sequence = translation initiation enhancer
EGFP = enhanced green fluorescent protein

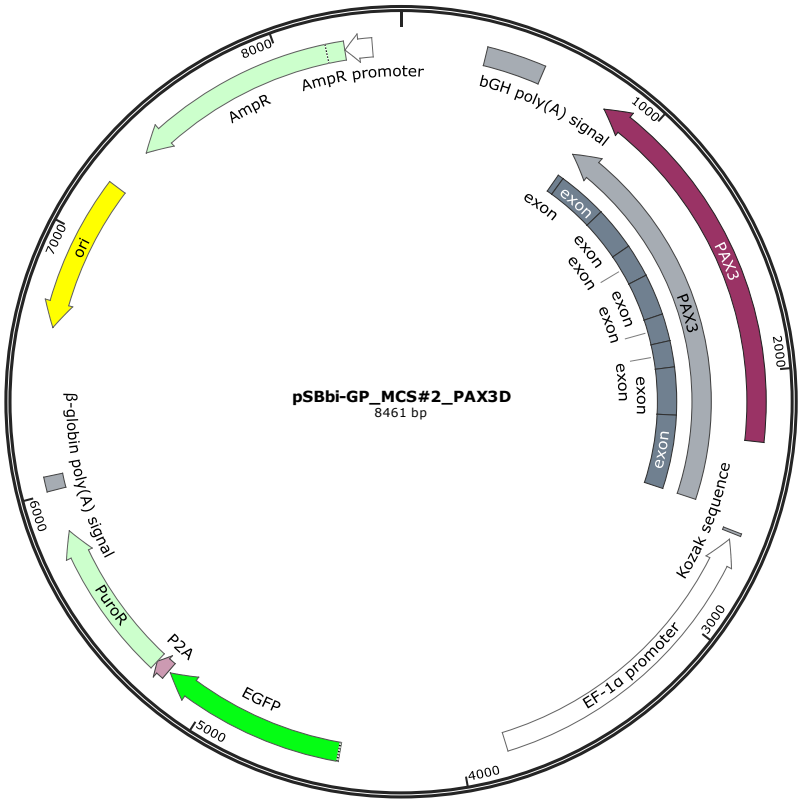

Figure 3.2: Sleeping Beauty vector containing *GFP* and *PAX3*.

This newly ligated vector combines the initial SB plasmid pSBbi-GFP with the inserted gene of interest *PAX3*. This vector was used to create SCP1$^{PAX3}_{high}$ and SCP1$^{PAX3}_{low}$ cells.

Ori = origin of replication
AmpR = Ampicillin resistance (for use in bacteria)
PuroR = Puromycin resistance (for use in eucaryotic cells)
MCS = multiple cloning site; contains restriction sites to enable insertion of DNA in this region
Kozak sequence = translation initiation enhancer
EGFP = enhanced green fluorescent protein

3.10.4 C2C12 cells

The coding sequence for *RFP* (red fluorescent protein) was stably inserted into C2C12 (CRL-1772™, ATCC, USA) cells to generate RFP-positive myogenic cells. Using the 4D-Nucleofector™ Core Unit for nucleofection, 500,000 native C2C12 cells were mixed with 0,4 µl SB transposon plasmid (pSBbi-RP; #60513, Addgene, USA), 0,9 µg transposase (pCMV(CAT)T7-SB100, #34879, Addgene, USA) and 20 µl of nucleofector solution (Amaxa™ Cell Line Nucleofactor™ Kit V, Lonza, Switzerland) (202). The cells were seeded in 6-well plates and selection was performed with 2 µg/ml puromycin for 10 days (202). These cells were FACS sorted and the red fluorescent C2C12$^{RFP}_{high}$ cells (called C2C12) were used as a myogenic cell population for comparison with SCP1 cells in my study.

3.11 Cell culture

3.11.1 Thawing cells

After the cells were removed from the nitrogen tank, they were put on dry ice. They were thawed in the water bath at 37°C. During this process the lid was opened at times to prevent overpressure. After they thawed completely, 1 ml of cell suspension was mixed with 4 ml DMEM and centrifuged for 5 min at 500 g to eliminate DMSO. The supernatant was discarded, and fresh media was added onto the cells. SCP1 and C2C12 cells were put into T175 flasks filled with 25 ml DMEM and cultivated at 37°C with 5% CO_2 in the incubator (Thermo Fisher Scientific, USA).

3.11.2 Cultivation of cells

Both SCP1 and C2C12 cells were cultivated in DMEM with 10% FBS and 1% penicillin/streptomycin. The media was changed twice a week. When cells were too confluent, they were passaged.

3.11.3 Passaging of cells

The cells were passaged when cell density was too high. For this purpose, the media was removed, and the cells were washed with D-PBS. 1x Trypsin, which was added on the cells for 5 min at 37°C, detached the cells from the bottom of the flask. The reaction was stopped by pipetting double the amount of DMEM onto the cells. The Trypsin, media and cells mixture was centrifuged for 5 min at 5 g. The supernatant was sucked, and the

cell pellet was dissolved in culture media. Lastly, the cells were put in flasks to be cultivated or frozen.

3.11.4 Counting cells

A Neubauer counting chamber was used to count the cells. Four quadrants were counted, and the total cell number was calculated with this formula:

$$cell\ number\ per\ ml = \frac{\text{total cell number of all four quadrants}}{4} \times 10^4$$

3.11.5 Freezing cells

Cells were counted and passaged. The abovementioned formula (see 3.11.4) was used to calculate the necessary amount of cell suspension to get 1 million cells in 1 ml per cryo vial. The vials were stored on dry ice before putting them into the nitrogen tank.

3.12 Validation of PAX3-overexpression in SCP1 cells

3.12.1 RNA isolation and cDNA synthesis

RNA was isolated using the RNeasy Micro Kit (Qiagen, Germany). For cDNA synthesis, 300 ng RNA was used in the Transcriptor First Strand cDNA Synthesis kit (Roche, Switzerland). The PCR program described in the manufacturer's instructions was run on a peqSTAR 2x thermocycler (VWR, USA).

3.12.2 Quantitative real-time PCR

cDNA was diluted in ddH_2O (1:5). Forward and reverse primers (primer 1: AGCTTGCTTCCTCCATCTTG; primer 2: GAGAGAACTCATTACCCTGACAT) were mixed and diluted in ddH_2O to a final concentration of 10 µM. For each reaction, 4.8 µl of SYBR green (Roche, Switzerland) was mixed with 0.2 µl of the primer mix and 5 µl of diluted cDNA.

The quantitative real-time PCR (RT-PCR) was performed using Prime Time Gene Expression Master Mix (IDT #1055772) in a LightCycler 96 Instrument (45 cycles, 2-step amplification, per step 95°C for 180 sec) (Roche, Switzerland).

3.12.3 Western Blot

Proteins were harvested by trypsinization and kept on ice until Laemmli buffer was added. Lysates were incubated at 95°C for 5 min to denature proteins. Protein concentrations were measured using the Pierce BCA assay kit (Thermo Fisher Scientific, USA) according to manufacturer's instructions. Proteins were separated based on their molecular weight by Sodium dodecyl sulfate polyacrylamide gel electrophoresis (SDS-PAGE). 20 µg protein in 2x Laemmli buffer + 10 mM DTT were run on 10% SDS gels immersed in SDS running buffer at 50 mA for 1 h.

Subsequently, proteins were transferred from gels to nitrocellulose membranes, sandwiched between Whatman papers, using the Trans-Blot SD semi-dry Transfer Cell (Bio-Rad Laboratories Inc., USA) for 1 h at 60 mA per gel. The membranes were blocked in 5% milk TBS + 0.05% Tween (TBST) for 1 h at room temperature.

Primary antibodies were added overnight at 4°C in 5% BSA TBST at the following dilutions.

Table 10: Primary antibodies and dilutions for Western Blot.

Antibody	Product information	Dilution
Mouse anti-β-actin-HRP	#sc-47778, Santa Cruz, USA	1:1000
Chicken anti-GFP	#ab13790, Abcam, UK	1:1000
Mouse anti-Pax3	# AB_528426, DSHB, USA	1:100

The next day, the membranes for PAX3 and GFP detection were incubated with respective secondary antibodies in 5% BSA TBST for 90 min. This step was flanked by extensive washing steps with PBST (3x10 min, each).

Table 11: Secondary antibodies and dilutions for Western Blot.

Target	Product information	Dilution
anti-chicken-HRP	#A16054, Invitrogen, USA	1:2500
Anti-mouse-HRP	#7076S, Cell Signaling, USA	1:2500

The signal was visualised by applying Pierce ECL Western blotting Substrate (Thermo Fisher Scientific, USA) onto the membranes and imaged on a Western Blot developer (Vilber Lourmat, France). ImageJ was used to quantify band intensities.

3.12.4 Next-Generation RNA-Sequencing and Bioinformatic Analysis

Total RNA from 12 SCP1 samples (4 SCP1^{GFP} cells, 4 SCP1$^{PAX3}{}_{low}$ cells and 4 SCP1$^{PAX3}{}_{high}$ cells) were isolated by Trizol Reagent. RNA-seq libraries were generated using the SENSE mRNA-Seq Library Prep Kit V2 (Lexogen, Austria) according to the manufacturer's protocol. Sequencing was performed on a HiSeq1500 device (Illumina, USA) with a read length of 50 bp and a sequencing depth of approximately 18 million reads per sample.

FASTQ files were demultiplexed by the barcodes used for the generation of each library. Reads were aligned to the human genome (release GRCh38.101) using STAR (version 2.7.2b). Low gene counts were filtered out by minimum 10 reads per gene, and 20,533 genes remained for further analysis. Normalisation was performed through variance stabilising transformation (vst) for Principal Component Analysis (PCA). Differential gene expression was analysed by DESeq2 (version 1.28.1) in R software (version 4.0.3) with an adjusted p-value (p-adj) cut off of < 0.05 and a Log2FoldChange of ±1 cut off for each cell population: SCP1^{GFP}, SCP1$^{PAX3}{}_{low}$ and SCP1$^{PAX3}{}_{high}$ cells. Only protein-expressing genes were included in further analysation.

3.13 Setup of experiments

3.13.1 Cell Proliferation Assay

To evaluate and compare growth rates of SCP1 cell populations, cumulative population doublings (cumPD) and population doubling time (PDT) were determined. Therefore, cells were quantified over a period of 28 days.

50,000 cells of each population (SCP1^{GFP}, SCP1$^{PAX3}{}_{low}$ or SCP1$^{PAX3}{}_{high}$) were seeded into three T25 cell culture flasks per cell population. Over the course of 4 weeks, cells were trypsinated and counted twice a week (on days 4, 7, 11, 14, 18, 21, 25 and 28 after seeding). After counting, 50,000 cells of each kind were seeded back into T25 flasks again. PD was calculated using the following formula:

$$PD = \frac{\log \frac{N_n}{N_0}}{\log 2}$$

N_n = cell number at trypsination

N_0 = number of initially seeded cells (=50 000)

Population doubling time (PDT) is defined as the time a cell population needs to double itself. To determine PDT, the following formula was used:

$$PDT = \frac{time\ priod\ (day)}{PD}$$

CumPD is made up of the sum of the single PDT values. It demonstrates how often the population of each reviewed cell type doubled in 28 days *in vitro*.

$$\mathrm{cumPD} = \Sigma \mathrm{PD}(1, \mathrm{d})$$

d = day 4, 7, 11, 14, 18, 21, 25 and 28 after seeding

3.13.2 Colony Forming Unit Assay (CFU)

To analyse the clonogenic potential of SCP1 cell populations, 700 cells (SCP1^{GFP}, SCP1$^{PAX3_{low}}$ or SCP1$^{PAX3_{high}}$) in 7 ml DMEM were seeded into 10 cm^2 Petri dishes. Media (DMEM) was changed once after 7 days. CFU assay was reproduced 4 times in triplicates.

After cultivating cells for 14 days, they were fixated and stained with 0.5% crystal violet in methanol and the visible, intensely stained colonies with a range from clusters of 25 cells upwards were counted using a transmitted light microscope Leica M165 FC (10x magnification). CFU efficiency was calculated using the following formula:

$$CFU\ efficiency\ = \frac{N_n}{N_0} \times 100$$

N_n= number of counted colonies

N_0= number of plated cells

Crystal Violet Staining was used to analyse the Colony Forming Unit Assay. The cells were stained with 3 ml of 0.5% crystal violet in methanol in 10 cm dishes after being washed with PBS twice. Afterwards, they were incubated at room temperature for 10 min under mild shaking. Crystal violet was removed, and the plates were rinsed with PBS. The dishes were left to dry at room temperature.

3.13.3 Fusion Assay

Two combinations of cell populations were used in direct co-cultures to evaluate cell fusion. Each cell population (SCP1^{GFP}, SCP1$^{PAX3}{}_{low}$, SCP1$^{PAX3}{}_{high}$ or C2C12 cells) isolated or a mixture of C2C12 cells combined with each SCP1 cell population (SCP1^{GFP}, SCP1$^{PAX3}{}_{low}$ or SCP1$^{PAX3}{}_{high}$ cells) was analysed. Therefore, a 24-well plate was filled with 100,000 cells in 1 ml DMEM per well. Different ratios were chosen (C2C12 cells are first, second ratio is the other cell line: SCP1^{GFP}, SCP1$^{PAX3}{}_{low}$ or SCP1$^{PAX3}{}_{high}$) 2:1, 1:1 and 1:2. 5 h after seeding, media was changed to DMEM with 2% HS and 1% penicillin/streptomycin to support the differentiation and fusion process of the cells. After days 3, 5 and 7, the cells were fixated in 4% PFA for 15 min and stained according to antibody staining/immunocytochemistry protocols (see 3.13.4). Images were taken with a 10x objective at Fluorescence microscope Axio Observer Z1 (Zeiss, Germany) (10x magnification). The relative fused myofiber area was quantified using ImageJ (NIH, USA). Fusion assay was reproduced 4 times independently.

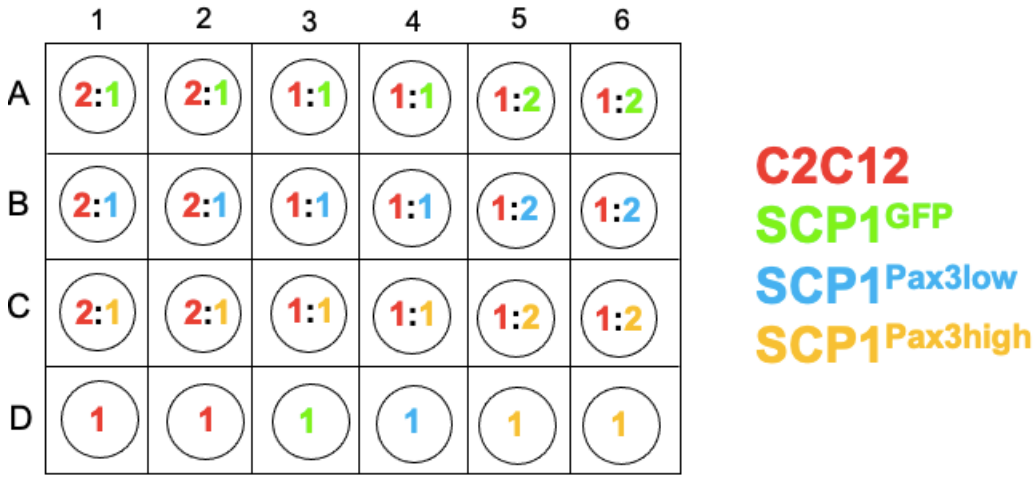

Figure 3.3: Experimental setup for cell fusion assay.

A 24-well plate is represented here. Cells were mixed in different ratios (1:0/ 0:1, 1:1, 1:2, 2:1; C2C12 is always referred to as the first number of the ratios) to analyse relative fused myofiber area.

3.13.4 Antibody Staining/ Immunocytochemistry

To evaluate the relative fused myofiber area in the cell fusion assay, cells in the 24-well plate were fixated and stained. First, they were washed with PBS and fixated in 4% paraformaldehyde for 15 min. Then, they were washed with PBS once more before adding blocking solution (PBS+0.1% Triton+10% HS) for 1 h at room temperature. Next, the solution was discarded and the primary antibody against the myosin heavy chain 1E (MYH1E, clone MF20, acquired from the Developmental Studies Hybridoma Bank developed under the auspices of the NICHD and maintained by The University of Iowa,

Department of Biological Sciences, Iowa City, IA, USA 52242; MF 20 was deposited to the DSHB by Fischman, D.A. (DSHB Hybridoma Product MF 20)) was used. The antibody was diluted in blocking solution at 1:100 and added to the cells overnight at 4°C. The following day, cells were washed with PBS+0,1%Triton 3 times for 5 min each before the secondary antibody Donkey Anti-Mouse (Alexa Flour 647, abcam, UK) diluted in blocking solution 1:1000 was added. The samples were protected from light and gently shaken for at least 1 h at room temperature. Once more, they were washed with PBS twice and then stained with 200 µl DAPI (4',6-diamidino-2-phenylindole) per well for 30 sec. Afterwards, they were washed with PBS and a Covership (Sigma Aldrich, USA) was put onto each well after putting one drop of Fluoroshield (Sigma Aldrich, USA) on it.

3.13.5 Evaluation of Cell Morphology

For evaluating morphological changes in the cell populations, this study focuses on the cell area and aspect ratio (AR; cells' ratio of width to height). The cells with an area of $< 1.5x10^4$ µm^2 or aspect ratio of < 7 were included in further analysis, leaving a total of 734 SCP1^{GFP} cells, 756 SCP1$^{PAX3}{}_{low}$ cells, 749 SCP1$^{PAX3}{}_{high}$ cells and 451 C2C12 cells to evaluate.

SCP1 cell populations

19 h after trypsinisation, phase contrast images were taken of each SCP1 cell population (SCP1$^{PAX3}{}_{high}$ cells, SCP1$^{PAX3}{}_{low}$ cells or SCP1^{GFP} cells) to analyse cell morphology. 3 pictures were taken per flask and a minimum of 100 cells per passage were analysed using Image J concerning cell area and aspect ratio (AR). 7 passages and a minimum of 700 SCP1 cells were analysed using ImageJ (NIH, USA) for each cell population.

C2C12 cells

C2C12 cells were imaged 19 h after seeding on a 24-well plate. These plates were the preparation for the fusion assays. 3 pictures were taken per well in 3 different wells. C2C12 cells were evaluated like SCP1 cells concerning cell area and aspect ratio using ImageJ (NIH, USA).

3.13.6 Random Migration of Cells

A 6-well plate was coated with 1 ml of rat tail type I collagen (type I collagen; Sigma Aldrich; USA) (10 µg/ml) diluted in Opti-MEM media. It was put into the fridge at 4°C overnight. The next day, type I collagen was aspirated and 10,000 cells (SCP1$^{PAX3}{}_{high}$ cells, SCP1$^{PAX3}{}_{low}$ cells or SCP1^{GFP} cells) in 2 ml DMEM were added to each well. As a control group, 10,000 cells in 2 ml DMEM were seeded on uncoated 6-well plates. Time

lapse microscopy was started the day after seeding to examine the random migration of SCP1 cell populations for 72 h. 3 pictures were taken per well in 20 min intervals using a 10x objective (time lapse microscope Axiovert S100; Zeiss, Germany) at room temperature. On average, 40-50 cells were tracked per experiment. The migration of the cells was evaluated using ImageJ (NIH, USA). The random migration assay was reproduced 4 times independently. Relevant aspects were the cells' mean velocity and maximum velocity both surfaces (type I collagen-coated and non-coated).

3.14 Statistical analysis

The data was assessed for statistical significance in R (version 4.0.3). Results were standardly displayed in box-and-whisker plots. Boxes represent the interquartile range, and the median is marked by a line inside the box. The variability of the data outside the interquartile range is displayed by the whiskers. Cell culture experiments were conducted at least 3 times each in triplicates. Significance was determined via a p-value of 0.05 or lower. The Gaussian distribution was checked using the Shapiro-Wilk Normality test. The Wilcoxon test was used for variables or measurements that were not normally distributed. In figures, n and w were added for further description meaning n = number of independent experiments and w = number of cell culture dishes used per experiment (well plates, cell culture dishes, cell culture flasks).

4. Results

4.1 Characterisation of SCP1 cell populations

4.1.1 Sorting of SCP1 cells according to GFP intensities via FACS

The SCP1 cell populations were sorted into groups of high and low GFP intensities via fluorescence-activated cell sorting (FACS). SCP1$^{GFP}{}_{high}$ cells were used as the control group in future assays under the name of SCP1^{GFP} cells.

SCP1^{PAX3} cells containing *GFP* and *PAX3* on the same plasmid were also sorted for high and low GFP fluorescence intensity by FACS. These cells were divided into SCP1$^{PAX3}{}_{low}$ cells (with lower GFP expression levels) and SCP1$^{PAX3}{}_{high}$ cells (with higher GFP expression levels). At this point, I assumed that GFP intensity levels correlated with GFP expression levels and with expression levels of PAX3.

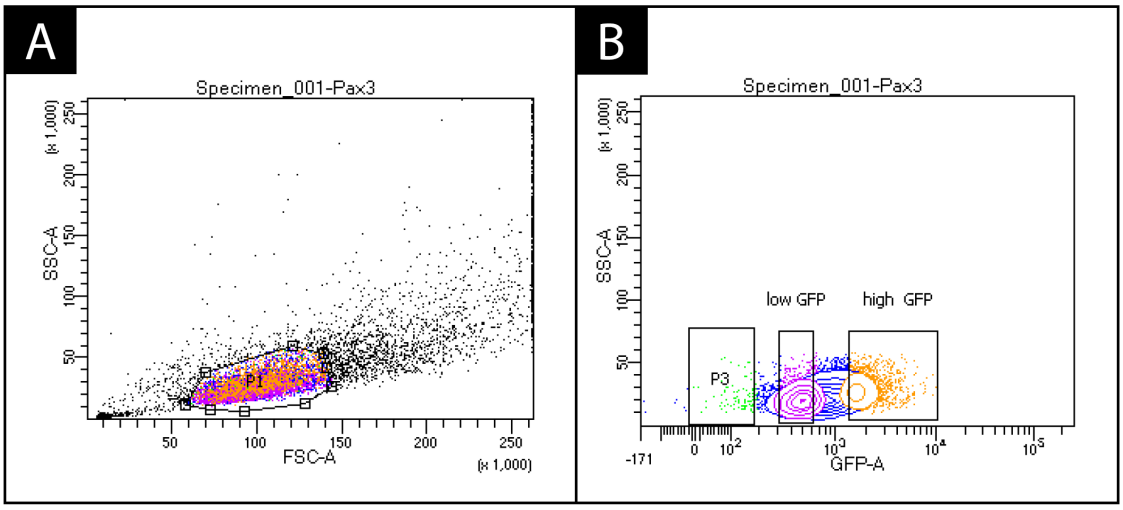

Figure 4.1: FACS of SCP1^{PAX3} cells by GFP fluorescence intensities.

A) SCP1^{PAX3} cells: Depiction of the total population of PAX3-overexpressing SCP1 cells (P1) before sorting. The P1 population excluded cell debris and cell clusters and was identified by SSC-A (y-axis) describing the granularity of cells and FSC-A (x-axis), describing the cell size.

B) SCP1^{PAX3} cells: Gate P3 depicts non-GFP expressing SCP1 cells. Gate low GFP shows low GFP intensity SCP1 cells namely SCP1$^{PAX3}{}_{low}$ (assumed correlation of low GFP intensity and low PAX3 expression). Gate high GFP depicts high GFP intensity SCP1 cells: SCP1$^{PAX3}{}_{high}$ (assumed correlation of high GFP intensity and high PAX3 expression).

4.1.2 SCP1$^{PAX3}_{high}$ cells show a significant higher *PAX3* expression, when compared to native SCP1 cells

Quantitative real-time PCR (RT-PCR) was performed to validate the overexpression of *PAX3* on RNA levels. There was no significant difference in the levels of *PAX3* expression between SCP1$^{PAX3}_{high}$ and SCP1$^{PAX3}_{low}$ cells (p = 0.180). The same applies to SCP1^{GFP} and SCP1$^{PAX3}_{low}$ cells (p = 0.180). However, on RNA levels via RT-PCR, a significant difference in the *PAX3* levels of SCP1$^{PAX3}_{high}$ cells compared to SCP1^{GFP} cells (p = 0.007) was confirmed.

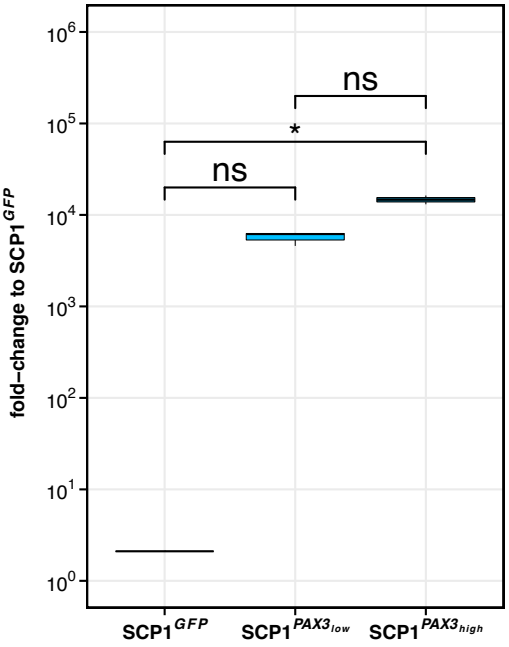

Figure 4.2: SCP1$^{PAX3}_{high}$ cells show a significant higher *PAX3* expression, when compared to native SCP1.

Positive fold change shows that *PAX3* was overexpressed in both cell populations, when compared to native SCP1^{GFP} cells. A significant difference was found in the levels of *PAX3* expression comparing SCP1$^{PAX3}_{high}$ and SCP1^{GFP} cells on RNA levels (p = 0.007).

Significance levels*: p ≤ 0.05, ns: not significant. Statistical method: Wilcoxon test; n = 3

4.1.3 PAX3 is expressed in SCP1^{PAX3} cell populations, but GFP and PAX3 levels are unaltered between SCP1$^{PAX3}{}_{high}$ and SCP1$^{PAX3}{}_{low}$ cells

GFP protein expression was assessed in different SCP1 cell populations (SCP1$^{PAX3}{}_{low}$ cells and SCP1$^{PAX3}{}_{high}$ cells) through Western blotting (Figure 4.3). SCP1^{GFP} cells containing pSBbi-GP plasmid were used as a control group for GFP presence.

All three cell populations depicted bands of the same intensity around 40 kDa for the "housekeeping" protein beta-actin. This confirms that a similar amount of total protein was loaded per sample.

Surprisingly, the GFP blot depicts two bands, one slightly above 25 kDa and one slightly below 25 kDa. Since the expected molecular weight of eGFP is 26.9 kDa, I cannot conclusively determine which band belongs to eGFP. The lower band in question is decreased in intensity in SCP1$^{PAX3}{}_{low}$ cells compared to SCP1^{GFP} and SCP1$^{PAX3}{}_{high}$ cells, whereas the upper band is equally intense in all conditions. Further methods would need to be employed to distinguish between nonspecific bands and those specific to GFP. Nevertheless, the lower band aligns with the expected decreased GFP-expression levels in the SCP1$^{PAX3}{}_{low}$ population compared to the SCP1$^{PAX3}{}_{high}$ population, as per the FACS sorting criteria. I will talk about this in more detail in the discussion (see 5.7).

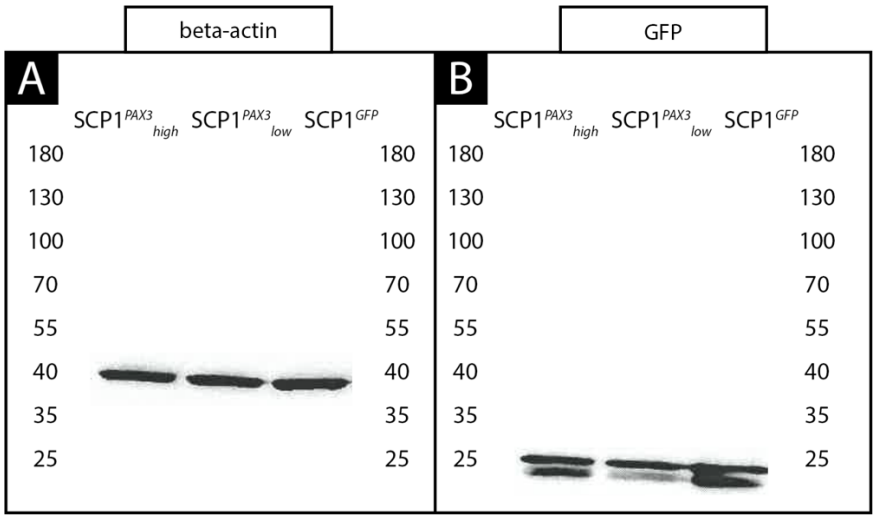

Figure 4.3: Detection of GFP and beta-actin in SCP1 cell populations.

A) Beta-actin was used as a housekeeping protein and its band was expected to be around 42 kDa. All SCP1 cell populations expressed this protein equally because of the homogenous bands with similar intensities in the area of 40 kDa.

B) Unexpectedly, the GFP blot depicts two bands. The first band is just above 25 kDa and the second is a little below 25 kDa. GFP bands are expected at 27 kDa. I cannot inconclusively correlate the bands to GFP. Presumably, it is the upper band that correlates with eGFP. The intensity of the lower band decreased in SCP1$^{PAX3}{}_{low}$ cells compared to SCP1^{GFP} and SCP1$^{PAX3}{}_{high}$ cells. The upper band, however, shows equal intensity in all conditions.

Further, PAX3 protein expression in SCP1$^{PAX3}_{high}$ and SCP1$^{PAX3}_{low}$ cells was assessed by Western Blot (Figure 4.4). SCP1^{GFP} cells were used as control and a signal intensity decrease in PAX3 at 56 kDa in SCP1$^{PAX3}_{low}$ cells was found. This correlates with the signal decrease in the housekeeping protein beta-actin. ImageJ was used to quantify band intensities and similar PAX3-to-beta-actin ratios for SCP1$^{PAX3}_{high}$ and SCP1$^{PAX3}_{low}$ cells were found (Table 12).

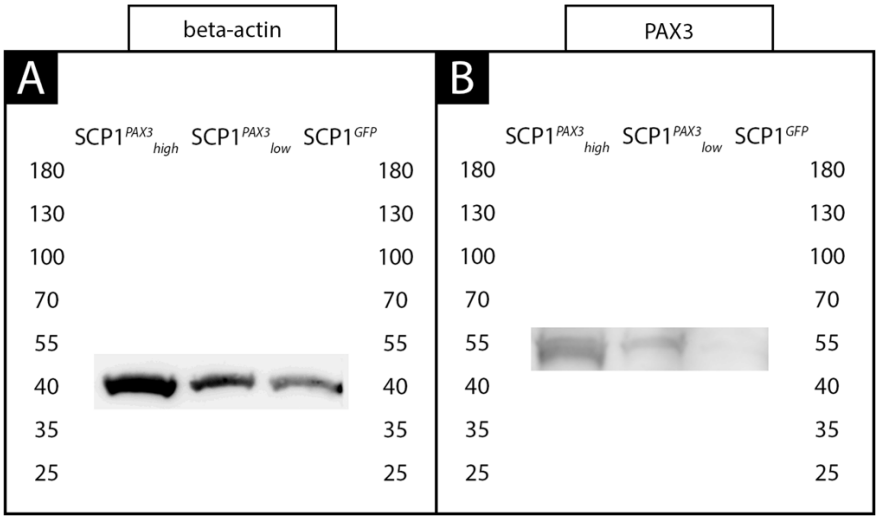

Figure 4.4: Detection of PAX3 expression in SCP1 cell populations.

A) Loading control with beta-actin (molecular weight of 42 kDa): All SCP1 cell populations exhibited different intensities which correlated with PAX3 intensities (B).

B) Western Blot with PAX3 antibodies: SCP1^{GFP} cells were used as a negative control. The drop in signal intensity in SCP1$^{PAX3}_{low}$ cells in PAX3 at 56 kDa matches the signal decrease in the housekeeping protein beta-actin. Quantification of band intensities using ImageJ revealed similar PAX3-to-beta-actin ratios for SCP1$^{PAX3}_{high}$ and SCP1$^{PAX3}_{low}$ cells.

Table 12: Signal intensity ratio PAX3-to-beta-actin as determined by ImageJ.

	Signal intensity ratios (PAX3-to-beta-actin) in R.U.
SCP1$^{PAX3}_{low}$	0.781983
SCP1$^{PAX3}_{high}$	0.753076

This means that PAX3 protein levels per cell number did not differ within different SCP1 populations. Instead, partial protein degradation might have occurred, especially in the SCP1$^{PAX3}_{low}$ and the SCP1^{GFP} samples.

The intensities of the GFP bands, however, were not measured due to uncertainty as to which band is specific for GFP. In addition, GFP levels serve as an indirect indicator of PAX3 protein levels, which is the primary protein of interest.

In conclusion, despite differing GFP fluorescence intensities as detected by FACS and eventually by Western blot, PAX3 protein levels did not differ in SCP1$^{PAX3}_{high}$ versus SCP1$^{PAX3}_{low}$ cells.

4.1.4 PAX3-overexpression leads to significant transcriptional changes in SCP1 cells in a dose independent manner

Next-gen RNA-sequencing was performed to detect changes in the transcriptome of the newly generated SCP1 cell populations. Out of 20.533 filtered genes (> ten reads per gene), 711 genes were differentially expressed between SCP1^{GFP} and SCP1$^{PAX3}_{high}$ cells and 484 genes between SCP1^{GFP}and SCP1$^{PAX3}_{low}$ cells.

PAX3-overexpressing SCP1 cell populations are distinct from native SCP1 cells according to Principal component analysis

Principal component analysis (PCA) of the transcriptome of SCP1 cell populations was performed to analyse exploratory data from next-gen RNA-sequencing and to reduce the data set's dimensions.

The scree plot in Figure 4.5 (A) shows that PC1 and PC2 are collectively responsible for about 51% of explained variances. Therefore, PC1 and PC2 were used exclusively for the discussion of further results.

Moreover, when visualising the results of PC1 and PC2, a clear distinction between SCP1$^{PAX3}_{high}$ and SCP1$^{PAX3}_{low}$ cells was found, when compared to SCP1^{GFP} cells as the plot (Figure 4.5 (B)) depicts clusters of samples based on their resemblance. There were more similarities between PAX3-expressing SCP1 cell populations in comparison to SCP1^{GFP} cells.

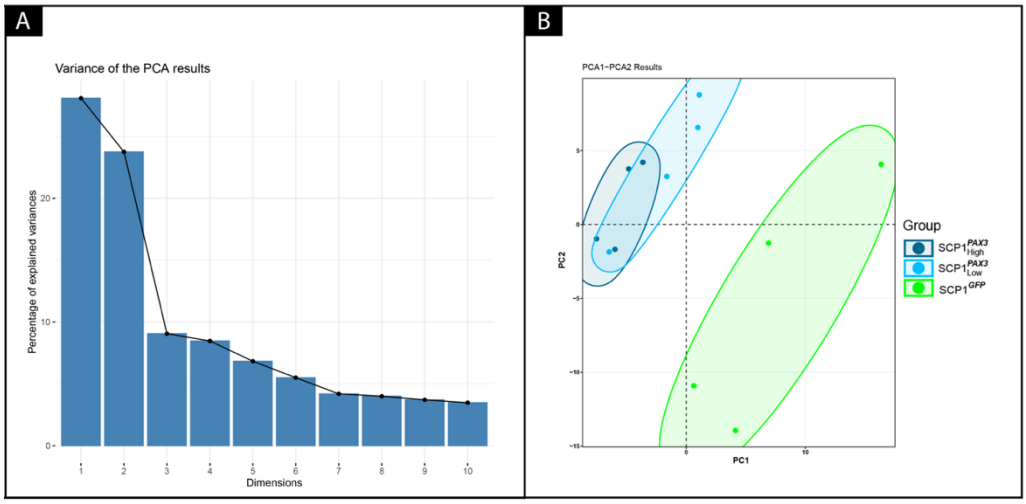

Figure 4.5: Principal component analysis (PCA) plots.

A) The percentages of explained variances were matched to each of the ten dimensions of the PCA. PC1 on the left-hand side with approximately 27% and PC2 with approximately 24% of explained variances comprised around 51%. PC1 and PC2 were used exclusively for the following analysis.

B) PC1 and PC2 results were visualised concerning the genes of the three different SCP1 cell populations: SCP1^{GFP}, SCP1$^{PAX3}{}_{low}$ cells and SCP1$^{PAX3}{}_{high}$ cells. The PCA plots show clusters based on the similarity of cell populations. A clear separation of the PAX3-expressing samples, which show more similarities and even overlap, and the non-PAX3-expressing samples can be observed.

Overexpression of PAX3 activates pathway of muscle organ development in SCP1 cells

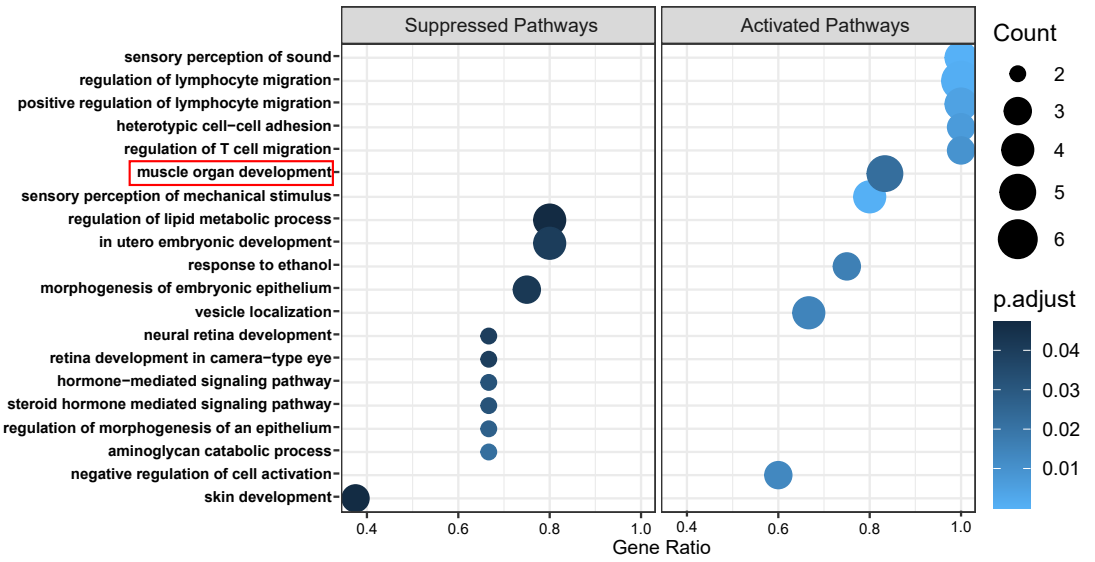

Figure 4.6: Gene Ontology (GO) enrichment analysis of activated and suppressed biological processes in SCP1$^{PAX3}{}_{high}$ cells compared to SCP1^{GFP} cells.

Suppressed and activated pathways in SCP1$^{PAX3}{}_{high}$ cells compared to SCP1^{GFP} cells are shown. Muscle organ development was an activated pathway which indicates the requirement of PAX3-overexpression for detecting a slightly positive effect in the tendency of alterations of the transcriptome towards muscle development.

X-axis shows gene ratio; y-axis shows affected pathways. The number of counts is indicated by the size of the dots.

I performed a gene ontology (GO) enrichment analysis to allow functional interpretation of data regarding the function of PAX3 in SCP1 cells. In these results, I only focus on the biological processes affected significantly by the overexpression of PAX3 in SCP1$^{PAX3}{}_{high}$ cells compared to the control group (SCP1^{GFP} cells).

As determined by RT-PCR (see 4.1.2), there was no significant difference in *PAX3* expression between SCP1$^{PAX3}{}_{high}$ and SCP1$^{PAX3}{}_{low}$ cells ($p = 0.180$) or between SCP1^{GFP} and SCP1$^{PAX3}{}_{low}$ cells ($p = 0.180$). However, a notable difference in *PAX3* levels was found between SCP1$^{PAX3}{}_{high}$ cells and SCP1^{GFP} cells ($p = 0.007$). Therefore, only SCP1$^{PAX3}{}_{high}$ cells are considered for analysing activated and suppressed biological processes (GO enrichment analysis) compared to SCP1^{GFP} cells.

In the graph (Figure 4.6), I illustrated the twenty most influenced pathways, showing the effect of PAX3-overexpression on SCP1 cells. Some of these biological processes were suppressed and others were activated due to PAX3-overexpression. I found that muscle organ development is an activated pathway in SCP1$^{PAX3}{}_{high}$ cells compared to SCP1^{GFP} cells.

Muscle organ development is defined as a process that aims to develop muscle over time, starting with early muscle formation up to mature structure (203-205). My study detected that the genes involved in this process were *PAX3, COL11A1, KEL, STRA6* and *RGS2*. All of these five genes are also involved in the biological process of muscle structure development (206). Additionally, *COL11A1, KEL, STRA6* and *RGS2* are part of muscle tissue development (206).

To me, finding that muscle organ development is an activated pathway in SCP1$^{PAX3}{}_{high}$ cells is essential for my study. This result emphasises the role of PAX3 concerning slight tendencies of human mesenchymal stem cells on their way to start the transformation into functional myoblasts. As I saw in all performed assays, more than PAX3 on its own is required to achieve a proper myogenic transformation. Still, it is important to note this slightly positive effect in the tendency of the transcriptome towards a myogenic lineage due to this activated pathway of muscle organ development.

Via GO enrichment analysis, I also found that PAX3 was involved in more pathways than only muscle organ development. It was also associated with the sensory perception of sound, mechanical stimulus, and system process.

To sum up, this GO enrichment analysis supported the tendency of a role of PAX3 concerning myogenic development in SCP1 cells by activating the pathway of muscle organ

development. PAX3, by itself, was not able to induce myogenic differentiation in SCP1 cells. Still, I want to stress that PAX3-overexpression enabled slight changes in the transcriptome of SCP1 cell populations towards a more myogenic lineage.

4.2 Overexpression of PAX3 does not affect the proliferation of SCP1 cells

The proliferation of muscle precursor cells is essential for myogenic differentiation to allow skeletal muscle formation (207). Cell proliferation is also important in muscle regeneration (207). Pax3 holds an essential role in the proliferation of muscle precursor cells because of Pax3/7BP (151, 181). This is a protein that binds Pax3 and Pax7 and is linked to histone 3 lysine 4 (H3K4) methyltransferase (HMT) activity which is vital for the regulation of proliferation in muscle precursor cells (151, 181). Knockdown of Pax3/7BP deactivates H3K4 HMT, thereby hindering muscle precursor cell proliferation *in vitro* and *in vivo* (181). Ling et al. found that in goats *Pax3* accelerates the proliferation of skeletal muscle satellite cells (208). Therefore, Pax3 is essential for the proliferation of muscle (precursor) cells. For this reason, I analysed cumulative population doublings (cumPD) and population doubling time (PDT) of SCP1 cell populations.

4.2.1 Low overexpression of PAX3 in SCP1 cells leads to a slightly higher cell proliferation

This cumPD assay demonstrates how often the population of each reviewed cell type doubled in the time of four weeks *in vitro*.

Over a period of 28 days, it was found that the cell proliferation was fastest in SCP1$^{PAX3}{}_{low}$ cells (with a mean cumPD value of 3.28 ± 0.22 after 4 days, 9.72 ± 1.57 after 14 days and 18.04 ± 1.74 after 28 days), followed by SCP1$^{PAX3}{}_{high}$ cells (with a mean cumPD value of 2.67 ± 0.93 after four days, 9.08 ± 1.42 after 14 days and 15.35 ± 1.60 after 28 days). The slowest cell proliferation was observed in SCP1^{GFP} cells (with a mean cumPD value of 2.55 ± 0.21 after four days, 7.97 ± 1.01 after 14 days and 13.74 ± 1.40 after 28 days). With RT-PCR, next-gen RNA-sequencing and Western blotting results it was found that SCP1$^{PAX3}{}_{low}$ cells and SCP1$^{PAX3}{}_{high}$ cells did not differ in levels of PAX3 expression. Thus, via the cumPD assay, it was shown that PAX3-expressing cell populations proliferated slightly faster than the control group of SCP1^{GFP} cells.

After 28 days SCP1$^{PAX3}{}_{low}$ cells showed a slight increase in proliferation compared to SCP1^{GFP} cells (mean cumPD after 28 days: SCP1$^{PAX3}{}_{low}$ cells: 18.04 ± 1.74; SCP1^{GFP} cells: 13.74 ± 1.40). Compared to SCP1^{GFP} cells, SCP1$^{PAX3}{}_{high}$ cells also had a faster

population doubling time (mean cumPD after 28 days: SCP1$^{PAX3}_{high}$ cells: 15.35 ± 1.60; SCP1^{GFP} cells: 13.74 ± 1.40).

Compared to the control group, a slight increase in cell proliferation of PAX3-overexpressing SCP1 cell populations was detected. To corroborate these findings, population doubling times (PDT) were also analysed.

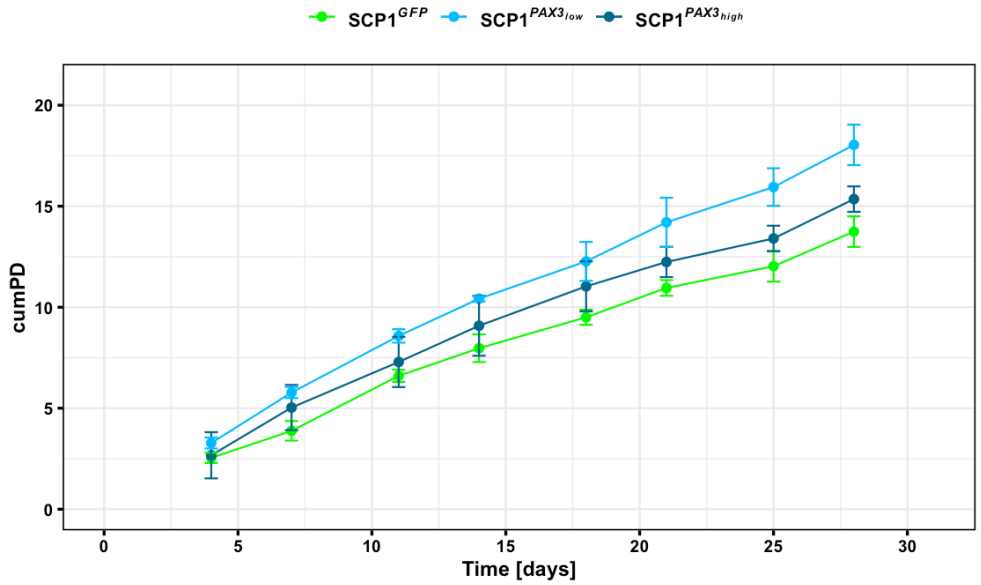

Figure 4.7: Impact of PAX3-overexpression on SCP1 cells regarding cumulative population doublings.

After 28 days, SCP1$^{PAX3}_{low}$ cells had a faster cumPD than SCP1$^{PAX3}_{high}$ cells. At this point, they also were faster than SCP1^{GFP} cells. (Mean cum PD at day 28: SCP1$^{PAX3}_{low}$ cells: 18.04 ± 1.74; SCP1$^{PAX3}_{high}$ cells: 15.35 ± 1.60; SCP1^{GFP} cells: 13.74 ± 1.40)

Dots represent mean value, and vertical lines attached to dots represent standard deviation. n = 8; w = 3

When analysing the population doubling time (PDT) it was found that SCP1$^{PAX3}_{low}$ cells might exhibit a slight tendency towards increased proliferation, when compared to SCP1^{GFP} cells. All SCP1 cell populations (SCP1$^{PAX3}_{high}$ cells, SCP1$^{PAX3}_{low}$ cells or SCP1^{GFP} cells) were counted for 28 weeks to investigate their growth rate. The following findings regarding the PDT were noted. According to cumPD results, a slight difference in cell proliferation regarding PAX3 and non-PAX3-expressing cell populations was expected. It was found that the mean PDT of SCP1^{GFP} cells was 2.84 days ± 1.85. The mean PDT of SCP1$^{PAX3}_{low}$ cells was 1.56 days ± 0.41 and the mean PDT of SCP1$^{PAX3}_{high}$ cells was 2.09 days ± 0.91. There were no significant differences between all analysed SCP1 cell populations regarding the growth rate measured by PDT; however, the p-value between SCP1^{GFP} cells and SCP1$^{PAX3}_{low}$ cells was close to significance ($p = 0.058$). Therefore, a slight tendency towards an increased proliferation of SCP1$^{PAX3}_{low}$ cells compared to SCP1^{GFP} cells (other p-values: SCP1^{GFP} cells to SCP1$^{PAX3}_{high}$ cells: $p = 0.495$;

SCP1$^{PAX3}{}_{high}$ cells to SCP1$^{PAX3}{}_{low}$ cells: p = 0.083) could be suspected. However, this assumption still needs to be validated in future studies. Overall, it was found that low levels of PAX3 expression in SCP1 cells might lead to a possible tendency of increased cell proliferation in comparison to SCP1^{GFP} cells.

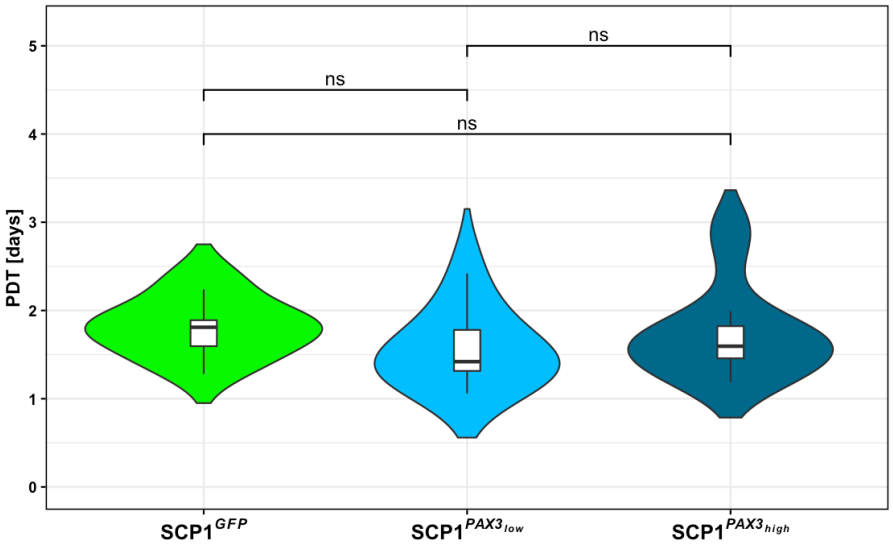

Figure 4.8: Population doubling time (PDT) of SCP1 cells populations.

Population doubling time is depicted in days summarised over a total period of 28 days. Mean PDT values were 2.84 days ± 1.85 for SCP1^{GFP} cells, 1.56 days ± 0.41 for SCP1$^{PAX3}{}_{low}$ cells and 2.09 days ± 0.91 for SCP1$^{PAX3}{}_{high}$ cells. No significant differences in PDT between SCP1$^{PAX3}{}_{high}$ cells, SCP1$^{PAX3}{}_{low}$ cells or SCP1^{GFP} cells were found. When comparing SCP1$^{PAX3}{}_{low}$ cells to SCP1^{GFP} cells (p = 0.058), a minimal tendency of increased proliferation could be assumed and should be verified in future studies.

Box plots represent the median, quartiles, and range. Significance levels*: p ≤ 0.05, ns: not significant. Statistical method: Wilcoxon test; n = 8; w = 3

4.2.2 Overexpression of PAX3 does not affect the clonogenic potential of SCP1 cells

After performing the CFU assay, the relative CFU efficiency of all SCP1 cell populations was determined to see whether PAX3 expression would change the clonogenic potential of cells. In this assay, the clonogenic ability and *in vitro* changes in the colony formation of SCP1 cell populations was evaluated.

SCP1^{GFP} cells had a mean relative CFU efficiency of 12.91 ± 9.25%. For SCP1$^{PAX3}{}_{high}$ cells, the mean relative CFU efficiency was 13.63 ± 5.85%; for SCP1$^{PAX3}{}_{low}$ cells it was 18.69 ± 11.31%. There were no significant differences in relative CFU efficiency between all SCP1 cell populations. Therefore, it can be concluded that the overexpression of PAX3 did not change the clonogenic ability of SCP1 cell populations.

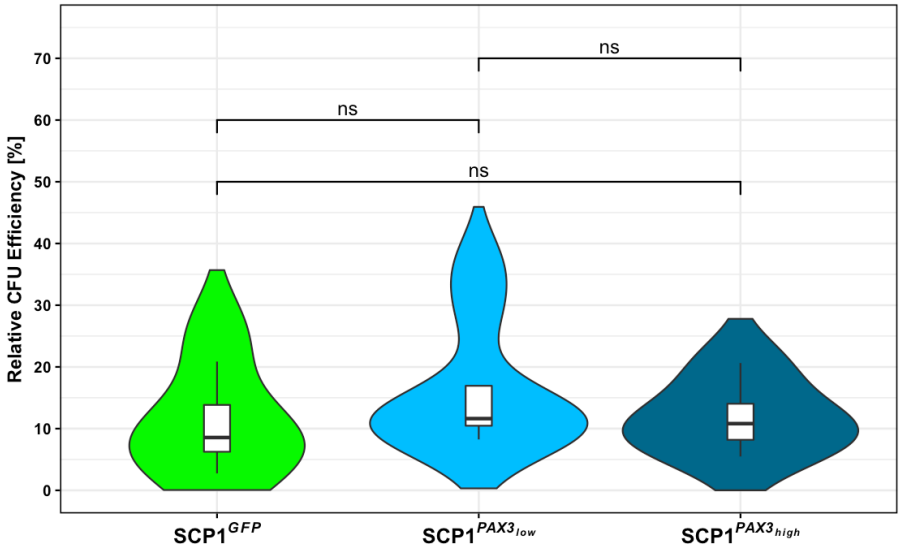

Figure 4.9: Relative CFU Efficiency of SCP1 cell populations.

Mean relative CFU efficiency was 12.91 ± 9.25% for SCP1^{GFP} cells, 13.63 ± 5.85% for SCP1$^{PAX3}{}_{high}$ cells and 18.69 ± 11.31% for SCP1$^{PAX3}{}_{low}$ cells. No significant differences in CFU efficiency were found between all SCP1 cell populations.

Box plots represent the median, quartiles, and range. Significance levels*: $p \leq 0.05$, ns: not significant. Statistical method: Wilcoxon test; n = 4; w = 3

4.3 Morphology of SCP1 cells is not affected by PAX3-overexpression

Since I wanted to describe the effect of PAX3-overexpression on SCP1 cells and detect possible modifications of the cells towards a more myogenic lineage, morphological changes in shape and size were important to evaluate.

The fusion of myoblasts forms myotubes (209). During this complex process, various cellular events take place. After migration to the desired position, cells adhere and then elongate, followed by cell-cell recognition (209). Finally, myoblasts align, and their membranes fuse (209). In this cascade, the elongation of cells is vital (209). The myoblasts alter their shape to enable further fusion and thereby muscle formation (209). With the following assay, I offer insight into these morphological changes. On one hand, I compared PAX3-overexpressing cell populations (SCP1$^{PAX3}{}_{high}$ cells and SCP1$^{PAX3}{}_{low}$ cells) to native SCP1^{GFP} cells. On the other hand, I compared them to C2C12 cells, a mouse myoblast cell line. In this assay, I examined the morphological aspects of cell area and the aspect ratio to compare the configuration of all cell populations.

Cell area and aspect ratio were used to analyse morphological changes in PAX3-overexpressing SCP1 cell populations. They were compared to SCP1^{GFP} cells (control group) and C2C12 myoblasts.

The confidence interval (CI) (see Figure 4.10) was defined with 95% of C2C12 data. It is depicted as a dashed red line in the graph (3.96 at the x-axis, which depicts AR; 2.82x10^3 µm^{2}on the y-axis for cell area). With the CI, every column is divided into four quadrants, with the first quadrant in the lower left corner. Here, data of cells with little area and little AR accumulates – small and round cells. The quadrants have been numbered clockwise, ending with the fourth quadrant at the bottom right. Data from small, spindle-shaped cells are collected here. Table 13 provides an overview of the data collected.

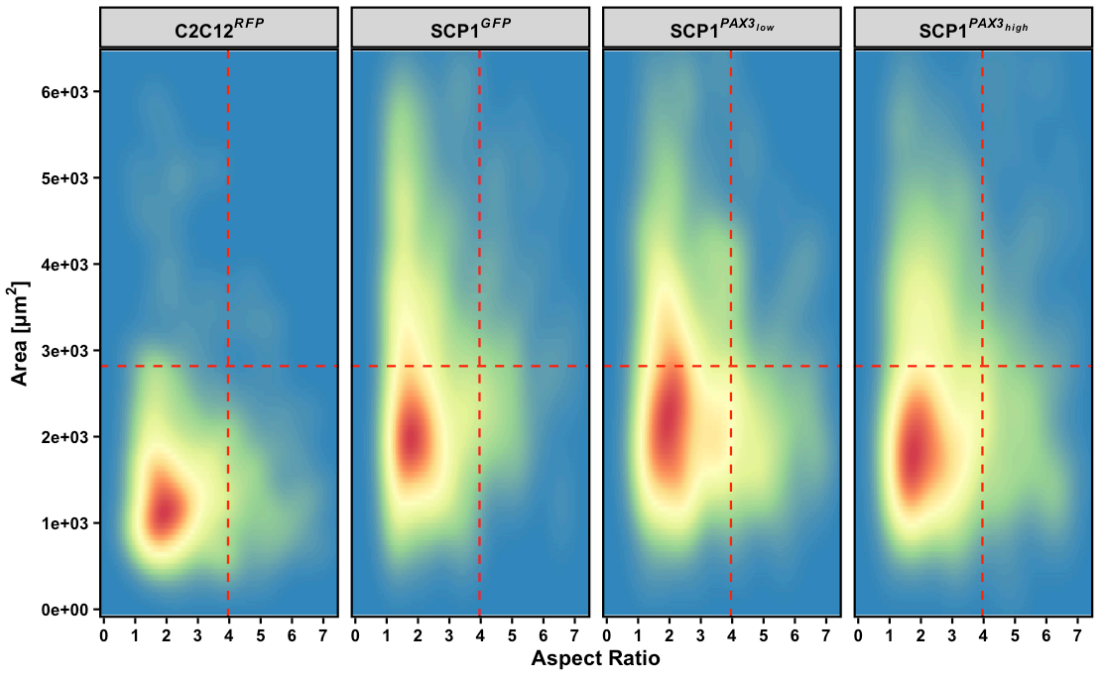

Figure 4.10: Comparison of area and aspect ratio of analysed cell populations.

The confidence interval (red dashed lines: 3.96 on the x-axis; 2,82x10^{3}µm^2 on the y-axis) was determined with 95% of data from C2C12 cells. This results in four quadrants within each depicted cell population counted from one (lower left compartment) clockwise to four (lower right compartment). n = 7; w = 3

Most C2C12 cells (72.28% in the first quadrant) were small and round. All SCP1 cell populations had the majority of data in the first quadrant (51.63% of SCP1^{GFP} cells, 45.63% of SCP1$^{PAX3}{}_{low}$ cells, and 50.60% of SCP1$^{PAX3}{}_{high}$ cells) which means they were small and round as well.

Table 13: Cell morphology based on area and aspect ratio as shown in Figure 4.10.

	SCP1^{GFP} cells	SCP1$^{PAX3}{}_{low}$ cells	SCP1$^{PAX3}{}_{high}$ cells	C2C12 cells
1st quadrant: small, round cells	51.63%	45.63%	50.60%	72.28%
2nd quadrant: big, round cells	33.12%	30.42%	26.84%	6.65%
3rd quadrant: big, spindle-shaped cells	6.54%	5.16%	6.54%	2.22%
4th quadrant: small, spindle-shaped cells	8.72%	18.78%	16.02%	18.85%

Overall, as shown in Figure 4.10, I found that most of the cells were small and round as most of the data accumulated in the first quadrant (51.63% of SCP1^{GFP} cells, 45.63% of SCP1$^{PAX3}{}_{low}$ cells, 50.60% of SCP1$^{PAX3}{}_{high}$ cells and 72.28% of C2C12 cells). All SCP1 cell populations had the second largest number of cells in the second quadrant, indicating that they were big and round (33.12% of SCP1^{GFP} cells, 30.42% of SCP1$^{PAX3}{}_{low}$ cells, 26.84% of SCP1$^{PAX3}{}_{high}$ cells). C2C12 cells had their second largest population in the fourth quadrant (18.85%). These cells were small and spindle-shaped. With this assay I can show that the majority of C2C12 cells were small (round or spindle-shaped), and the majority of SCP1 cell populations were round (big or small).

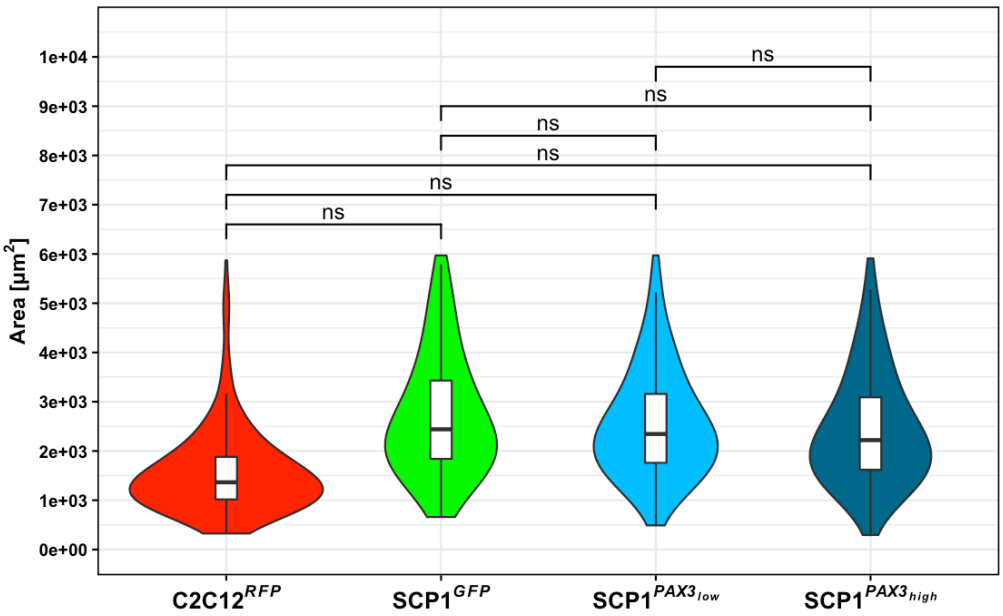

Figure 4.11: Cell area of C2C12 myoblasts and SCP1 cell populations.

The mean cell area of C2C12 cells was $1.71x10^3$ µm² ± $1.43x10^3$. The mean area of $SCP1^{GFP}$ cells was $2.90x10^3$ µm² ± $1.58x10^3$, of $SCP1^{PAX3_{low}}$ cells it was $2.76x10^3$ µm² ± $1.52x10^3$ and of $SCP1^{PAX3_{high}}$ cells it was $2.67x10^3$ µm² ± $1.58x10^3$. There were no significant differences regarding cell area between all analysed cell populations.

Box plots represent the median, quartiles, and range. Significance levels*: p ≤ 0.05, ns: not significant. Statistical method: Wilcoxon test; n = 7; w = 3

Cell area of C2C12 cells and SCP1 cell populations (Figure 4.11) was not significantly different. The mean cell area of C2C12 cells was $1.71x10^3$ µm² ± $1.43x10^3$. The mean cell area of $SCP1^{GFP}$ cells was $2.90x10^3$ µm² ± $1.58x10^3$, of $SCP1^{PAX3_{low}}$ cells it was $2.76x10^3$ µm² ± $1.52x10^3$ and of $SCP1^{PAX3_{high}}$ cells the mean area was $2.67x10^3$ µm² ± $1.58x10^3$.

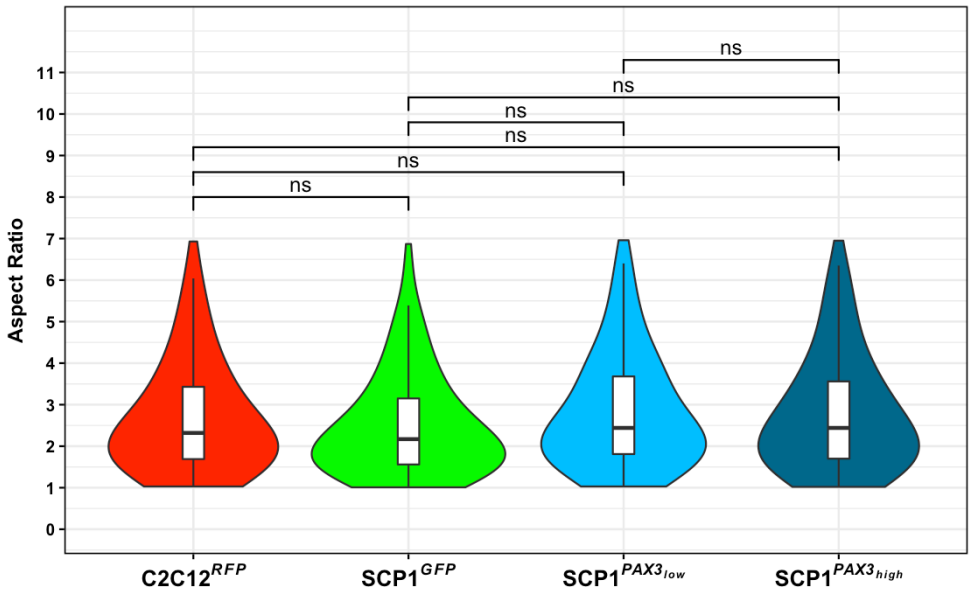

Figure 4.12: Aspect Ratio of C2C12 cells and SCP1 cell populations.

The mean aspect ratio (AR) of C2C12 myoblasts was 2.97 ± 1.82; of SCP1^{GFP} cells it was 2.63 ± 1.49. The mean AR of SCP1$^{PAX3_{low}}$ cells was 3.13 ± 1.79; of SCP1$^{PAX3_{high}}$ cells it was 3.03 ± 1.73. There were no significant differences when comparing the AR of all analysed cell populations.

Box plots represent the median, quartiles, and range. Significance levels*: $p \leq 0.05$, ns: not significant. Statistical method: Wilcoxon test; n = 7; w = 3

The aspect ratio (AR) describes the ratio of each cell's width to its length. There were no significant differences when comparing C2C12 cells, SCP1^{GFP} cells, SCP1$^{PAX3_{low}}$ cells and SCP1$^{PAX3_{high}}$ cells (Figure 4.12). The mean aspect ratio of C2C12 cells was 2.97 ± 1.82. The mean AR of SCP1^{GFP} cells was 2.63 ± 1.49; of SCP1$^{PAX3_{low}}$ cells it was 3.13 ± 1.79 and of SCP1$^{PAX3_{high}}$ cells the mean AR was 3.03 ± 1.73.

4.4 The velocity of randomly migrating SCP1 cells is not altered by overexpression of PAX3

Pax3 plays an important role for muscle progenitor cells as they delaminate from the dermomyotome and subsequently migrate to far-off locations of myogenesis, such as the limbs, to form muscle tissue (151, 180). A study by Epstein et al. showed that Pax3 regulates c-met expression, which is necessary for proper migration of myogenic precursors to the limb (159). Epstein et al. also confirmed the need for Pax3 for the migration of myogenic progenitor cells from the ventrolateral lip of the dermomyotome to the limb bud in *Pax3* mutant mice, where the development of limb muscles was severely impaired (159, 190). Therefore, I analysed the random migration of PAX3-overexpressing SCP1 cells and compared it to SCP1^{GFP} cells.

The extracellular matrix protein type I collagen was chosen as a base coating in cell culture dishes to compare to the uncoated polystyrene. Type I collagen was chosen because it is specific to muscle tissue in the dermomyotome, as myogenic progenitor cells express collagen type 1 α2 in the dermomyotome (210). Although it is muscle specific, laminin was not used as a coating because laminin forms at later stages of myofiber formation (newly formed myotubes) (163) and the focus of my assay lies on earlier stages of myogenesis.

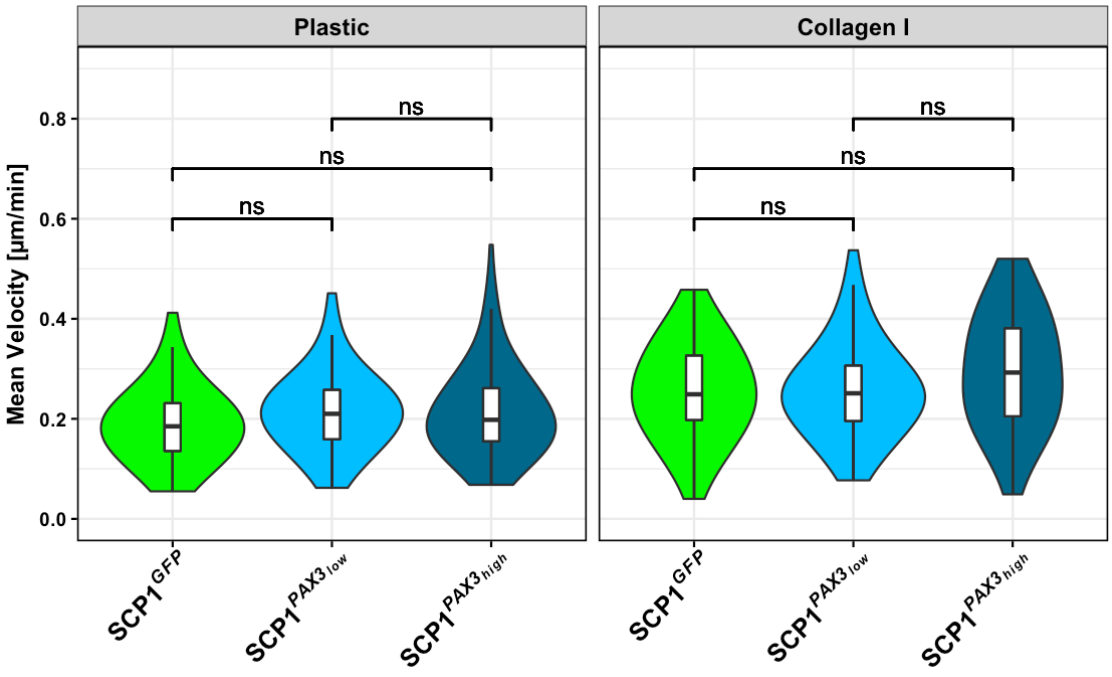

Figure 4.13: Mean velocity of migrating SCP1 cell populations on polystyrene and type I collagen.

I found no significant differences in the mean velocity between all SCP1 cell populations on polystyrene and type I collagen. The mean velocities on polystyrene were 0.19 µm/min ± 0.07 for SCP1^{GFP} cells, 0.21 µm/min ± 0.08 for SCP1$^{PAX3}{}_{low}$ cells and 0.21 µm/min ± 0.09 for SCP1$^{PAX3}{}_{high}$ cells. On type I collagen, SCP1^{GFP} cells

had a mean velocity of 0.25 µm/min ± 0.09; SCP1$^{PAX3_{low}}$ cells of 0.26 µm/min ± 0.11 and SCP1$^{PAX3_{high}}$ cells had a mean velocity of 0.30 µm/min ± 0.11 on the type I collagen-coated surface.

Box plots represent the median, quartiles, and range. Significance levels*: p ≤ 0.05, ns: not significant. Statistical method: Wilcoxon test; n = 4; w = 1

The mean velocity of SCP1^{GFP} cells on the collagen-coated surface was 0.25 µm/min ± 0.09, 0.26 µm/min ± 0.11 for SCP1$^{PAX3_{low}}$ cells and 0.30 µm/min ± 0.11 for SCP1$^{PAX3_{high}}$ cells.

On polystyrene, SCP1$^{PAX3_{low}}$ cells and SCP1$^{PAX3_{high}}$ cells both had a mean velocity of 0.21 µm/min (SCP1$^{PAX3_{low}}$ 0.21 µm/min ± 0.08; SCP1$^{PAX3_{high}}$ 0.21 µm/min ± 0.09). SCP1^{GFP} cells had a mean velocity of 0.19 µm/min ± 0.07. I detected no significant differences between the mean velocity of all migrating SCP1 cell populations.

Regarding overall mean velocity, I found that, on average, SCP1^{GFP} cells were 24.00% faster on collagen compared to polystyrene, and SCP1$^{PAX3_{low}}$ cells were also 19.23% faster on collagen as well. Also, SCP1$^{PAX3_{high}}$ cells were 30.00% faster on collagen compared to the non-coated polystyrene surface.

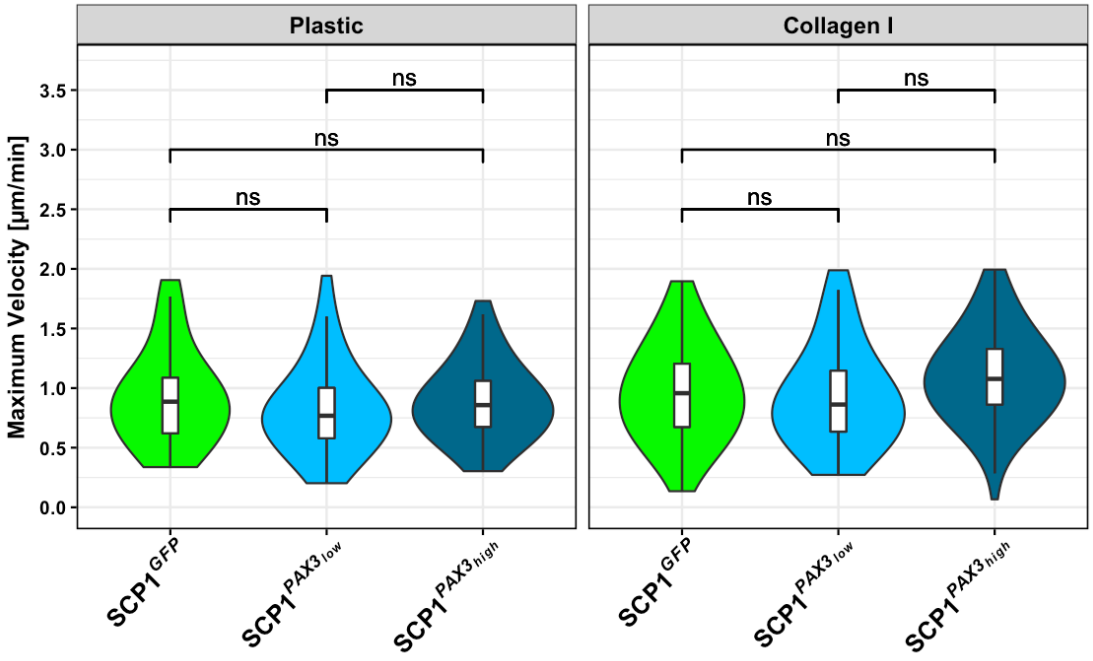

Figure 4.14: Maximum velocity in random migration of SCP1 cell populations.

There were no significant differences when comparing the maximum velocity of randomly migrating SCP1^{GFP} cells, SCP1$^{PAX3_{low}}$ cells and SCP1$^{PAX3_{high}}$ cells on polystyrene or type I collagen. On polystyrene, the maximum velocities were 1.01 µm/min ± 0.54 for SCP1^{GFP} cells, 0.93 µm/min ± 0.62 for SCP1$^{PAX3_{low}}$ cells and 0.90 µm/min ± 0.32 for SCP1$^{PAX3_{high}}$ cells. On type I collagen, the maximum velocities were 0.97 µm/min ± 0.37 for SCP1^{GFP} cells, 0.99 µm/min ± 0.49 for SCP1$^{PAX3_{low}}$ cells and 1.18 µm/min ± 0.49 for SCP1$^{PAX3_{high}}$ cells.

Box plots represent the median, quartiles, and range. Significance levels*: p ≤ 0.05, ns: not significant. Statistical method: Wilcoxon test; n = 4; w = 1

The mean maximum velocity of SCP1^{GFP} cells on the type I collagen-coated surface was 0.97 µm/min ± 0.37, 0.99 µm/min ± 0.49 for SCP1$^{PAX3_{low}}$ cells and 1.18 µm/min ± 0.49 for SCP1$^{PAX3_{high}}$ cells. On polystyrene, the mean maximum velocity was 1.01 µm/min ± 0.54 for SCP1^{GFP} cells, 1.02 µm/min ± 0.62 for SCP1$^{PAX3_{low}}$ cells and 0.90 µm/min ± 0.32 for SCP1$^{PAX3_{high}}$ cells. I found no significant differences in the maximum velocities of all analysed cell populations.

Regarding the average maximum velocity, SCP1$^{PAX3_{high}}$ cells were 23.73% faster on type I collagen than on polystyrene. SCP1$^{PAX3_{low}}$ cells were 2.94% faster on polystyrene; the same applies to SCP1^{GFP} cells which were 3.96% faster on polystyrene.

It can be concluded that there were no significant differences between the different SCP1 cell populations on either substrate. This indicates that PAX3 does not affect the random migration velocity of cells.

4.5 Overexpression of PAX3 in SCP1 cells does not induce cell fusion *in vitro*

I investigated direct cell fusion in this assay. It is one of the most important aspects I examined since the fusion of myoblasts is crucial for muscle development and regeneration. Through the fusion of myoblasts, multi-nucleated myotubes are formed (209). They are the basis of muscle tissue. I analysed the cell populations to see whether they would fuse or not. C2C12 myoblasts were added in this assay because fusion of these cells is certain which makes them a suitable control group. The relative fused myofiber area was analysed after three, five or seven days. SCP1 cell populations were mixed in different ratios (1:1, 1:2, 2:1) with C2C12 cells to see whether there would be an effect on fusion behaviour and therefore differentiation of cells. All cell populations were also cultured alone as a control (1:0/ 0:1) and to investigate the fusion of SCP1 cell populations by themselves.

It was found that C2C12 cells (not mixed; 1:0) increased their relative fused myofiber area by 187.43% from day three to day five and by 200.43% from day five to day seven. From day three to day seven, a 375.67% increase in the fused myofiber area of C2C12 cells was noted. After seven days, the relative fused myofiber area of C2C12 cells was significantly different from SCP1^{GFP} cells ($p \leq 0.001$), SCP1$^{PAX3}{}_{low}$ cells ($p \leq 0.001$) or SCP1$^{PAX3}{}_{high}$ cells ($p \leq 0.001$), which did not fuse.

On day five, C2C12 cells mixed with SCP1^{GFP} cells in a 1:2 ratio had a significantly different relative fused myofiber area compared to C2C12 cells mixed with SCP1$^{PAX3}{}_{low}$ cells in a 1:2 ratio ($p = 0.001$). There were no other significant differences detected in cell mixtures of C2C12 cells and SCP1 cell populations. Note that the experimental condition C2C12 & SCP1$^{PAX3}{}_{low}$ (1:2, day 5) contained a significant outlier (GraphPad Outlier Calculator: significant outlier, $p \geq 0.05$).

I found that the SCP1 cell populations did not fuse by themselves. These cells did not differentiate and therefore cell fusion did not occur. I saw that SCP1 cell populations did not express myosin heavy chain, which is a structural component of muscle, as immunohistochemistry showed (MYH1E, clone MF20). MYH1E (Developmental Studies Hybridoma Bank, USA) is a primary antibody against the myosin heavy chain 1E. The myosin heavy chain is known as the motor protein for thick muscle filaments and is needed to define specific muscle properties (211). I found that overexpression of PAX3 was insufficient to induce cell fusion in SCP1 cell populations.

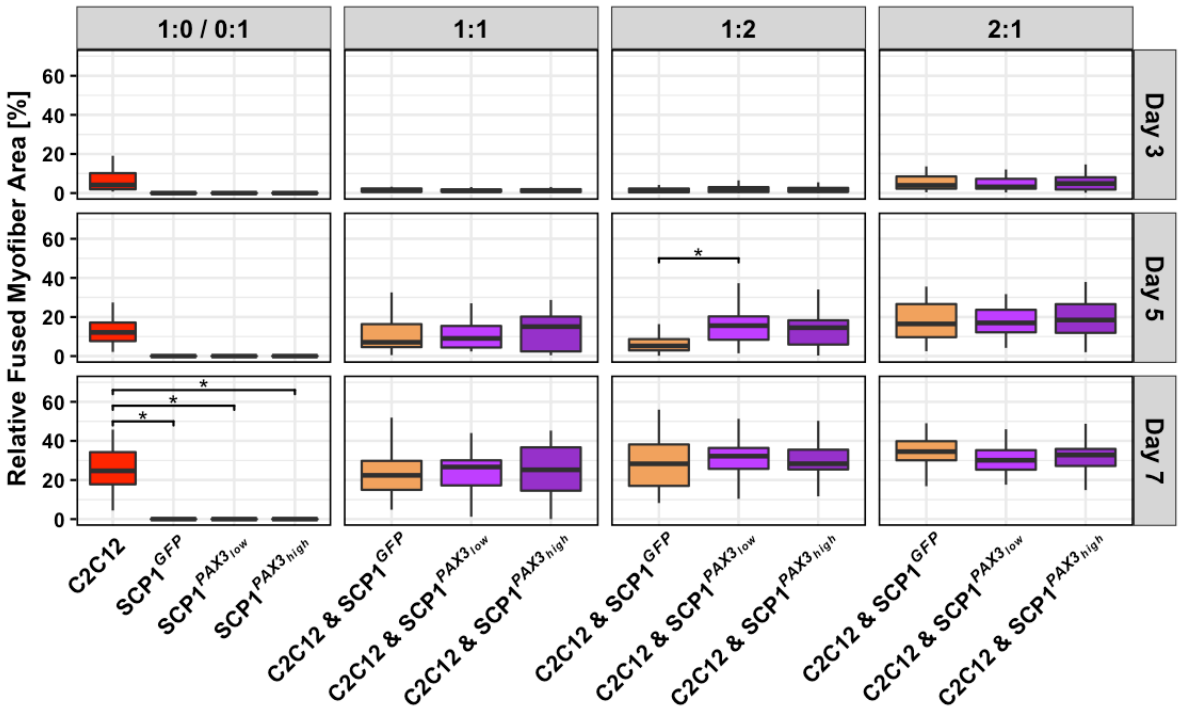

Figure 4.15: Relative fused myofiber area of C2C12 cells and SCP1 cell populations.

The relative fused myofiber area of the cells was analysed after three, five and seven days. SCP1 cell populations (SCP1^{GFP}, SCP1$^{PAX3}{}_{low}$ or SCP1$^{PAX3}{}_{high}$ cells) were mixed with C2C12 cells in different ratios: 1:1, 1:2 or 2:1. The first number of the ratio always refers to the amount of C2C12 cells used in the mixture.

C2C12 cells (not mixed; ratio 1:0) increased their relative fused myofiber area by 187.43% from day three to day five and by 200.43% from day five to day seven. From day three to day seven, they raised the relative fused myofiber area by 376.67%. After seven days, relative fused myofiber area of C2C12 cells was significantly different from relative fused myofiber area of SCP1^{GFP} cells ($p \leq 0.001$), SCP1$^{PAX3}{}_{low}$ cells ($p \leq 0.001$) and from SCP1$^{PAX3}{}_{high}$ cells ($p \leq 0.001$).

SCP1 cell populations did not fuse by themselves. I observed that the overexpression of PAX3 did not enable cell fusion of SCP1 cells.

Box plots represent the median, quartiles, and range. Significance levels*: $p \leq 0.05$. Statistical methods: t-test, Bonferroni correction; n = 4; w = 2

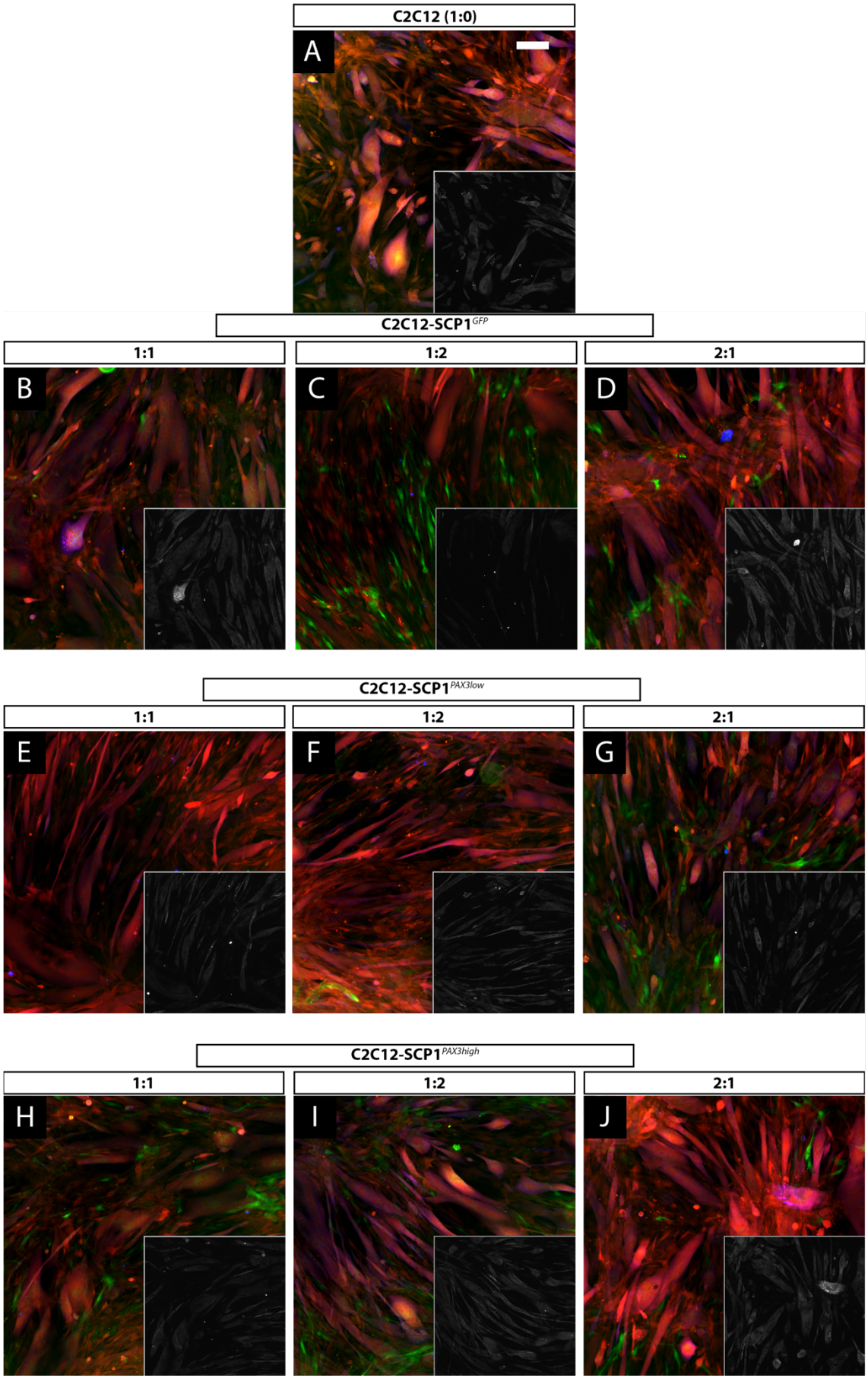

Figure 4.16: Fusion of different cell combinations on day 7.

Representative fluorescence microscopy images for GFP (SCP1 cell populations) and RFP (C2C12 cells) are shown. The black-and-white images are the same images as the coloured red and green ones but allow to better visualise myotubes after immunocytochemistry using MYH1E (Developmental Studies Hybridoma Bank, USA), a primary antibody against the myosin heavy chain 1E.

A) C2C12 cells (1:0) alone have fused to myofibers on day seven.

B-J) C2C12 cells mixed with SCP1^{GFP} cells, SCP1$^{PAX3_{low}}$ cells or SCP1$^{PAX3_{high}}$ cells in different ratios (1:1, 1:2, 2:1) on day seven. As expected, C2C12 myoblasts fused which can be seen in the black-and-white images. In these pictures, fused myofiber areas match with RFP marked C2C12 cells in the coloured images. SCP1 cell populations did not fuse.

Scale bars: 100 µm

5. Discussion

5.1 Overexpressing PAX3 slightly shifted SCP1 cells towards a myogenic program

The main finding of my study is that the mere overexpression of PAX3 in SCP1 cells was insufficient to initiate a myogenic program, though I was able to detect slight changes in myogenic cell fate.

In a 2011 study, Darabi et al. showed that Pax3 controls the myogenic induction of iPSCs (212). In embryoid body-derived cells, Pax3 induced myogenesis (191). Sato et al. believed that upregulating vital myogenic transcription factors like MyoD, Pax7 and Pax3 was an important requirement for inducing myogenesis in non-skeletal muscle cells (213).

Owing to these studies, I first expected PAX3 to induce myogenic differentiation in SCP1 cells; however, I did not find that the SCP1cells overexpressing PAX3 transformed into functional myoblasts. I detected minor changes in the characteristic of the cells, towards a more myogenic lineage, specifically in the transcriptome of SCP1 cell populations. Most importantly, activating the pathway of muscle organ development indicates that the tendencies towards myogenic differentiation existed in the SCP1 cell populations expressing PAX3 (see 5.2). Nonetheless, most cellular properties of the newly created SCP1 cell populations did not change compared to PAX3-negative SCP1 cells.

I will discuss my findings in more detail the following subsections.

5.2 Activating the pathway of “muscle organ development” through PAX3-overexpression

A key finding of next-gen RNA-sequencing was that overexpressing PAX3 in SCP1$^{PAX3}{}_{high}$ cells activated the pathway of muscle organ development compared to SCP1^{GFP} cells. The GO pathway of muscle organ development is understood as a process resulting in cells turning into muscle over time – starting with initial muscle formation until mature muscle structure is formed (203-205). This is particularly exciting because one of the aims of my study was to identify muscle-related molecular signatures of PAX3-overexpressing SCP1 cell populations. Using GO enrichment analysis, I showed that the overexpression of PAX3 could contribute to a potential transformation of SCP1 cells into a myogenic lineage. In contrast to the *in vivo* situation, however, the expression of PAX3

in the newly created SCP1 cell populations did not decrease due to the constitutive overexpression system. This means cells were constantly overexpressing PAX3 *in vitro* and thereby staying in an - “early”- native state instead of differentiating, which does not happen *in vivo*. *In vivo*, Pax3 is downregulated at the early stages of myogenesis when Pax7, MyF5 and MyoD are upregulated (183). It remains unclear, in my study, whether the PAX3-overexpressing SCP1 cell populations underwent the physiological cascade of different factors orchestrating and inducing the myogenic program. This limitation of my study is essential, and I will discuss it in more detail (see 5.9).

Next-gen RNA-sequencing confirmed that PAX3-expressing SCP1 cell populations differed from SCP1^{GFP} cells as revealed by PCA.

5.3 The possible tendency towards increased cell proliferation in PAX3-overexpressing cells

When analysing the cell proliferation of PAX3-overexpressing SCP1 cells and comparing them to SCP1^{GFP} cells, I expected to discover changes in cell proliferation since other *in vitro* studies found that overexpressing PAX3 controls cell proliferation and differentiation in skeletal muscle lineage development (151). Boudjadi et al. found that Pax3 triggers the proliferation of muscle precursor cells because of its interaction with Pax3/7BP (an adaptor that links Pax3 and Pax7 with the H3K4 methyltransferase complex) (151, 181). Ling et al. showed that Pax3 accelerates the proliferation of skeletal muscle satellite cells in goats (208).

I expected to find alterations in the proliferation of PAX3-overexpressing SCP1 cell populations but could not confirm them by cumPD and PDT assays.

Nevertheless, when I analysed PDT, there seemed to be a slight tendency towards increased cell proliferation, as seen in SCP1$^{PAX3_{low}}$ cells compared to the control group. With a p-value of $p = 0.058$, it was close to significance and therefore a slight tendency towards increased cell proliferation might exist. Since I found no difference in the levels of PAX3 expression between SCP1$^{PAX3_{high}}$ and SCP1$^{PAX3_{low}}$ cells (see 5.7), this tendency towards increased cell proliferation is probably independent of PAX3 and needs further studies to be investigated.

The proliferation assays should be repeated. If the trend towards increased cell proliferation is consistent, it would be interesting to investigate its molecular basis in future studies. My study found no significant differences in the growth rate, measured by PDT, among all the SCP1 cell populations analysed. I suspect a possible tendency towards

increased cell proliferation. This cannot be confirmed through my study alone but could be investigated in future studies.

5.4 No morphological changes in SCP1 cell populations due to PAX3-overexpression

Analysing the cell morphology of the PAX3-overexpressing SCP1 cells, C2C12 cells and the control group of SCP1^{GFP} cells, I found no significant differences in the cell area and aspect ratio.

In my study, 72.28% of C2C12 cells were small and round. Most cells of SCP1 cell populations were also small and round (51.63% of SCP1^{GFP} cells, 45.63% of SCP1$^{PAX3}{}_{low}$ cells, 50.60% of SCP1$^{PAX3}{}_{high}$ cells). SCP1 cell populations also contained many big and round cells (33.12% of SCP1^{GFP} cells, 30.42% of SCP1$^{PAX3}{}_{low}$ cells, 26.84% of SCP1$^{PAX3}{}_{high}$ cells).

McMahon et al. showed that C2C12 cells have a mean diameter of 12 µm (range 5-25 µm) and a mean length of 290 µm (range 130-520 µm) (214). Taking these measurements (diameter of 12 µm, length of 290 µm (214)) and approximating C2C12 cells to an elliptical shape, a mean cell area of 2.73×10^3 µm^2 is left. In my study, the C2C12 cells had a mean cell area of 1.71×10^3 µm^2 ± 1.43×10^3. When I calculated the supposed elliptic cell area with the smallest values measured in the study by McMahon et al. (diameter of 5 µm and mean length of 130 µm (214)), I estimated a cell area of 5.11×10^2 µm^2. The area of the C2C12 cells I used in this study is within this range. I infer, therefore, that the experimental conditions in my study were appropriate and the C2C12 cells were adequately cultivated.

In a 2009 study, Haasters et al. characterised SCP1 cells with a cell diameter of < 157 µm and cell area of < 6.62×10^3 µm^2 (215). In my study, the mean cell area of SCP1^{GFP} cells was 2.90×10^3 µm^2 ± 1.58×10^3; in SCP1$^{PAX3}{}_{low}$ cells, the mean cell area was 2.76×10^3 µm^2 ± 1.52×10^3, and in SCP1$^{PAX3}{}_{high}$ cells, it was 2.67×10^3 µm^2 ± 1.58×10^3. All the SCP1 cell populations I analysed had an area approximately three times smaller than Haasters et al. found in their study (215). This could be because I used different machines in my research, poor cell fitness, different culturing conditions, or the genetic modifications introduced in my project. Ten years of selection pressure or the many passages of the SCP1 cells I used could also explain this. When considering the results of both above-mentioned studies (214, 215), it is fair to say that SCP1 cells usually have a larger diameter than C2C12 cells. In my study, however, there was no difference in the cell area and

aspect ratio of the C2C12 and SCP1 cells. Overall, all the C2C12 and SCP1 cells I observed were primarily small and round (see 4.3).

According to Yaffe et al., C2C12 cells usually differentiate after changing from high serum to low serum conditions (from 10% FBS to 2-5% horse serum) (216, 217). Multinucleated myotubes are formed following the fusion of single cells (216, 218). The newly formed myotubes elongate in the ongoing differentiation and fusion process and express myosin, α-actin and numerous other proteins (216, 218).

I changed the medium in which I cultivated C2C12 myoblasts to DMEM with 2% HS and 1% penicillin/streptomycin five hours after seeding cells. Pictures of the cells were taken nineteen hours after seeding; the cells were already in low serum conditions for fourteen hours. Had I chosen a later time, the C2C12 cells would have had more time to differentiate and hence alter their cell morphology (see 4.3) to form a more muscle related configuration such as becoming larger and more elongated for instance. For more studies in this field, I think it would be an interesting aspect to keep in mind and maybe take pictures of C2C12 cells at a later stage or at more than one point to detect more differences/more muscle cell-like morphological properties. Still, when analysing C2C12 cells care needs to be taken as they fuse rapidly, complicating the characterisation of single cells. This should also be considered. Time lapse microscopy could be used in this area to provide further insights.

Overall, my study's morphological obversions showed no differences in cell area or aspect ratio. Also, I did not observe the significant elongation of cells typical of muscle formation.

5.5 Migration of cells was not affected by PAX3

As stated before, muscle precursor cells require Pax3 to migrate from the dermomyotome to the limb buds (163, 180). *In vivo*, *Pax3* controls de-epithelialisation of muscle precursor cells and their following migration by activating *c-met* (which encodes a transmembrane tyrosine kinase receptor that is expressed by cells of the dermomyotome (160, 163). The c-met receptor is vital for migrating myogenic progenitors into the limb bud (160). A study by Epstein et al. showed that *Pax3* regulates *c-met* expression (159, 178).

For these reasons, I analysed the migration of PAX3-overexpressing SCP1 cells in my study. I found that the random migration of SCP1 cells was not affected by PAX3-overexpression, neither in terms of the maximum nor the mean velocity. I found no significant differences in SCP1 cells compared to the control group.

The ongoing overexpression of PAX3 in the recently created cell populations may have played a role in the changes seen in cell migration by constitutively activating, and thereby altering, the cascade of important factors. It would be interesting, in future studies, to upregulate PAX3 temporarily (see 5.9) so that gene expression resembles the dynamics of *in vivo* cascades.

Studies show that placement on surfaces coated with type I collagen stimulates cell migration (219-221). In my study, there was no difference in the mean velocity or the maximum velocity of cell migration in SCP1 cell populations on a type I collagen-coated surface when compared to the control group of SCP1^{GFP} cells. Since Western Blot analysis and RT-PCR results showed no differences in PAX3 expression between SCP1$^{PAX3_{low}}$ cells and SCP1$^{PAX3_{high}}$ cells (see 5.7), I did not expect differences in random migration between those two cell populations.

5.6 PAX3-overexpressing SCP1 cells neither differentiated nor fused

I established direct co-cultures of C2C12 cells and SCP1 cell populations (SCP1$^{PAX3_{high}}$ cells, SCP1$^{PAX3_{low}}$ cells or SCP1^{GFP} cells) in the fusion assay. I visualised the formation of myotubes by immunocytochemistry with MYH1E (Developmental Studies Hybridoma Bank, USA), a primary antibody against the myosin heavy chain 1E. As expected, the mouse myoblast cell line C2C12 fused and expressed MYH1E by itself (1:0) and when mixed with all SCP1 cell populations in different ratios.

Despite this, the SCP1 cell populations neither differentiated, fused nor expressed MYH1E. It is possible, that the constant overexpression of PAX3 hindered the process of differentiation and prevented the SCP1 cell populations from fusing (see 5.9).

Investigating differentiation in indirect co-cultures (222) of SCP1 cell populations and C2C12 cells could be interesting for future experiments, as communication mediated by soluble factors could be clearly separated from direct communication mechanisms. In such a setting, the cells could communicate biochemically via their secretome, and their effects on each other could be evaluated. In this way, one could investigate whether C2C12 cells differentiate differently in an indirect co-culture due to the presence of PAX3.

5.7 SCP1$^{PAX3}_{high}$ and SCP1$^{PAX3}_{low}$ cells have the same PAX3 expression levels

I found no significant difference in PAX3 expression levels when comparing SCP1$^{PAX3}_{high}$ cells and SCP1$^{PAX3}_{low}$ cells in RT-PCR and Western Blot results. Using next-gen RNA-sequencing, I confirmed that these cell populations were similar. The PCA results confirmed that both SCP1 populations differed from SCP1^{GFP} cells.

At the FACS stage (see 4.1.1), I assumed that the levels of GFP intensity would correlate with the levels of PAX3 expression; however, I found no correlation between those two factors, as PAX3 levels did not significantly differ in SCP1 cell populations. Varying levels of GFP intensity could be linked to other factors, such as variations in plasmid integration events or integration sites per cell. It could also be explained by the cells' general health status, post-transcriptional regulation or the initial transfection efficiency.

Generally, since SCP1$^{PAX3}_{high}$ cells and SCP1$^{PAX3}_{low}$ cells had the same levels of PAX3 expression (as shown by PCR and Western blot), the assays conducted can be interpreted as PAX3-expressing SCP1 cell populations compared to non-PAX3-expressig SCP1^{GFP} cells or C2C12 myoblasts. Retrospectively, this provides a reasonable control for determining PAX3-dependent effects from background biological effects. If the levels of PAX3 expression had been different between the two SCP1 cell populations, meaning that SCP1$^{PAX3}_{high}$ cells really expressed higher levels of PAX3 than SCP1$^{PAX3}_{low}$ cells, it would have been interesting to see a correlation between those levels and the potential induction of a myogenic program. Cell lines with differing PAX3 levels would have allowed a "titration" down to physiological conditions.

A correlation between the GFP protein and GFP intensities could not be confirmed in my study. Two bands were depicted when analysing GFP expression on protein levels via Western Blot (see 4.1.3). Typically, only a single band is expected for GFP (223, 224). This could be due to unspecific binding of the chicken anti-GFP antibody or inferior protein sample quality, for example due to degradation. The Western Blot should be repeated with a new GFP antibody specific to eGFP (present in the original plasmid) and with freshly harvested protein samples.

5.8 Recap of experimental results

In this section, I would like to briefly summarise my findings:

Although Pax3 is involved in the proliferation of cells (181, 225), in my study, overexpressing PAX3 did not affect cell proliferation. There might be a tendency of increased

cell proliferation in SCP1$^{PAX3}_{low}$ cells; however, whether this depends on PAX3 is unclear and could be an avenue of future research (see 5.3).

I did not alter the cell area and aspect ratio of SCP1 cells by overexpressing PAX3. Compared to C2C12 myoblasts, there were no significant differences in the cell morphology of all SCP1 cell populations, as most of the SCP1 and C2C12 cells I analysed were small and round, and I did not detect any changes in their morphology (see 5.4).

Although Pax3's functions are essential in early myogenesis and the migration of myogenic progenitor cells (180), I found that the mean and maximum velocity of migrating PAX3-expressing cells did not differ from the control group (see 5.5).

Cell fusion is an essential characteristic of myoblasts. In the fusion assay, I found that the C2C12 myoblasts fused as expected. After seven days, the relative area of fused muscle fibre differed significantly from all the SCP1 cell populations, which did not fuse. The PAX3-expressing SCP1 cells neither differentiated, nor expressed MYH1E (see 5.6).

Another point worth discussing is the lack of variation in PAX3 levels in SCP1$^{PAX3}_{low}$ and SCP1$^{PAX3}_{high}$ cells, as demonstrated by RT-PCR, Western Blot and next-gen RNA-sequencing: both SCP1$^{PAX3}_{low}$ and SCP1$^{PAX3}_{high}$ cells had equal levels of PAX3. In view of this, I am not surprised to see that these two cell populations never showed significant differences in any of the assays performed. I consider the significant differences in the data of PAX3-overexpressing SCP1 cell populations compared to SCP1^{GFP} cells or C2C12 myoblasts as a general tendency, unconnected to varying levels of PAX3 expression (see 5.7). One, therefore, could interpret the results of my study as PAX3-overexpressing cells (regardless of whether they are SCP1$^{PAX3}_{low}$ or SCP1$^{PAX3}_{high}$ cells) being compared to a control group (SCP1^{GFP} cells) and to C2C12 myoblasts. Significant differences in the results of, for example, SCP1$^{PAX3}_{high}$ cells and not SCP1$^{PAX3}_{low}$ cells compared to SCP1^{GFP} cells or C2C12 cells can be interpreted as SCP1^{PAX3} cells, independent of the distinction in SCP1$^{PAX3}_{low}$ and SCP1$^{PAX3}_{high}$ cells, as there was no difference in the levels of PAX3 in these two cell populations.

5.9 Downregulation of PAX3 during *in vivo* myogenesis

It is crucial to reiterate that when I worked with the newly generated SCP1 cell populations (SCP1$^{PAX3}_{high}$ and SCP1$^{PAX3}_{low}$ cells), they constantly overexpressed PAX3. PAX3 was not downregulated at any stage of the experiments, so these cells remained in a native early state *in vitro*. This continuous overexpression of PAX3, as it occurs during my study, is not natural as it occurs during myogenesis *in vivo*.

Myogenesis *in vivo* is regulated through a hierarchy of various interacting transcription factors which are up- and downregulated at different developmental stages (183). A genetic network consisting of numerous extrinsic and intrinsic factors has power over myogenesis (183). Pax3 is a master regulator of early muscle lineage specification *in vivo* together with Pax7, Six1 and Six4 (183). Pax3 is downregulated during early myogenesis while Pax7, MyF5 and MyoD are upregulated (183). The downregulation of PAX3 is essential to allow other factors to be activated. In my study, it would have been interesting to insert crucial genes other than PAX3 and allow the cascade to occur as it would naturally. Overall, there is an elaborate feedback and feed-forward system of transcription factors associated with myogenic lineage progression (183). Muscle lineage is controlled by many factors (183). Although I could show that PAX3-overexpression can bring potential changes to SCP1 cells, shifting them towards myogenesis, it was insufficient to induce myogenic differentiation in these cell populations.

In future studies, working with cells expressing more factors would be interesting, rather than PAX3 exclusively. However, this could be difficult, especially since all factors involved must be timed precisely. Exclusive overexpression of PAX3, as it occurred in my study, must not be considered natural and cannot be compared to myogenesis *in vivo*. For this study, single overexpression of PAX3 was a way to focus on its effects and specific gene function.

I identified muscle-related changes in the newly created SCP1^{PAX} cell populations. These muscle-related molecular signatures partially occurred, as some results showed. The remaining problem that may have hindered PAX3-expressing SCP1 cell populations from terminal differentiation is that, as stated in this chapter, PAX3 was not downregulated but constantly overexpressed. Another interesting approach for future research could be the temporary upregulation of PAX3 in SCP1 cell populations. This could “prime/prepare” the cells for the first steps towards myogenic differentiation. A subsequent downregulation of PAX3 at later stages of the differentiation process might enable proper cell maturation.

5.10 Working with immortalised SCP1 cell populations

Immortalised cell lines were established to study biological and molecular processes (226). They offer the possibility to research cellular lineages, cancer malignancies and molecular pathways in cells (226). Immortalised cell lines are used for research in regenerative medicine, and in the treatment of incurable diseases (226). Immortalised cells drop their cell cycle checkpoint pathways, thereby avoiding ageing (227). Human mesenchymal stem cells are essential in regenerative medicine (228). Getting hold of these cells is non-invasive, and they can differentiate into numerous cell types (228). SCP1 cells can differentiate into osteogenic, adipogenic and chondrogenic lineages (200, 228).

In this project, I worked with immortalised human mesenchymal stem cells (hMSCs) – SCP1 cells. In this study, I wanted to identify muscle-related molecular signatures in SCP1 cells overexpressing PAX3 and perhaps induce a myogenic differentiation in SCP1 cells. To date, SCP1 cells have not been successfully differentiated into myogenic cells. Strenzke et al. found that the fusion of myoblasts was significantly boosted due to exposure to the secretome of *SCX* overexpressing SCP1 cells (229).

SCP1 cells were established 15 years ago, in 2008, by Böcker et al. (200). This mesenchymal stem cell population was immortalised by the expression of hTERT after retroviral transformation (200). Cells in a culture for an extended period are prone to genetic drift (230). This may modify the phenotype of the cells as well as introduce changes in growth patterns (230). Laboratory studies can be impeded by genetic drift and other factors such as cross-contamination; these studies are difficult to reproduce and can be problematic to compare (230). Torsvik et al. compared sub-clones of the U-251 glioblastoma cell line to the original U-251MG line and found differences in those cells due to genetic drift in culture (230). There is a possibility that over time, phenotypic consequences and genetic changes have occurred in my SCP1 cells after all these years in culture (230). Some of their features might have altered, potentially hindering their ability to differentiate and/or fully initiate a myogenic program.

I only worked with cell lines and did not use primary mesenchymal stem cells. Ideally, I would have first carried out my experiments with cell lines such as SCP1 or C2C12 and afterwards validated my results using primary cells to corroborate my findings. This would have been an important step since cell lines cannot precisely recreate the properties of primary cells (231). In my study, however, I used cell lines as they are a valuable tool for studying biomolecular processes (231). The benefits of using cell lines include cost effectiveness, simple usage, an endless stocks of cells and bypassing eventual ethical matters that can occur when working with tissue from humans or animals (231). They are popular for studying gene function (231), such as in my study. Nonetheless, care

must be taken when working with cell lines instead of primary cells (231). Cell lines might respond differently to stimuli or display modifications in their phenotype or original functions (231). As mentioned before, genetic drift might result in genotypic or phenotypic changes in the cells (231). For this reason, cell lines may differ from primary cells, and varying results might be generated (231). Nelson-Rees et al. showed that most cell lines used globally were contaminated by HeLa cells at some point (231, 232). This is still a current issue, many years later (231, 233, 234). For this reason, primary cells should be used to recheck the results of conducted studies, especially regarding crucial findings (231).

Verifying my results with primary cells would have been helpful and might be of interest in future studies regarding this topic.

6. Conclusion & Outlook

My project aimed to generate PAX3-overexpressing SCP1 cell populations and characterise them *in vitro* to identify muscle-related molecular signatures of these newly created cell populations. Based on the results, the following can be concluded:

1. The transcriptome of SCP1 cells was shifted by PAX3-overexpression, as shown by next-gen RNA-sequencing and PCA. I found that the muscle organ development pathway was activated in SCP1$^{PAX3}{}_{high}$ cells.
2. The overexpression of PAX3 had no effect on the proliferation of SCP1 cells. However, there may be a tendency towards increased proliferation in PAX3-expressing cells compared to SCP1^{GFP} cells. Future studies are needed to confirm this.
3. The clonogenic potential of cell populations overexpressing PAX3 did not change compared to the control group.
4. Overexpressing PAX3 did not affect the morphology of SCP1 cells in terms of cell area or aspect ratio.
5. PAX3-overexpression had no impact on the random migration of SCP1 cells regarding the mean or the maximum velocity.
6. Cell fusion of SCP1 cells could not be induced by overexpression of PAX3. Newly created SCP1 cell populations did not express MYH1E and therefore did not differentiate or fuse.

The essence of this study could be described as follows:

Overexpression of PAX3 in SCP1 cells allowed partial myogenic changes in the transcriptomes and properties of these cells, which I interpret as a slight tendency towards a more myogenic lineage; however, terminal myogenic differentiation (and fusion) of these cell populations did not occur. The constant overexpression of PAX3 may have prevented the cells from undergoing terminal myogenic differentiation. In future studies, PAX3 levels need to be more dynamic, for example by using a doxycycline-inducible promoter system.

I believe that my findings will be helpful for future research into the potential and limitations of PAX3 expression in SCP1 cells and for a better understanding of the challenges of studying PAX3 in myogenesis in 2D cell culture models.

For future studies, it would be interesting to generate cell populations that overexpress PAX3 transiently rather than continuously. With this approach, PAX3 expression could ‘support’ or ‘prime’ cells *in vitro* as they begin to differentiate towards a myogenic lineage. However, it should be possible to downregulate PAX3 at later stages, as it occurs *in vivo*.

Transient transfection could be another way for future studies to temporarily overexpress a specific protein. Another approach could be the temporary expression of PAX3 by transient transfection, as opposed to the stable integration used in my study.

It would be interesting for future experiments to create cell populations that express various factors instead of PAX3 alone. Regulator genes of early myogenesis could be up and then downregulated, especially PAX3, while other factors take the lead. Pax7, Six1 and Six4 specify early muscle lineages and would be promising candidates for future studies. MRFs such as Myf5, MyoD, Myogenin or Mrf4 could also be compelling factors. It would be interesting to see what combination of factors could induce myogenic differentiation in SCP1 cells. A mixture of early and late regulators would be helpful, as PAX3 controls the early stages of myogenesis. Future experiments aimed at myogenic induction would benefit from overexpressing a combination of these key transcription factors in SCP1 cells.

Summing up the results of this study reminds me of the bigger picture. The whole process of myogenesis is very complex. I have zoomed in and analysed a single, specific gene involved in the earliest stages of myogenesis. By zooming out and thinking about the context of muscle loss, the barriers to satisfactory treatment for affected patients, and the attempts in regenerative medicine to address these problems, I see my study as a useful addition and hope to have an impact on the progress of research into skeletal muscle wasting.

7. Bibliography

1. Fanzani A, Conraads VM, Penna F, Martinet W. Molecular and cellular mechanisms of skeletal muscle atrophy: an update. J Cachexia Sarcopenia Muscle. 2012;3(3):163-79.

2. Evans WJ. Skeletal muscle loss: cachexia, sarcopenia, and inactivity. Am J Clin Nutr. 2010;91(4):1123s-7s.

3. Dunn A, Talovic M, Patel K, Patel A, Marcinczyk M, Garg K. Biomaterial and stem cell-based strategies for skeletal muscle regeneration. J Orthop Res. 2019;37(6):1246-62.

4. Janas J. Muscular dystrophy. Nurse Pract Forum. 1996;7(4):167-73.

5. Evans WJ, Campbell WW. Sarcopenia and age-related changes in body composition and functional capacity. J Nutr. 1993;123(2 Suppl):465-8.

6. Evans WJ. What is sarcopenia? J Gerontol A Biol Sci Med Sci. 1995;50 Spec No:5-8.

7. Muscaritoli M, Anker SD, Argilés J, Aversa Z, Bauer JM, Biolo G, Boirie Y, Bosaeus I, Cederholm T, Costelli P, Fearon KC, Laviano A, Maggio M, Rossi Fanelli F, Schneider SM, Schols A, Sieber CC. Consensus definition of sarcopenia, cachexia and pre-cachexia: joint document elaborated by Special Interest Groups (SIG) "cachexia-anorexia in chronic wasting diseases" and "nutrition in geriatrics". Clin Nutr. 2010;29(2):154-9.

8. Frontera WR, Hughes VA, Fielding RA, Fiatarone MA, Evans WJ, Roubenoff R. Aging of skeletal muscle: a 12-yr longitudinal study. J Appl Physiol (1985). 2000;88(4):1321-6.

9. Lexell J, Henriksson-Larsén K, Winblad B, Sjöström M. Distribution of different fiber types in human skeletal muscles: effects of aging studied in whole muscle cross sections. Muscle Nerve. 1983;6(8):588-95.

10. Kortebein P, Ferrando A, Lombeida J, Wolfe R, Evans WJ. Effect of 10 days of bed rest on skeletal muscle in healthy older adults. Jama. 2007;297(16):1772-4.

11. Morley JE. Hormones and the aging process. J Am Geriatr Soc. 2003;51(7 Suppl):S333-7.

12. Visser M, Deeg DJ, Lips P. Low vitamin D and high parathyroid hormone levels as determinants of loss of muscle strength and muscle mass (sarcopenia): the Longitudinal Aging Study Amsterdam. J Clin Endocrinol Metab. 2003;88(12):5766-72.

13. Cesari M, Penninx BW, Pahor M, Lauretani F, Corsi AM, Rhys Williams G, Guralnik JM, Ferrucci L. Inflammatory markers and physical performance in older persons: the InCHIANTI study. J Gerontol A Biol Sci Med Sci. 2004;59(3):242-8.

14. Cesari M, Kritchevsky SB, Baumgartner RN, Atkinson HH, Penninx BW, Lenchik L, Palla SL, Ambrosius WT, Tracy RP, Pahor M. Sarcopenia, obesity, and inflammation--results from the Trial of Angiotensin Converting Enzyme Inhibition and Novel Cardiovascular Risk Factors study. Am J Clin Nutr. 2005;82(2):428-34.

15. Morley JE. Sarcopenia: diagnosis and treatment. J Nutr Health Aging. 2008;12(7):452-6.

16. Dhillon RJ, Hasni S. Pathogenesis and Management of Sarcopenia. Clin Geriatr Med. 2017;33(1):17-26.

17. Abellan van Kan G, Cderbaum JM, Cesari M, Dahinden P, Fariello RG, Fielding RA, Goodpaster BH, Hettwer S, Isaac M, Laurent D, Morley JE, Pahor M, Rooks D, Roubenoff R, Rutkove SB, Shaheen A, Vamvakas S, Vrijbloed JW, Vellas B. Sarcopenia: biomarkers and imaging (International Conference on Sarcopenia research). J Nutr Health Aging. 2011;15(10):834-46.

18. Cesari M, Fielding RA, Pahor M, Goodpaster B, Hellerstein M, van Kan GA, Anker SD, Rutkove S, Vrijbloed JW, Isaac M, Rolland Y, M'Rini C, Aubertin-Leheudre M, Cedarbaum JM, Zamboni M, Sieber CC, Laurent D, Evans WJ, Roubenoff R, Morley JE, Vellas B. Biomarkers of sarcopenia in clinical trials-recommendations from the International Working Group on Sarcopenia. J Cachexia Sarcopenia Muscle. 2012;3(3):181-90.

19. Cruz-Jentoft AJ, Baeyens JP, Bauer JM, Boirie Y, Cederholm T, Landi F, Martin FC, Michel JP, Rolland Y, Schneider SM, Topinková E, Vandewoude M, Zamboni M. Sarcopenia: European

consensus on definition and diagnosis: Report of the European Working Group on Sarcopenia in Older People. Age Ageing. 2010;39(4):412-23.

20. Roth SM, Ferrell RF, Hurley BF. Strength training for the prevention and treatment of sarcopenia. J Nutr Health Aging. 2000;4(3):143-55.

21. Sakuma K, Yamaguchi A. Sarcopenia and age-related endocrine function. Int J Endocrinol. 2012;2012:127362.

22. Wakabayashi H, Sakuma K. Comprehensive approach to sarcopenia treatment. Curr Clin Pharmacol. 2014;9(2):171-80.

23. Pötsch MS, Tschirner A, Palus S, von Haehling S, Doehner W, Beadle J, Coats AJ, Anker SD, Springer J. The anabolic catabolic transforming agent (ACTA) espindolol increases muscle mass and decreases fat mass in old rats. J Cachexia Sarcopenia Muscle. 2014;5(2):149-58.

24. Dingemans AM, de Vos-Geelen J, Langen R, Schols AM. Phase II drugs that are currently in development for the treatment of cachexia. Expert Opin Investig Drugs. 2014;23(12):1655-69.

25. Rondanelli M, Miccono A, Peroni G, Guerriero F, Morazzoni P, Riva A, Guido D, Perna S. A Systematic Review on the Effects of Botanicals on Skeletal Muscle Health in Order to Prevent Sarcopenia. Evid Based Complement Alternat Med. 2016;2016:5970367.

26. Harimoto N, Shirabe K, Yamashita YI, Ikegami T, Yoshizumi T, Soejima Y, Ikeda T, Maehara Y, Nishie A, Yamanaka T. Sarcopenia as a predictor of prognosis in patients following hepatectomy for hepatocellular carcinoma. Br J Surg. 2013;100(11):1523-30.

27. Zhang XM, Chen D, Xie XH, Zhang JE, Zeng Y, Cheng AS. Sarcopenia as a predictor of mortality among the critically ill in an intensive care unit: a systematic review and meta-analysis. BMC Geriatr. 2021;21(1):339.

28. Sayer AA, Robinson SM, Patel HP, Shavlakadze T, Cooper C, Grounds MD. New horizons in the pathogenesis, diagnosis and management of sarcopenia. Age Ageing. 2013;42(2):145-50.

29. von Haehling S, Anker SD. Cachexia as a major underestimated and unmet medical need: facts and numbers. J Cachexia Sarcopenia Muscle. 2010;1(1):1-5.

30. Evans WJ, Morley JE, Argilés J, Bales C, Baracos V, Guttridge D, Jatoi A, Kalantar-Zadeh K, Lochs H, Mantovani G, Marks D, Mitch WE, Muscaritoli M, Najand A, Ponikowski P, Rossi Fanelli F, Schambelan M, Schols A, Schuster M, Thomas D, Wolfe R, Anker SD. Cachexia: a new definition. Clin Nutr. 2008;27(6):793-9.

31. von Haehling S, Lainscak M, Springer J, Anker SD. Cardiac cachexia: a systematic overview. Pharmacol Ther. 2009;121(3):227-52.

32. Nunes EA, Stokes T, McKendry J, Currier BS, Phillips SM. Disuse-induced skeletal muscle atrophy in disease and nondisease states in humans: mechanisms, prevention, and recovery strategies. Am J Physiol Cell Physiol. 2022;322(6):C1068-c84.

33. Gao Y, Arfat Y, Wang H, Goswami N. Muscle Atrophy Induced by Mechanical Unloading: Mechanisms and Potential Countermeasures. Front Physiol. 2018;9:235.

34. Kirwan R, McCullough D, Butler T, Perez de Heredia F, Davies IG, Stewart C. Sarcopenia during COVID-19 lockdown restrictions: long-term health effects of short-term muscle loss. Geroscience. 2020;42(6):1547-78.

35. McKendry J, Thomas ACQ, Phillips SM. Muscle Mass Loss in the Older Critically Ill Population: Potential Therapeutic Strategies. Nutr Clin Pract. 2020;35(4):607-16.

36. Rosa KYA, Pádua KLC, Maldaner VZ, Franco de Oliveira LV, de Melo FX, Santos DB. Musculoskeletal Consequences from COVID-19 and the Importance of Pulmonary Rehabilitation Program. Respiration. 2021;100(10):1038-40.

37. Visser M, Goodpaster BH, Kritchevsky SB, Newman AB, Nevitt M, Rubin SM, Simonsick EM, Harris TB. Muscle mass, muscle strength, and muscle fat infiltration as predictors of incident mobility limitations in well-functioning older persons. J Gerontol A Biol Sci Med Sci. 2005;60(3):324-33.

38. de Santana FM, Premaor MO, Tanigava NY, Pereira RMR. Low muscle mass in older adults and mortality: A systematic review and meta-analysis. Exp Gerontol. 2021;152:111461.

39. Atherton PJ, Greenhaff PL, Phillips SM, Bodine SC, Adams CM, Lang CH. Control of skeletal muscle atrophy in response to disuse: clinical/preclinical contentions and fallacies of evidence. Am J Physiol Endocrinol Metab. 2016;311(3):E594-604.

40. Rudrappa SS, Wilkinson DJ, Greenhaff PL, Smith K, Idris I, Atherton PJ. Human Skeletal Muscle Disuse Atrophy: Effects on Muscle Protein Synthesis, Breakdown, and Insulin Resistance-A Qualitative Review. Front Physiol. 2016;7:361.

41. Conraads VM, Beckers P, Bosmans J, De Clerck LS, Stevens WJ, Vrints CJ, Brutsaert DL. Combined endurance/resistance training reduces plasma TNF-alpha receptor levels in patients with chronic heart failure and coronary artery disease. Eur Heart J. 2002;23(23):1854-60.

42. Penna F, Busquets S, Pin F, Toledo M, Baccino FM, López-Soriano FJ, Costelli P, Argilés JM. Combined approach to counteract experimental cancer cachexia: eicosapentaenoic acid and training exercise. J Cachexia Sarcopenia Muscle. 2011;2(2):95-104.

43. Van Berendoncks AM, Garnier A, Beckers P, Hoymans VY, Possemiers N, Fortin D, Van Hoof V, Dewilde S, Vrints CJ, Ventura-Clapier R, Conraads VM. Exercise training reverses adiponectin resistance in skeletal muscle of patients with chronic heart failure. Heart. 2011;97(17):1403-9.

44. Palus S, Schur R, Akashi YJ, Bockmeyer B, Datta R, Halem H, Dong J, Culler MD, Adams V, Anker SD, Springer J. Ghrelin and its analogues, BIM-28131 and BIM-28125, improve body weight and regulate the expression of MuRF-1 and MAFbx in a rat heart failure model. PLoS One. 2011;6(11):e26865.

45. Malkin CJ, Pugh PJ, West JN, van Beek EJ, Jones TH, Channer KS. Testosterone therapy in men with moderate severity heart failure: a double-blind randomized placebo controlled trial. Eur Heart J. 2006;27(1):57-64.

46. Schmidt K, von Haehling S, Doehner W, Palus S, Anker SD, Springer J. IGF-1 treatment reduces weight loss and improves outcome in a rat model of cancer cachexia. J Cachexia Sarcopenia Muscle. 2011;2(2):105-9.

47. Chung ES, Packer M, Lo KH, Fasanmade AA, Willerson JT. Randomized, double-blind, placebo-controlled, pilot trial of infliximab, a chimeric monoclonal antibody to tumor necrosis factor-alpha, in patients with moderate-to-severe heart failure: results of the anti-TNF Therapy Against Congestive Heart Failure (ATTACH) trial. Circulation. 2003;107(25):3133-40.

48. Mann DL, McMurray JJ, Packer M, Swedberg K, Borer JS, Colucci WS, Djian J, Drexler H, Feldman A, Kober L, Krum H, Liu P, Nieminen M, Tavazzi L, van Veldhuisen DJ, Waldenstrom A, Warren M, Westheim A, Zannad F, Fleming T. Targeted anticytokine therapy in patients with chronic heart failure: results of the Randomized Etanercept Worldwide Evaluation (RENEWAL). Circulation. 2004;109(13):1594-602.

49. Mantovani G, Macciò A, Madeddu C, Serpe R, Antoni G, Massa E, Dessì M, Panzone F. Phase II nonrandomized study of the efficacy and safety of COX-2 inhibitor celecoxib on patients with cancer cachexia. J Mol Med (Berl). 2010;88(1):85-92.

50. Tawa NE, Jr., Odessey R, Goldberg AL. Inhibitors of the proteasome reduce the accelerated proteolysis in atrophying rat skeletal muscles. J Clin Invest. 1997;100(1):197-203.

51. Carmignac V, Quéré R, Durbeej M. Proteasome inhibition improves the muscle of laminin α2 chain-deficient mice. Hum Mol Genet. 2011;20(3):541-52.

52. Huh Y, Son KY. Association between total protein intake and low muscle mass in Korean adults. BMC Geriatr. 2022;22(1):319.

53. Qualls AE, Southern WM, Call JA. Mitochondria-cytokine crosstalk following skeletal muscle injury and disuse: a mini-review. Am J Physiol Cell Physiol. 2021;320(5):C681-c8.

54. Armstrong RB, Warren GL, Warren JA. Mechanisms of exercise-induced muscle fibre injury. Sports Med. 1991;12(3):184-207.

55. Baker BA. An Old Problem: Aging and Skeletal-Muscle-Strain Injury. J Sport Rehabil. 2017;26(2):180-8.

56. Wall BT, Morton JP, van Loon LJ. Strategies to maintain skeletal muscle mass in the injured athlete: nutritional considerations and exercise mimetics. Eur J Sport Sci. 2015;15(1):53-62.

57. Pandey SN, Kesari A, Yokota T, Pandey GS. Muscular Dystrophy: Disease Mechanisms and Therapies. Biomed Res Int. 2015;2015:456348.

58. Chemello F, Bassel-Duby R, Olson EN. Correction of muscular dystrophies by CRISPR gene editing. J Clin Invest. 2020;130(6):2766-76.

59. Shieh PB. Muscular dystrophies and other genetic myopathies. Neurol Clin. 2013;31(4):1009-29.

60. Annexstad EJ, Lund-Petersen I, Rasmussen M. Duchenne muscular dystrophy. Tidsskr Nor Laegeforen. 2014;134(14):1361-4.

61. Gupta RM, Musunuru K. Expanding the genetic editing tool kit: ZFNs, TALENs, and CRISPR-Cas9. J Clin Invest. 2014;124(10):4154-61.

62. Bonaldo P, Sandri M. Cellular and molecular mechanisms of muscle atrophy. Dis Model Mech. 2013;6(1):25-39.

63. Kline WO, Panaro FJ, Yang H, Bodine SC. Rapamycin inhibits the growth and muscle-sparing effects of clenbuterol. J Appl Physiol (1985). 2007;102(2):740-7.

64. Zhou X, Wang JL, Lu J, Song Y, Kwak KS, Jiao Q, Rosenfeld R, Chen Q, Boone T, Simonet WS, Lacey DL, Goldberg AL, Han HQ. Reversal of cancer cachexia and muscle wasting by ActRIIB antagonism leads to prolonged survival. Cell. 2010;142(4):531-43.

65. Supinski GS, Vanags J, Callahan LA. Effect of proteasome inhibitors on endotoxin-induced diaphragm dysfunction. Am J Physiol Lung Cell Mol Physiol. 2009;296(6):L994-l1001.

66. Caron AZ, Haroun S, Leblanc E, Trensz F, Guindi C, Amrani A, Grenier G. The proteasome inhibitor MG132 reduces immobilization-induced skeletal muscle atrophy in mice. BMC Musculoskelet Disord. 2011;12:185.

67. Jamart C, Raymackers JM, Li An G, Deldicque L, Francaux M. Prevention of muscle disuse atrophy by MG132 proteasome inhibitor. Muscle Nerve. 2011;43(5):708-16.

68. Ciciliot S, Schiaffino S. Regeneration of mammalian skeletal muscle. Basic mechanisms and clinical implications. Curr Pharm Des. 2010;16(8):906-14.

69. Collins CA, Olsen I, Zammit PS, Heslop L, Petrie A, Partridge TA, Morgan JE. Stem cell function, self-renewal, and behavioral heterogeneity of cells from the adult muscle satellite cell niche. Cell. 2005;122(2):289-301.

70. Pannérec A, Marazzi G, Sassoon D. Stem cells in the hood: the skeletal muscle niche. Trends Mol Med. 2012;18(10):599-606.

71. Jones DL, Wagers AJ. No place like home: anatomy and function of the stem cell niche. Nat Rev Mol Cell Biol. 2008;9(1):11-21.

72. Moss FP, Leblond CP. Satellite cells as the source of nuclei in muscles of growing rats. Anat Rec. 1971;170(4):421-35.

73. Dumont NA, Bentzinger CF, Sincennes MC, Rudnicki MA. Satellite Cells and Skeletal Muscle Regeneration. Compr Physiol. 2015;5(3):1027-59.

74. Sousa-Victor P, García-Prat L, Muñoz-Cánoves P. Control of satellite cell function in muscle regeneration and its disruption in ageing. Nat Rev Mol Cell Biol. 2022;23(3):204-26.

75. Nagata Y, Partridge TA, Matsuda R, Zammit PS. Entry of muscle satellite cells into the cell cycle requires sphingolipid signaling. J Cell Biol. 2006;174(2):245-53.

76. Tatsumi R, Liu X, Pulido A, Morales M, Sakata T, Dial S, Hattori A, Ikeuchi Y, Allen RE. Satellite cell activation in stretched skeletal muscle and the role of nitric oxide and hepatocyte growth factor. Am J Physiol Cell Physiol. 2006;290(6):C1487-94.

77. Tatsumi R, Anderson JE, Nevoret CJ, Halevy O, Allen RE. HGF/SF is present in normal adult skeletal muscle and is capable of activating satellite cells. Dev Biol. 1998;194(1):114-28.

78. Conboy IM, Rando TA. The regulation of Notch signaling controls satellite cell activation and cell fate determination in postnatal myogenesis. Dev Cell. 2002;3(3):397-409.

79. Brack AS, Conboy IM, Conboy MJ, Shen J, Rando TA. A temporal switch from notch to Wnt signaling in muscle stem cells is necessary for normal adult myogenesis. Cell Stem Cell. 2008;2(1):50-9.

80. Yin H, Price F, Rudnicki MA. Satellite cells and the muscle stem cell niche. Physiol Rev. 2013;93(1):23-67.

81. Asfour HA, Allouh MZ, Said RS. Myogenic regulatory factors: The orchestrators of myogenesis after 30 years of discovery. Exp Biol Med (Maywood). 2018;243(2):118-28.

82. Cornelison DD, Olwin BB, Rudnicki MA, Wold BJ. MyoD(-/-) satellite cells in single-fiber culture are differentiation defective and MRF4 deficient. Dev Biol. 2000;224(2):122-37.

83. Asakura A, Komaki M, Rudnicki M. Muscle satellite cells are multipotential stem cells that exhibit myogenic, osteogenic, and adipogenic differentiation. Differentiation. 2001;68(4-5):245-53.

84. Schmalbruch H. The morphology of regeneration of skeletal muscles in the rat. Tissue Cell. 1976;8(4):673-92.

85. Grefte S, Kuijpers-Jagtman AM, Torensma R, Von den Hoff JW. Skeletal muscle development and regeneration. Stem Cells Dev. 2007;16(5):857-68.

86. Berdeaux R, Stewart R. cAMP signaling in skeletal muscle adaptation: hypertrophy, metabolism, and regeneration. Am J Physiol Endocrinol Metab. 2012;303(1):E1-17.

87. Cohen S, Nathan JA, Goldberg AL. Muscle wasting in disease: molecular mechanisms and promising therapies. Nat Rev Drug Discov. 2015;14(1):58-74.

88. Yoshida T, Delafontaine P. Mechanisms of IGF-1-Mediated Regulation of Skeletal Muscle Hypertrophy and Atrophy. Cells. 2020;9(9).

89. Barton-Davis ER, Shoturma DI, Musaro A, Rosenthal N, Sweeney HL. Viral mediated expression of insulin-like growth factor I blocks the aging-related loss of skeletal muscle function. Proc Natl Acad Sci U S A. 1998;95(26):15603-7.

90. Dunshea FR, Chung CS, Owens PC, Ballard JF, Walton PE. Insulin-like growth factor-I and analogues increase growth in artificially-reared neonatal pigs. Br J Nutr. 2002;87(6):587-93.

91. Garcia JM, Polvino WJ. Pharmacodynamic hormonal effects of anamorelin, a novel oral ghrelin mimetic and growth hormone secretagogue in healthy volunteers. Growth Horm IGF Res. 2009;19(3):267-73.

92. Porporato PE, Filigheddu N, Reano S, Ferrara M, Angelino E, Gnocchi VF, Prodam F, Ronchi G, Fagoonee S, Fornaro M, Chianale F, Baldanzi G, Surico N, Sinigaglia F, Perroteau I, Smith RG, Sun Y, Geuna S, Graziani A. Acylated and unacylated ghrelin impair skeletal muscle atrophy in mice. J Clin Invest. 2013;123(2):611-22.

93. Chen JA, Splenser A, Guillory B, Luo J, Mendiratta M, Belinova B, Halder T, Zhang G, Li YP, Garcia JM. Ghrelin prevents tumour- and cisplatin-induced muscle wasting: characterization of multiple mechanisms involved. J Cachexia Sarcopenia Muscle. 2015;6(2):132-43.

94. Nagaya N, Moriya J, Yasumura Y, Uematsu M, Ono F, Shimizu W, Ueno K, Kitakaze M, Miyatake K, Kangawa K. Effects of ghrelin administration on left ventricular function, exercise capacity, and muscle wasting in patients with chronic heart failure. Circulation. 2004;110(24):3674-9.

95. Nagaya N, Itoh T, Murakami S, Oya H, Uematsu M, Miyatake K, Kangawa K. Treatment of cachexia with ghrelin in patients with COPD. Chest. 2005;128(3):1187-93.

96. Burdet L, de Muralt B, Schutz Y, Pichard C, Fitting JW. Administration of growth hormone to underweight patients with chronic obstructive pulmonary disease. A prospective, randomized, controlled study. Am J Respir Crit Care Med. 1997;156(6):1800-6.

97. Nagaya N, Kojima M, Kangawa K. Ghrelin, a novel growth hormone-releasing peptide, in the treatment of cardiopulmonary-associated cachexia. Intern Med. 2006;45(3):127-34.

98. Lynch GS, Ryall JG. Role of beta-adrenoceptor signaling in skeletal muscle: implications for muscle wasting and disease. Physiol Rev. 2008;88(2):729-67.

99. Sandri M. Signaling in muscle atrophy and hypertrophy. Physiology (Bethesda). 2008;23:160-70.

100. Ryall JG, Schertzer JD, Lynch GS. Attenuation of age-related muscle wasting and weakness in rats after formoterol treatment: therapeutic implications for sarcopenia. J Gerontol A Biol Sci Med Sci. 2007;62(8):813-23.

101. Hinkle RT, Hodge KMB, Cody DB, Sheldon RJ, Kobilka BK, Isfort RJ. Skeletal muscle hypertrophy and anti-atrophy effects of clenbuterol are mediated by the beta2-adrenergic receptor. Muscle Nerve. 2002;25(5):729-34.

102. Busquets S, Figueras MT, Fuster G, Almendro V, Moore-Carrasco R, Ametller E, Argilés JM, López-Soriano FJ. Anticachectic effects of formoterol: a drug for potential treatment of muscle wasting. Cancer Res. 2004;64(18):6725-31.

103. Endres S, Fülle HJ, Sinha B, Stoll D, Dinarello CA, Gerzer R, Weber PC. Cyclic nucleotides differentially regulate the synthesis of tumour necrosis factor-alpha and interleukin-1 beta by human mononuclear cells. Immunology. 1991;72(1):56-60.

104. Rabe KF. Update on roflumilast, a phosphodiesterase 4 inhibitor for the treatment of chronic obstructive pulmonary disease. Br J Pharmacol. 2011;163(1):53-67.

105. Ifegwu OC, Awale G, Rajpura K, Lo KW, Laurencin CT. Harnessing cAMP signaling in musculoskeletal regenerative engineering. Drug Discov Today. 2017;22(7):1027-44.

106. Gold MG, Gonen T, Scott JD. Local cAMP signaling in disease at a glance. J Cell Sci. 2013;126(Pt 20):4537-43.

107. Keshwani MM, Kanter JR, Ma Y, Wilderman A, Darshi M, Insel PA, Taylor SS. Mechanisms of cyclic AMP/protein kinase A- and glucocorticoid-mediated apoptosis using S49 lymphoma cells as a model system. Proc Natl Acad Sci U S A. 2015;112(41):12681-6.

108. Chen AE, Ginty DD, Fan CM. Protein kinase A signalling via CREB controls myogenesis induced by Wnt proteins. Nature. 2005;433(7023):317-22.

109. Griffin CA, Kafadar KA, Pavlath GK. MOR23 promotes muscle regeneration and regulates cell adhesion and migration. Dev Cell. 2009;17(5):649-61.

110. Zalin RJ, Montague W. Changes in cyclic AMP, adrenylate cyclase and protein kinase levels during the development of embryonic chick skeletal muscle. Exp Cell Res. 1975;93(1):55-62.

111. Hawke TJ, Garry DJ. Myogenic satellite cells: physiology to molecular biology. J Appl Physiol (1985). 2001;91(2):534-51.

112. Ryall JG, Schertzer JD, Alabakis TM, Gehrig SM, Plant DR, Lynch GS. Intramuscular beta2-agonist administration enhances early regeneration and functional repair in rat skeletal muscle after myotoxic injury. J Appl Physiol (1985). 2008;105(1):165-72.

113. Stewart R, Flechner L, Montminy M, Berdeaux R. CREB is activated by muscle injury and promotes muscle regeneration. PLoS One. 2011;6(9):e24714.

114. Sinha-Hikim I, Artaza J, Woodhouse L, Gonzalez-Cadavid N, Singh AB, Lee MI, Storer TW, Casaburi R, Shen R, Bhasin S. Testosterone-induced increase in muscle size in healthy young men is associated with muscle fiber hypertrophy. Am J Physiol Endocrinol Metab. 2002;283(1):E154-64.

115. Sinha-Hikim I, Roth SM, Lee MI, Bhasin S. Testosterone-induced muscle hypertrophy is associated with an increase in satellite cell number in healthy, young men. Am J Physiol Endocrinol Metab. 2003;285(1):E197-205.

116. Curran MJ, Bihrle W, 3rd. Dramatic rise in prostate-specific antigen after androgen replacement in a hypogonadal man with occult adenocarcinoma of the prostate. Urology. 1999;53(2):423-4.

117. Bhasin S, Calof OM, Storer TW, Lee ML, Mazer NA, Jasuja R, Montori VM, Gao W, Dalton JT. Drug insight: Testosterone and selective androgen receptor modulators as anabolic therapies for chronic illness and aging. Nat Clin Pract Endocrinol Metab. 2006;2(3):146-59.

118. Kuang S, Gillespie MA, Rudnicki MA. Niche regulation of muscle satellite cell self-renewal and differentiation. Cell Stem Cell. 2008;2(1):22-31.

119. Motohashi N, Asakura Y, Asakura A. Isolation, culture, and transplantation of muscle satellite cells. J Vis Exp. 2014(86).

120. Sacco A, Doyonnas R, Kraft P, Vitorovic S, Blau HM. Self-renewal and expansion of single transplanted muscle stem cells. Nature. 2008;456(7221):502-6.

121. Xu X, Wilschut KJ, Kouklis G, Tian H, Hesse R, Garland C, Sbitany H, Hansen S, Seth R, Knott PD, Hoffman WY, Pomerantz JH. Human Satellite Cell Transplantation and Regeneration from Diverse Skeletal Muscles. Stem Cell Reports. 2015;5(3):419-34.

122. Garcia SM, Tamaki S, Lee S, Wong A, Jose A, Dreux J, Kouklis G, Sbitany H, Seth R, Knott PD, Heaton C, Ryan WR, Kim EA, Hansen SL, Hoffman WY, Pomerantz JH. High-Yield Purification, Preservation, and Serial Transplantation of Human Satellite Cells. Stem Cell Reports. 2018;10(3):1160-74.

123. Sun C, Serra C, Lee G, Wagner KR. Stem cell-based therapies for Duchenne muscular dystrophy. Exp Neurol. 2020;323:113086.

124. Skuk D, Tremblay JP. Myoblast transplantation: the current status of a potential therapeutic tool for myopathies. J Muscle Res Cell Motil. 2003;24(4-6):285-300.

125. Skuk D, Tremblay JP. Intramuscular cell transplantation as a potential treatment of myopathies: clinical and preclinical relevant data. Expert Opin Biol Ther. 2011;11(3):359-74.

126. Skuk D, Goulet M, Tremblay JP. Intramuscular transplantation of myogenic cells in primates: importance of needle size, cell number, and injection volume. Cell Transplant. 2014;23(1):13-25.

127. Kinoshita I, Vilquin JT, Guérette B, Asselin I, Roy R, Tremblay JP. Very efficient myoblast allotransplantation in mice under FK506 immunosuppression. Muscle Nerve. 1994;17(12):1407-15.

128. Naranjo JD, Dziki JL, Badylak SF. Regenerative Medicine Approaches for Age-Related Muscle Loss and Sarcopenia: A Mini-Review. Gerontology. 2017;63(6):580-9.

129. Ohnuki M, Takahashi K. Present and future challenges of induced pluripotent stem cells. Philos Trans R Soc Lond B Biol Sci. 2015;370(1680):20140367.

130. Goudenege S, Lebel C, Huot NB, Dufour C, Fujii I, Gekas J, Rousseau J, Tremblay JP. Myoblasts derived from normal hESCs and dystrophic hiPSCs efficiently fuse with existing muscle fibers following transplantation. Mol Ther. 2012;20(11):2153-67.

131. Maffioletti SM, Sarcar S, Henderson ABH, Mannhardt I, Pinton L, Moyle LA, Steele-Stallard H, Cappellari O, Wells KE, Ferrari G, Mitchell JS, Tyzack GE, Kotiadis VN, Khedr M, Ragazzi M, Wang W, Duchen MR, Patani R, Zammit PS, Wells DJ, Eschenhagen T, Tedesco FS. Three-Dimensional Human iPSC-Derived Artificial Skeletal Muscles Model Muscular Dystrophies and Enable Multilineage Tissue Engineering. Cell Rep. 2018;23(3):899-908.

132. Mizuno Y, Chang H, Umeda K, Niwa A, Iwasa T, Awaya T, Fukada S, Yamamoto H, Yamanaka S, Nakahata T, Heike T. Generation of skeletal muscle stem/progenitor cells from murine induced pluripotent stem cells. Faseb j. 2010;24(7):2245-53.

133. Tateno H, Onuma Y, Ito Y, Minoshima F, Saito S, Shimizu M, Aiki Y, Asashima M, Hirabayashi J. Elimination of tumorigenic human pluripotent stem cells by a recombinant lectin-toxin fusion protein. Stem Cell Reports. 2015;4(5):811-20.

134. Gussoni E, Soneoka Y, Strickland CD, Buzney EA, Khan MK, Flint AF, Kunkel LM, Mulligan RC. Dystrophin expression in the mdx mouse restored by stem cell transplantation. Nature. 1999;401(6751):390-4.

135. Corbel SY, Lee A, Yi L, Duenas J, Brazelton TR, Blau HM, Rossi FM. Contribution of hematopoietic stem cells to skeletal muscle. Nat Med. 2003;9(12):1528-32.

136. Goldman SM, Henderson BEP, Corona BT. Evaluation of bone marrow mononuclear cells as an adjunct therapy to minced muscle graft for the treatment of volumetric muscle loss injuries. Stem Cell Res Ther. 2017;8(1):142.

137. Boppart MD, De Lisio M, Zou K, Huntsman HD. Defining a role for non-satellite stem cells in the regulation of muscle repair following exercise. Front Physiol. 2013;4:310.

138. Sheng G. The developmental basis of mesenchymal stem/stromal cells (MSCs). BMC Dev Biol. 2015;15:44.

139. Cianfarani F, Toietta G, Di Rocco G, Cesareo E, Zambruno G, Odorisio T. Diabetes impairs adipose tissue-derived stem cell function and efficiency in promoting wound healing. Wound Repair Regen. 2013;21(4):545-53.

140. Scala P, Rehak L, Giudice V, Ciaglia E, Puca AA, Selleri C, Della Porta G, Maffulli N. Stem Cell and Macrophage Roles in Skeletal Muscle Regenerative Medicine. Int J Mol Sci. 2021;22(19).

141. Matziolis G, Winkler T, Schaser K, Wiemann M, Krocker D, Tuischer J, Perka C, Duda GN. Autologous bone marrow-derived cells enhance muscle strength following skeletal muscle crush injury in rats. Tissue Eng. 2006;12(2):361-7.

142. Lee JH, Kosinski PA, Kemp DM. Contribution of human bone marrow stem cells to individual skeletal myotubes followed by myogenic gene activation. Exp Cell Res. 2005;307(1):174-82.

143. Mueller GM, O'Day T, Watchko JF, Ontell M. Effect of injecting primary myoblasts versus putative muscle-derived stem cells on mass and force generation in mdx mice. Hum Gene Ther. 2002;13(9):1081-90.

144. Qu-Petersen Z, Deasy B, Jankowski R, Ikezawa M, Cummins J, Pruchnic R, Mytinger J, Cao B, Gates C, Wernig A, Huard J. Identification of a novel population of muscle stem cells in mice: potential for muscle regeneration. J Cell Biol. 2002;157(5):851-64.

145. Uezumi A, Fukada S, Yamamoto N, Takeda S, Tsuchida K. Mesenchymal progenitors distinct from satellite cells contribute to ectopic fat cell formation in skeletal muscle. Nat Cell Biol. 2010;12(2):143-52.

146. Joe AW, Yi L, Natarajan A, Le Grand F, So L, Wang J, Rudnicki MA, Rossi FM. Muscle injury activates resident fibro/adipogenic progenitors that facilitate myogenesis. Nat Cell Biol. 2010;12(2):153-63.

147. Tanaka KK, Hall JK, Troy AA, Cornelison DD, Majka SM, Olwin BB. Syndecan-4-expressing muscle progenitor cells in the SP engraft as satellite cells during muscle regeneration. Cell Stem Cell. 2009;4(3):217-25.

148. Doyle MJ, Zhou S, Tanaka KK, Pisconti A, Farina NH, Sorrentino BP, Olwin BB. Abcg2 labels multiple cell types in skeletal muscle and participates in muscle regeneration. J Cell Biol. 2011;195(1):147-63.

149. Buckingham M, Relaix F. PAX3 and PAX7 as upstream regulators of myogenesis. Semin Cell Dev Biol. 2015;44:115-25.

150. Esteves de Lima J, Bou Akar R, Mansour M, Rocancourt D, Buckingham M, Relaix F. M-Cadherin Is a PAX3 Target During Myotome Patterning. Front Cell Dev Biol. 2021;9:652652.

151. Boudjadi S, Chatterjee B, Sun W, Vemu P, Barr FG. The expression and function of PAX3 in development and disease. Gene. 2018;666:145-57.

152. Buckingham M. Myogenic progenitor cells and skeletal myogenesis in vertebrates. Curr Opin Genet Dev. 2006;16(5):525-32.

153. Hutcheson DA, Zhao J, Merrell A, Haldar M, Kardon G. Embryonic and fetal limb myogenic cells are derived from developmentally distinct progenitors and have different requirements for beta-catenin. Genes Dev. 2009;23(8):997-1013.

154. Bober E, Franz T, Arnold HH, Gruss P, Tremblay P. Pax-3 is required for the development of limb muscles: a possible role for the migration of dermomyotomal muscle progenitor cells. Development. 1994;120(3):603-12.

155. Daston G, Lamar E, Olivier M, Goulding M. Pax-3 is necessary for migration but not differentiation of limb muscle precursors in the mouse. Development. 1996;122(3):1017-27.

156. Shin J, Watanabe S, Hoelper S, Krüger M, Kostin S, Pöling J, Kubin T, Braun T. BRAF activates PAX3 to control muscle precursor cell migration during forelimb muscle development. Elife. 2016;5.

157. Borycki AG, Li J, Jin F, Emerson CP, Epstein JA. Pax3 functions in cell survival and in pax7 regulation. Development. 1999;126(8):1665-74.

158. Relaix F, Rocancourt D, Mansouri A, Buckingham M. A Pax3/Pax7-dependent population of skeletal muscle progenitor cells. Nature. 2005;435(7044):948-53.

159. Epstein JA, Shapiro DN, Cheng J, Lam PY, Maas RL. Pax3 modulates expression of the c-Met receptor during limb muscle development. Proc Natl Acad Sci U S A. 1996;93(9):4213-8.

160. Bladt F, Riethmacher D, Isenmann S, Aguzzi A, Birchmeier C. Essential role for the c-met receptor in the migration of myogenic precursor cells into the limb bud. Nature. 1995;376(6543):768-71.

161. Williams BA, Ordahl CP. Pax-3 expression in segmental mesoderm marks early stages in myogenic cell specification. Development. 1994;120(4):785-96.

162. Kiefer JC, Hauschka SD. Myf-5 is transiently expressed in nonmuscle mesoderm and exhibits dynamic regional changes within the presegmented mesoderm and somites I-IV. Dev Biol. 2001;232(1):77-90.

163. Christ B, Brand-Saberi B. Limb muscle development. Int J Dev Biol. 2002;46(7):905-14.

164. Epstein DJ, Vekemans M, Gros P. Splotch (Sp2H), a mutation affecting development of the mouse neural tube, shows a deletion within the paired homeodomain of Pax-3. Cell. 1991;67(4):767-74.

165. Franz T. Persistent truncus arteriosus in the Splotch mutant mouse. Anat Embryol (Berl). 1989;180(5):457-64.

166. Chalepakis G, Stoykova A, Wijnholds J, Tremblay P, Gruss P. Pax: gene regulators in the developing nervous system. J Neurobiol. 1993;24(10):1367-84.

167. Franz T, Kothary R. Characterization of the neural crest defect in Splotch (Sp1H) mutant mice using a lacZ transgene. Brain Res Dev Brain Res. 1993;72(1):99-105.

168. Henderson DJ, Conway SJ, Copp AJ. Rib truncations and fusions in the Sp2H mouse reveal a role for Pax3 in specification of the ventro-lateral and posterior parts of the somite. Dev Biol. 1999;209(1):143-58.

169. Lakkis MM, Golden JA, O'Shea KS, Epstein JA. Neurofibromin deficiency in mice causes exencephaly and is a modifier for Splotch neural tube defects. Dev Biol. 1999;212(1):80-92.

170. Relaix F, Rocancourt D, Mansouri A, Buckingham M. Divergent functions of murine Pax3 and Pax7 in limb muscle development. Genes Dev. 2004;18(9):1088-105.

171. Bober E, Brand-Saberi B, Ebensperger C, Wilting J, Balling R, Paterson BM, Arnold HH, Christ B. Initial steps of myogenesis in somites are independent of influence from axial structures. Development. 1994;120(11):3073-82.

172. Goulding M, Lumsden A, Paquette AJ. Regulation of Pax-3 expression in the dermomyotome and its role in muscle development. Development. 1994;120(4):957-71.

173. Goulding MD, Chalepakis G, Deutsch U, Erselius JR, Gruss P. Pax-3, a novel murine DNA binding protein expressed during early neurogenesis. Embo j. 1991;10(5):1135-47.

174. Tajbakhsh S, Buckingham M. The birth of muscle progenitor cells in the mouse: spatiotemporal considerations. Curr Top Dev Biol. 2000;48:225-68.

175. Buckingham M, Relaix F. The role of Pax genes in the development of tissues and organs: Pax3 and Pax7 regulate muscle progenitor cell functions. Annu Rev Cell Dev Biol. 2007;23:645-73.

176. Tremblay P, Dietrich S, Mericskay M, Schubert FR, Li Z, Paulin D. A crucial role for Pax3 in the development of the hypaxial musculature and the long-range migration of muscle precursors. Dev Biol. 1998;203(1):49-61.

177. Franz T, Kothary R, Surani MA, Halata Z, Grim M. The Splotch mutation interferes with muscle development in the limbs. Anat Embryol (Berl). 1993;187(2):153-60.

178. Tajbakhsh S, Rocancourt D, Cossu G, Buckingham M. Redefining the genetic hierarchies controlling skeletal myogenesis: Pax-3 and Myf-5 act upstream of MyoD. Cell. 1997;89(1):127-38.

179. Mansouri A. The role of Pax3 and Pax7 in development and cancer. Crit Rev Oncog. 1998;9(2):141-9.

180. Nord H, Kahsay A, Dennhag N, Pedrosa Domellöf F, von Hofsten J. Genetic compensation between Pax3 and Pax7 in zebrafish appendicular muscle formation. Dev Dyn. 2022;251(9):1423-38.

181. Diao Y, Guo X, Li Y, Sun K, Lu L, Jiang L, Fu X, Zhu H, Sun H, Wang H, Wu Z. Pax3/7BP is a Pax7- and Pax3-binding protein that regulates the proliferation of muscle precursor cells by an epigenetic mechanism. Cell Stem Cell. 2012;11(2):231-41.

182. Wang Q, Kumar S, Mitsios N, Slevin M, Kumar P. Investigation of downstream target genes of PAX3c, PAX3e and PAX3g isoforms in melanocytes by microarray analysis. Int J Cancer. 2007;120(6):1223-31.

183. Bentzinger CF, Wang YX, Rudnicki MA. Building muscle: molecular regulation of myogenesis. Cold Spring Harb Perspect Biol. 2012;4(2).

184. Esteves de Lima J, Relaix F. Master regulators of skeletal muscle lineage development and pluripotent stem cells differentiation. Cell Regen. 2021;10(1):31.

185. Bryson-Richardson RJ, Currie PD. The genetics of vertebrate myogenesis. Nat Rev Genet. 2008;9(8):632-46.

186. Punch VG, Jones AE, Rudnicki MA. Transcriptional networks that regulate muscle stem cell function. Wiley Interdiscip Rev Syst Biol Med. 2009;1(1):128-40.

187. Bismuth K, Relaix F. Genetic regulation of skeletal muscle development. Exp Cell Res. 2010;316(18):3081-6.

188. Maroto M, Reshef R, Münsterberg AE, Koester S, Goulding M, Lassar AB. Ectopic Pax-3 activates MyoD and Myf-5 expression in embryonic mesoderm and neural tissue. Cell. 1997;89(1):139-48.

189. Kassar-Duchossoy L, Giacone E, Gayraud-Morel B, Jory A, Gomès D, Tajbakhsh S. Pax3/Pax7 mark a novel population of primitive myogenic cells during development. Genes Dev. 2005;19(12):1426-31.

190. Bajard L, Relaix F, Lagha M, Rocancourt D, Daubas P, Buckingham ME. A novel genetic hierarchy functions during hypaxial myogenesis: Pax3 directly activates Myf5 in muscle progenitor cells in the limb. Genes Dev. 2006;20(17):2450-64.

191. Darabi R, Gehlbach K, Bachoo RM, Kamath S, Osawa M, Kamm KE, Kyba M, Perlingeiro RC. Functional skeletal muscle regeneration from differentiating embryonic stem cells. Nat Med. 2008;14(2):134-43.

192. Buckingham M, Rigby PW. Gene regulatory networks and transcriptional mechanisms that control myogenesis. Dev Cell. 2014;28(3):225-38.

193. Moncaut N, Rigby PW, Carvajal JJ. Dial M(RF) for myogenesis. Febs j. 2013;280(17):3980-90.

194. Birlea SA, Costin GE, Roop DR, Norris DA. Trends in Regenerative Medicine: Repigmentation in Vitiligo Through Melanocyte Stem Cell Mobilization. Med Res Rev. 2017;37(4):907-35.

195. Yang R, Zheng Y, Li L, Liu S, Burrows M, Wei Z, Nace A, Herlyn M, Cui R, Guo W, Cotsarelis G, Xu X. Direct conversion of mouse and human fibroblasts to functional melanocytes by defined factors. Nat Commun. 2014;5:5807.

196. Zhang YX, Liu LP, Jin M, Sun H, Zhang HL, Li YM. Direct Reprogramming of Mouse Fibroblasts into Melanocytes. J Vis Exp. 2021(174).

197. Kang JS, Krauss RS. Muscle stem cells in developmental and regenerative myogenesis. Curr Opin Clin Nutr Metab Care. 2010;13(3):243-8.

198. Magli A, Schnettler E, Rinaldi F, Bremer P, Perlingeiro RC. Functional dissection of Pax3 in paraxial mesoderm development and myogenesis. Stem Cells. 2013;31(1):59-70.

199. Ridgeway AG, Skerjanc IS. Pax3 is essential for skeletal myogenesis and the expression of Six1 and Eya2. J Biol Chem. 2001;276(22):19033-9.

200. Böcker W, Yin Z, Drosse I, Haasters F, Rossmann O, Wierer M, Popov C, Locher M, Mutschler W, Docheva D, Schieker M. Introducing a single-cell-derived human mesenchymal stem cell line expressing hTERT after lentiviral gene transfer. J Cell Mol Med. 2008;12(4):1347-59.

201. Mátés L, Chuah MK, Belay E, Jerchow B, Manoj N, Acosta-Sanchez A, Grzela DP, Schmitt A, Becker K, Matrai J, Ma L, Samara-Kuko E, Gysemans C, Pryputniewicz D, Miskey C, Fletcher B, VandenDriessche T, Ivics Z, Izsvák Z. Molecular evolution of a novel hyperactive Sleeping Beauty transposase enables robust stable gene transfer in vertebrates. Nat Genet. 2009;41(6):753-61.

202. Pircher T, Wackerhage H, Akova E, Böcker W, Aszodi A, Saller MM. Fusion of Normoxic- and Hypoxic-Preconditioned Myoblasts Leads to Increased Hypertrophy. Cells. 2022;11(6).

203. Ashburner M, Ball CA, Blake JA, Botstein D, Butler H, Cherry JM, Davis AP, Dolinski K, Dwight SS, Eppig JT, Harris MA, Hill DP, Issel-Tarver L, Kasarskis A, Lewis S, Matese JC, Richardson JE, Ringwald M, Rubin GM, Sherlock G. Gene ontology: tool for the unification of biology. The Gene Ontology Consortium. Nat Genet. 2000;25(1):25-9.

204. Carbon S, Ireland A, Mungall CJ, Shu S, Marshall B, Lewis S. AmiGO: online access to ontology and annotation data. Bioinformatics. 2009;25(2):288-9.

205. The Gene Ontology resource: enriching a GOld mine. Nucleic Acids Res. 2021;49(D1):D325-d34.

206. Subramanian A, Tamayo P, Mootha VK, Mukherjee S, Ebert BL, Gillette MA, Paulovich A, Pomeroy SL, Golub TR, Lander ES, Mesirov JP. Gene set enrichment analysis: a knowledge-based approach for interpreting genome-wide expression profiles. Proc Natl Acad Sci U S A. 2005;102(43):15545-50.

207. Ciemerych MA, Archacka K, Grabowska I, Przewoźniak M. Cell cycle regulation during proliferation and differentiation of mammalian muscle precursor cells. Results Probl Cell Differ. 2011;53:473-527.

208. Ling YH, Sui MH, Zheng Q, Wang KY, Wu H, Li WY, Liu Y, Chu MX, Fang FG, Xu LN. miR-27b regulates myogenic proliferation and differentiation by targeting Pax3 in goat. Sci Rep. 2018;8(1):3909.

209. Lehka L, Rędowicz MJ. Mechanisms regulating myoblast fusion: A multilevel interplay. Semin Cell Dev Biol. 2020;104:81-92.

210. Sharma P, Ruel TD, Kocha KM, Liao S, Huang P. Single cell dynamics of embryonic muscle progenitor cells in zebrafish. Development. 2019;146(14).

211. Wells L, Edwards KA, Bernstein SI. Myosin heavy chain isoforms regulate muscle function but not myofibril assembly. Embo j. 1996;15(17):4454-9.

212. Darabi R, Santos FN, Filareto A, Pan W, Koene R, Rudnicki MA, Kyba M, Perlingeiro RC. Assessment of the myogenic stem cell compartment following transplantation of Pax3/Pax7-induced embryonic stem cell-derived progenitors. Stem Cells. 2011;29(5):777-90.

213. Sato T. Induction of Skeletal Muscle Progenitors and Stem Cells from human induced Pluripotent Stem Cells. J Neuromuscul Dis. 2020;7(4):395-405.

214. McMahon DK, Anderson PA, Nassar R, Bunting JB, Saba Z, Oakeley AE, Malouf NN. C2C12 cells: biophysical, biochemical, and immunocytochemical properties. Am J Physiol. 1994;266(6 Pt 1):C1795-802.

215. Haasters F, Prall WC, Anz D, Bourquin C, Pautke C, Endres S, Mutschler W, Docheva D, Schieker M. Morphological and immunocytochemical characteristics indicate the yield of early

progenitors and represent a quality control for human mesenchymal stem cell culturing. J Anat. 2009;214(5):759-67.

216. Veliça P, Bunce CM. A quick, simple and unbiased method to quantify C2C12 myogenic differentiation. Muscle Nerve. 2011;44(3):366-70.

217. Yaffe D, Saxel O. A myogenic cell line with altered serum requirements for differentiation. Differentiation. 1977;7(3):159-66.

218. Cabane C, Englaro W, Yeow K, Ragno M, Dérijard B. Regulation of C2C12 myogenic terminal differentiation by MKK3/p38alpha pathway. Am J Physiol Cell Physiol. 2003;284(3):C658-66.

219. Xu Q, Liu X, Liu W, Hayashi T, Yamato M, Fujisaki H, Hattori S, Tashiro SI, Onodera S, Ikejima T. Type I collagen-induced YAP nuclear expression promotes primary cilia growth and contributes to cell migration in confluent mouse embryo fibroblast 3T3-L1 cells. Mol Cell Biochem. 2019;450(1-2):87-96.

220. Liu X, Gao Y, Long X, Hayashi T, Mizuno K, Hattori S, Fujisaki H, Ogura T, Wang DO, Ikejima T. Type I collagen promotes the migration and myogenic differentiation of C2C12 myoblasts via the release of interleukin-6 mediated by FAK/NF-κB p65 activation. Food Funct. 2020;11(1):328-38.

221. Graf F, Horn P, Ho AD, Boutros M, Maercker C. The extracellular matrix proteins type I collagen, type III collagen, fibronectin, and laminin 421 stimulate migration of cancer cells. Faseb j. 2021;35(7):e21692.

222. Levorson EJ, Santoro M, Kasper FK, Mikos AG. Direct and indirect co-culture of chondrocytes and mesenchymal stem cells for the generation of polymer/extracellular matrix hybrid constructs. Acta Biomater. 2014;10(5):1824-35.

223. Bjørkøy G, Lamark T, Pankiv S, Øvervatn A, Brech A, Johansen T. Monitoring autophagic degradation of p62/SQSTM1. Methods Enzymol. 2009;452:181-97.

224. Tamamaki N, Yanagawa Y, Tomioka R, Miyazaki J, Obata K, Kaneko T. Green fluorescent protein expression and colocalization with calretinin, parvalbumin, and somatostatin in the GAD67-GFP knock-in mouse. J Comp Neurol. 2003;467(1):60-79.

225. Motohashi N, Alexander MS, Casar JC, Kunkel LM. Identification of a novel microRNA that regulates the proliferation and differentiation in muscle side population cells. Stem Cells Dev. 2012;21(16):3031-43.

226. Maqsood MI, Matin MM, Bahrami AR, Ghasroldasht MM. Immortality of cell lines: challenges and advantages of establishment. Cell Biol Int. 2013;37(10):1038-45.

227. Soice E, Johnston J. Immortalizing Cells for Human Consumption. Int J Mol Sci. 2021;22(21).

228. Reiprich S, Hofbauer E, Kiderlen S, Clausen-Schaumann H, Böcker W, Aszódi A, Schönitzer V. Adhesive Properties of the Hyaluronan Pericellular Coat in Hyaluronan Synthases Overexpressing Mesenchymal Stem Cells. Int J Mol Sci. 2020;21(11).

229. Strenzke M, Alberton P, Aszodi A, Docheva D, Haas E, Kammerlander C, Böcker W, Saller MM. Tenogenic Contribution to Skeletal Muscle Regeneration: The Secretome of Scleraxis Overexpressing Mesenchymal Stem Cells Enhances Myogenic Differentiation In Vitro. Int J Mol Sci. 2020;21(6).

230. Torsvik A, Stieber D, Enger P, Golebiewska A, Molven A, Svendsen A, Westermark B, Niclou SP, Olsen TK, Chekenya Enger M, Bjerkvig R. U-251 revisited: genetic drift and phenotypic consequences of long-term cultures of glioblastoma cells. Cancer Med. 2014;3(4):812-24.

231. Kaur G, Dufour JM. Cell lines: Valuable tools or useless artifacts. Spermatogenesis. 2012;2(1):1-5.

232. Nelson-Rees WA, Daniels DW, Flandermeyer RR. Cross-contamination of cells in culture. Science. 1981;212(4493):446-52.

233. Capes-Davis A, Theodosopoulos G, Atkin I, Drexler HG, Kohara A, MacLeod RA, Masters JR, Nakamura Y, Reid YA, Reddel RR, Freshney RI. Check your cultures! A list of cross-contaminated or misidentified cell lines. Int J Cancer. 2010;127(1):1-8.

234. Jiang L, Zeng X, Wang Z, Chen Q. Cell line cross-contamination: KB is not an oral squamous cell carcinoma cell line. Eur J Oral Sci. 2009;117(1):90-1.

8. Appendix

8.1 Abbreviations

Abbreviation	Meaning
AR	Aspect ratio
BSA	Bovine serum albumin
CFU	Colony forming unit
CI	Confidence interval
cumPD	Cumulative population doublings
DAPI	4',6-diamidino-2-phenylindole
ddH2O	Double-distilled water
DMEM	Dulbecco's Modified Eagle Medium
DMSO	Dimethyl sulfoxide
DTT	1,4-Dithiothreitol
eGFP	Enhanced green fluorescent protein
FACS	Fluorescence-activated cell sorting
FAPs	Fibro/adipogenic progenitor cells
FBS	Foetal bovine serum
GFP	Green fluorescent protein
GO	Gene Ontology
H3K4 HMT	Histone 3 lysine 4 methyltransferase
HGF	Hepatocyte growth factor
hMSCs	Human mesenchymal stem cells
HS	Heat-inactivated horse serum
HSCs	Hematopoietic stem cells
IGF1	Insulin-like growth factor 1
iPSCs	Induced pluripotent stem cells
LB	Lysogeny broth
MRFs	Myogenic Regulatory Factors
MSCs	Mesenchymal stem cells
MYH1E/MF20	Antibody against the myosin heavy chain 1E
n	Number of independent experiments
next-gen RNA-sequencing	next-generation RNA-sequencing
p	P-value
Pax3	Murine Paired Box 3 gene
PAX3	Human Paired Box 3 gene

PBS	Phosphate Buffered Saline
PCA	Principal Component Analysis
PD(T)	Population doubling (time)
PFA	Paraformaldehyde
RFP	Red fluorescent protein
SB	Sleeping Beauty
SP	Muscle side-population
SP cells	Muscle side population cells
w	Number of cell culture dishes used per experiment (well plates, cell culture dishes or cell culture flasks)

8.2 List of Genes

Gene Abbreviation	Gene/ Protein name
CD34	*CD34 molecule/* CD34 molecule
COL11A1	*collagen type XI alpha 1 chain*/ Collagen type XI alpha 1 chain
FGFR4	*fibroblast growth factor receptor 4*/ Fibroblast growth factor receptor 4
HES1	*hes family bHLH transcription factor 1*/ Hes family bHLH transcription factor 1
KEL	*Kell metallo-endopeptidase (Kell blood group)*/ Kell metallo-endopeptidase (Kell blood group)
Met/ MET	*MET proto-oncogene, receptor tyrosine kinase*/ MET proto-oncogene, receptor tyrosine kinase
MITF	*melanocyte inducing transcription factor*/ Melanocyte inducing transcription factor
Myf5	*myogenic factor 5*/ Myogenic factor 5
MyoD	*MyoD family inhibitor*/ Myogenic differentiation 1
MyoG	*Myogenin*/ Myogenin
PAX3/ Pax3	*paired box 3*/ Paired box 3
PAX7/ Pax7	*paired box 7*/ Paired box 7
RET	*ret proto-oncogene*/ Ret proto-oncogene
RGS2	*regulator of G protein signaling 2*/ Regulator of G protein signaling 2
SCX	*scleraxis bHLH transcription factor*/ Scleraxis bHLH transcription factor

Six1	*sine oculis-related homeobox 1*/ Homeobox protein SIX1
Six4	*sine oculis-related homeobox 4*/ Homeobox protein SIX4
STRA6	*signaling receptor and transporter of retinol STRA6*/ Signaling receptor and transporter of retinol STRA6

8.3 Danksagung

Ich möchte mich an dieser Stelle bei allen bedanken, die mich im Zuge meiner Arbeit unterstützt und begleitet haben.

Ich danke meinem Doktorvater **PD Dr. Attila Aszódi** für die Unterstützung und die Möglichkeit, meine Arbeit unter seiner Leitung durchzuführen.

Ich danke **Dr. rer. nat. Maximilian Saller** besonders für die konstruktive fachliche Betreuung und den kollegialen Austausch in allen Abschnitten dieser Dissertation. Vielen Dank für die enge Zusammenarbeit und die Einführung in das wissenschaftliche Arbeiten, welches ich durch ihn erlernen durfte.

Ebenso möchte ich mich herzlich bei **Martina Burggraf** für ihre Unterstützung bedanken.

Großer Dank gilt auch **Elif Akova** und **Sebastian Reiprich** die mich zu allen Zeiten bestärkt haben.

Ich danke meiner Familie und meinen Freunden:

Walter, **Elke**, **Lisbeth**, **Markus**, **Anusha**, **Luca**, **Catha**, **Sebastian**, **Ludwig**, **Lisa**,

Charlotte, **Paul** und **Annalena**.

8.4 Affidavit

Eidesstattliche Versicherung

Zimmermann Marlene

Name, Vorname

Ich erkläre hiermit an Eides statt, dass ich die vorliegende Dissertation mit dem Titel:

Overexpression of PAX3 in immortalised human mesenchymal stem cells initiates a myogenic program

selbständig verfasst, mich außer der angegebenen keiner weiteren Hilfsmittel bedient und alle Erkenntnisse, die aus dem Schrifttum ganz oder annähernd übernommen sind, als solche kenntlich gemacht und nach ihrer Herkunft unter Bezeichnung der Fundstelle einzeln nachgewiesen habe.

Ich erkläre des Weiteren, dass die hier vorgelegte Dissertation nicht in gleicher oder in ähnlicher Form bei einer anderen Stelle zur Erlangung eines akademischen Grades eingereicht wurde.

Wien, 25.03.25
Ort, Datum

Marlene Zimmermann
Unterschrift Doktorandin bzw. Doktorand